SYNTHESIS AND CHARACTERIZATION OF NEW SYSTEMS OF SIDE-CHAIN LIQUID CRYSTALLINE POLYMERS AND ORIENTATION STUDIES

by

Guoxiong Yuan

A thesis submitted in fulfillment of the requirement for the degree of master of science (M. Sc.) of Département de Chimie

FACULTÉ DES SCIENCES
UNIVERSITÉ DE SHERBROOKE

Sherbrooke, Québec, Canada, February 1997

SOMMAIRE

Les travaux de recherche décrits dans ce mémoire comprennent quatre projets séparés. Dans le premier projet, nous avons préparé une série de réseaux interpénétrés composés de deux polymères cristaux liquides à chaîne latérale (PCLCLs). Nous discutons la synthèse et la caractérisation ainsi que le potentiel de ce nouveau système cristallin liquide, démontré pour la toute première fois, dans la recherche de nouveaux matériaux fonctionnels. Dans le deuxième projet, deux PCLCLs sont greffés sur Styrène-Butadiène-Styrène (SBS), un copolymère à trois blocs, par une polymérisation radicalaire de monomères mesogènes dans une solution avec le SBS dissouts. Nous montrons que les matériaux résultants possèdent la caractéristique intéressante de se comporter comme un élastomère thermoplastique, et qu'une structure monodomaine des unités mesogènes peut être facilement induite par l'étirement d'un film et puis conservée par un traitement thermique à deux étapes. Cette technique spéciale peut être utilisée pour un grand nombre de PCLCLs, et représente une nouvelle approche pour arriver à un contrôle de la structure monodomaine. Dans le troisième projet, nous avons étudié l'orientation des unités mesogènes induite par l'effet mécanique dans deux séries de PCLCLs contenant des ions. Nous avons observé que dans un cas, où le groupe mesogène est un biphényle, les agrégats ioniques n'influencent pas l'orientation atteinte. Par contre, pour les ionomères dont le groupe mesogène est un benzoate de phényle, l'orientation maximale décroît en augmentant la concentration des ions, indiquant que les agrégats ioniques réduisent l'ordre moléculaire à l'intérieur de domaines nématiques. Finalement, dans le dernier projet, nous avons étudié le comportement en relaxation d'orientation d'un PCLCL étiré lorsqu'il est chauffé, tout en conservant la déformation du film, près de ses transitions de phases. Un phénomène de réorientation de groupes mesogènes induit par une transition de phases de nématique - smectique a été observé pour la première fois. Cette réorientation est caractérisée par une rotation de 90° de groupes mesogènes, passant d'une orientation perpendiculaire par

rapport à la direction d'étirement, laquelle est le résultat de l'étirement mécanique, à une orientation parallèle. Nous discutons ce phénomène ainsi que d'autres résultats obtenus dans cette étude.

ABSTRACT

The research work described in this thesis consists of four separate projects. In the first project, we have prepared a series of interpenetrating networks based on two covalently cross-linked side-chain liquid crystalline polymers (SCLCPs). We discuss the synthesis and characterization as well as the potential of this novel liquid crystalline system in the search of new functional materials. In the second project, two SCLCPs were grafted onto a styrene-butadiene-styrene (SBS) tri-block copolymer through a radical polymerization of the mesogenic monomers in a SBS solution. We show that the resulting SCLCP-based materials have the interesting feature to behave like a thermoplastic elastomer, and that a monodomain structure of the mesogens can easily be induced by a film stretching and then preserved after a two-step thermal annealing process. This special technique is applicable to a large number of SCLCPs, and represents a new approach for achieving a control the monodomain structure. In the third project, the mechanically-induced orientation of the mesogens in two groups of ion-containing SCLCPs was investigated. We found that in the case of a SCLCP carrying biphenyl mesogenic moieties the ionic aggregates show no influence on the orientation. By contrast, in the case of a SCLCP containing phenyl benzoate units, the achievable orientation decreases as the ion content increases, indicating that the ionic aggregates reduce the order inside nematic domains. In the last project, the orientational relaxation behavior of a stretched SCLCP was studied by heating the deformed film under strain to temperatures near its phase transitions. A mesophase-transition-induced reorientation phenomenon was observed for the first time. When the stretched SCLCP undergoes a smectic-nematic transition, the pendent mesogenic groups, which are initially oriented perpendicularly with respect to the stretching direction, flip 90° to give rise to a parallel orientation. We discuss this observation and other related phenomena.

ACKNOWLEDGEMENT

Firstly, I wish to thank my thesis' supervisor, Professor Yue Zhao, for his guidance, supervision, advice, support and assistance through my study and all research work pursuing in polymer science during my Master degree's program and in the preparation of this thesis.

Specially, I wish to thank my wife, Yan, for her giving me a continuing support in my study and research work.

Finally, I wish to acknowledge the Natural Sciences and Engineering Research Council of Canada and le Fonds pour la Formation de Chercheurs et l'Aide à la Recherche du Québec for financial support.

TABLE OF CONTENTS

LIST OF TABLES

LIST OF FIGURES

ABBREVIATIONS

Acronym	*Meaning*
SCLCPs	side-chain liquid crystalline polymers
LC	liquid crystalline
LCPs	liquid crystalline polymers
SCLCEs	side-chain liquid crystalline elastomers
ILCPNs	interpenetrating liquid crystalline polymer networks
IPNs	interpenetrating polymer networks
SBS	styrene-butadiene-styrene
FTIR	Fourier-transform infrared
DSC	differential scanning calorimetry
GPC	gel permeation chromatography
AIBN	azobisisobutyronitrile
PB	polybutadiene
PS	polystyrene
PVC	poly(vinyl chloride)
PMMA	poly(methyl methacrylate)
PVA	poly(vinyl alcohol)

INTRODUCTION

Side-chain liquid crystalline polymers (SCLCPs) are recognized as attractive functional materials because of a number of potential applications in various high-tech fields, including microelectronics, optical data storage, and nonlinear optics (1, 2). Since the first demonstration of SCLCPs in late Eighties and, in particular, during the last decade, a considerable amount of research works has been dedicated to the synthesis of new SCLCPs and to the understanding of the ordered structures in these polymers. The purpose of the present study is to make a contribution to the findings of novel systems based on SCLCPs, and, when possible, to investigate the induction of the monodomain structure in the materials. Before describing the contents of the subsequent chapters in this thesis, we will make a brief introduction to some important concepts in order to set a proper background for our studies.

SCLCPs are generally built up with three basic structural components: polymer backbone, mesogenic unit, which is the liquid crystal forming component, and flexible spacer, usually a short aliphatic chain (two to six CH_2 units). Unlike main-chain liquid crystalline polymers, in SCLCPs the rigid, rod-like mesogenic groups are linked to polymer main chain as pendent groups through the flexible spacer. The basic structure of SCLCPs is shown in *Figure 1*.

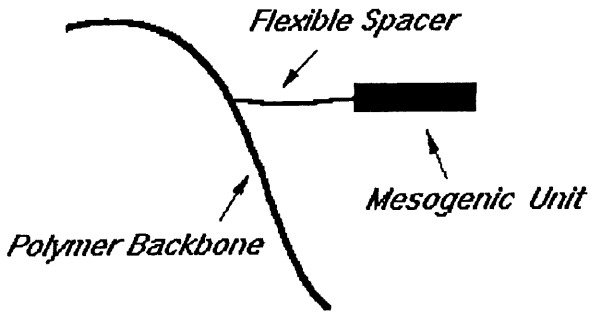

Figure 1. Schematic representation of the components of SCLCPs.

In the liquid crystal phases, these individual components have opposing tendencies. The polymer chains are entropically driven to a random coil type conformation, while the mesogenic units stabilize with long range orientational ordering. As individual units, the polymer chains and the mesogenic units would phase separate. However, the inherent chemical connectivity of the side-chain system inhibits this. As a result, there is a coupling of the behavior of the polymer chain and the mesogenic units. Now, it is known that the key to making SCLCPs is the incorporation of the flexible spacer between the mesogenic group and its attachment point to the backbone. With the spacer, the rigid groups can be sufficiently de-coupled from the perturbing influence of the backbone to pack as a mesophase. However, whatever length of the flexible spacer, coupling effects always exist and their effects may be strong or weak. This is why the SCLCPs with different length of flexible spacers have different liquid crystalline (LC) phases.

Because of the opposing influences of entropically disordered polymer chain conformation and the long range orientation ordering of the mesogenic units as mentioned above, SCLCPs exhibit a rich phase behaviours (1-3) which could be an isotropic, nematic, smectic, re-entrant nematic phase and a glass state. Generally, when SCLCPs are cooled from the isotropic state, the mesogenic groups can form a nematic phase, possessing long range orientational order along a direction called director (2). Upon further cooling, a smectic phase, in which there is not only an orientational order but also a positional order with a layered structure, could be formed. In this phase, there are two most common layered structures: smectic A and smectic C. In a smectic A phase, the director, **n**, lies along the layer normal, but in a smectic C phase, the director of each layer is inclined at an angle to the layer normal, this angle being identical for all layers. *Figure 2* shows the molecular arrangements in a nematic, a smectic A and a smectic C phase. On decreasing the temperature below the smectic phase, the re-entrant nematic phase appears for some SCLCPs. At last, the SCLCPs will stay in the glass state at lower temperature. In the three LC phases as mentioned above, some SCLCPs only has a

nematic phase (3-5); some of them presents both a nematic and a smectic phase (3-5); and a few of them possesses all three LC phases (3).

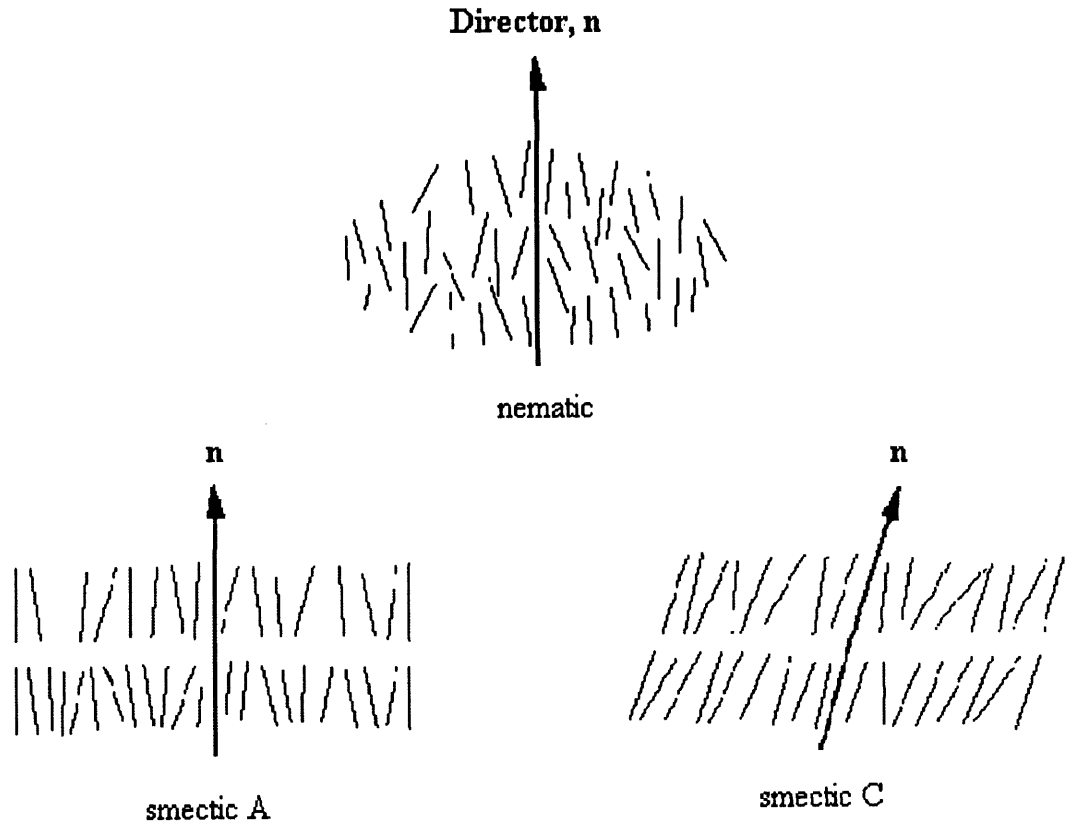

Figure 2. Schematic representation of the molecular arrangements in some LC phases.

LC phases are intrinsically oriented microstructures, i.e., the orientational order of the mesogenic groups exists in local LC domains, whose directors are randomly aligned. In other words, a SCLCP sample, such as a solution-cast film, is isotropic over a macroscopic scale, and does not have anisotropic properties. This is the so-called polydomain structure, as schematically depicted in *Figure 3.* When a polydomain-sample is subjected to the effects of an external field, including magnetic, electric, surface and mechanical field, an alignment of the LC domains can be induced, leading to a uniform orientation of the mesogenic groups along a reference direction throughout the sample. This resulting ordered structure is termed

monodomain structure. The transition from a polydomain to a monodomain as a result of a mechanical stretching is schematically shown in *Figure 3*.

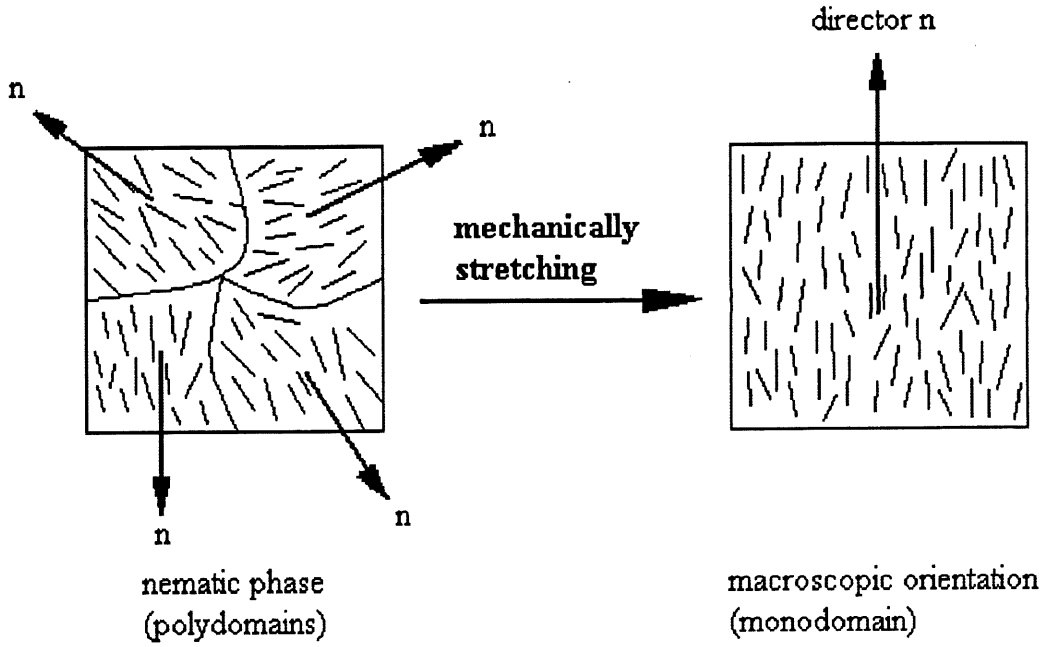

Figure 3. Schematic representation of a transition from polydomain to a monodomain and induced macroscopic orientation of mesogenic groups in nematic phase of SCLCPs.

From the technological point of view, the induction, control and manipulation of such a monodomain structure is of crucial importance because having a monodomain structure is a prerequisite for all main applications of SCLCPs. To this regard, it is of great interest to develop new SCLCPs whose monodomain structure can easily be achieved and controlled.

With the research and development of the liquid crystalline polymer (LCP) materials, a large number of SCLCPs, mostly based on poly(meth)acrylates and polysiloxanes, has been prepared. In the past several years, much effort has been made to explore new LC polymeric systems. The pertinent examples are the studies on the LC block and graft copolymers (6-8) which combine the LC order with immiscibility-induced microphase separation conferred on

block and graft copolymers, and on the ion-containing SCLCPs which display mesophases where the ionic aggregates, characteristic of the ionomers, are present (9). Another system showing a great potential is the side-chain liquid crystalline elastomers (SCLCEs) (10-12) prepared by cross-linking SCLCPs. SCLCEs are attracting more and more attention since they allow a macroscopic and uniform orientation of the mesogenic groups to be achieved and controlled by a mechanical stretching.

In view of the great interest of developing new LC functional materials, in the present study we have prepared and studied two novel systems based on SCLCPs. One is termed interpenetrating liquid crystalline polymer networks (ILCPNs) (13). The concept of interpenetrating polymer networks (IPNs) is well known, and a considerable amount of studies on conventional polymers were reported (14). We are the first to extend the concept to LCPs. Here, an ILCPN is a combination of two liquid crystalline elastomers, or simply two LCPs in network forms, whose networks are physically interlocked. Since phase separation in IPNs might be restricted to different extents by the cross-links, ILCPNs could offer new possibilities of making specialty materials with finely divided phases or a dual phase continuity which generally cannot be achieved by mixing two LCPs because of the immiscibility. The other novel system is a graft copolymer with a SCLCP component grafted on a styrene-butadiene-styrene (SBS) triblock copolymer (15). This graft copolymer system, which could have a SCLCP content of as much as 52 wt%, exhibits very interesting and improved properties as compared to the SBS/SCLCP blends, such as a homogeneous morphology and higher mechanical strength. As also will be shown in this thesis, a uniform macroscopic orientation of the mesogenic groups of the SCLCP component in such graft copolymers can easily be induced by stretching their elastic films and, more interestingly, the monodomain structure can almost be totally preserved in a relaxed free standing film after a special thermal treatment process.

The whole research work described in this thesis includes two parts. The first part consists in synthesis and characterization of two new SCLCP-based systems, i.e., the interpenetrating networks and the graft copolymers as briefly mentioned above, and the orientation induction of the graft copolymers. The second part is composed of two separate projects of physical studies of SCLCPs. In one, we have investigated the alignment of nematic domains of a series of ion-containing SCLCPs, namely LC ionomers, under the effect of a mechanical stretching. In the other project we have studied relaxation phenomena for a stretched SCLCP heating to the vicinity of its phase transitions under strain. The presentation of those studies is organized as follows.

Chapter 1 describes the synthesis and characterization of sequential ILCPNs prepared through 1) the combination of two covalent networks, and 2) the combination of a non-covalent and a covalent network. Chapter 2 discusses our research on the graft copolymers, including the synthesis, characterization and orientation induction. Chapter 3 presents the results of the orientation studies on LC ionomers, while Chapter 4 is dedicated to the thermally-induced relaxation and reorientation behavior of stretched SCLCPs. Finally, a general conclusion is given. Throughout this study, the characterization of the samples was carried out with several techniques. These are Fourier-transform infrared (FTIR) spectroscopy (on a Bomen MB-102 FTIR), differential scanning calorimetry (DSC) (on a Perkin-Elmer DSC-7), optical polarizing microscopy (on a Leitz DMP microscope equipped with an Instec hot stage), and, when necessary, gel permeation chromatography (GPC) and nuclear magnetic resonance (NMR) spectroscopy. The measurements of the molecular orientation, in terms of the orientation parameter, were performed through infrared dichroism. More details relative to each project will be given in the respective chapter.

CHAPTER 1

SYNTHESIS AND CHARACTERIZATION OF INTERPENETRATING LIQUID CRYSTALLINE POLYMER NETWORKS

1.1 Background

Interpenetrating polymer networks (IPNs) (14) are defined as a combination of two polymers in network form, at least one of which is synthesized or cross-linked in the immediate presence of the other. IPNs exhibit varying degrees of phase separation, dependent principally on the compatibility of the polymers. With highly incompatible polymers, their phase separation occurs strongly. In cases where the polymers are more compatible, phase separation can be almost completely circumvented. In many ways, IPNs are related closely to block copolymers. In the block copolymer systems, the length of the block determines the size of the domains. Correspondingly, the cross-link level (length of chain between cross-links) plays a major role in determining the domain size of IPNs. Short block or chain segments between cross-links both make for small domains under many conditions. IPNs represent one of the fastest growing fields in polymer science. Although most of these materials are phase separated, the presence of cross-links reduces the phase domain size and provides a method of controlling properties.

IPNs can be made in many different ways. According to the used different synthesis method they can be classified as several types, among which the most important are sequential and simultaneous IPNs. A sequential IPN is prepared by the following procedure: polymer network-1 is made and swollen in the monomer II plus cross-linker, and then the monomer II is polymerized *in-situ* (see *Figure 4*). A simultaneous interpenetrating network is obtained by

polymerization simultaneously in a mixture containing both monomers (or pre-polymers) plus cross-linkers.

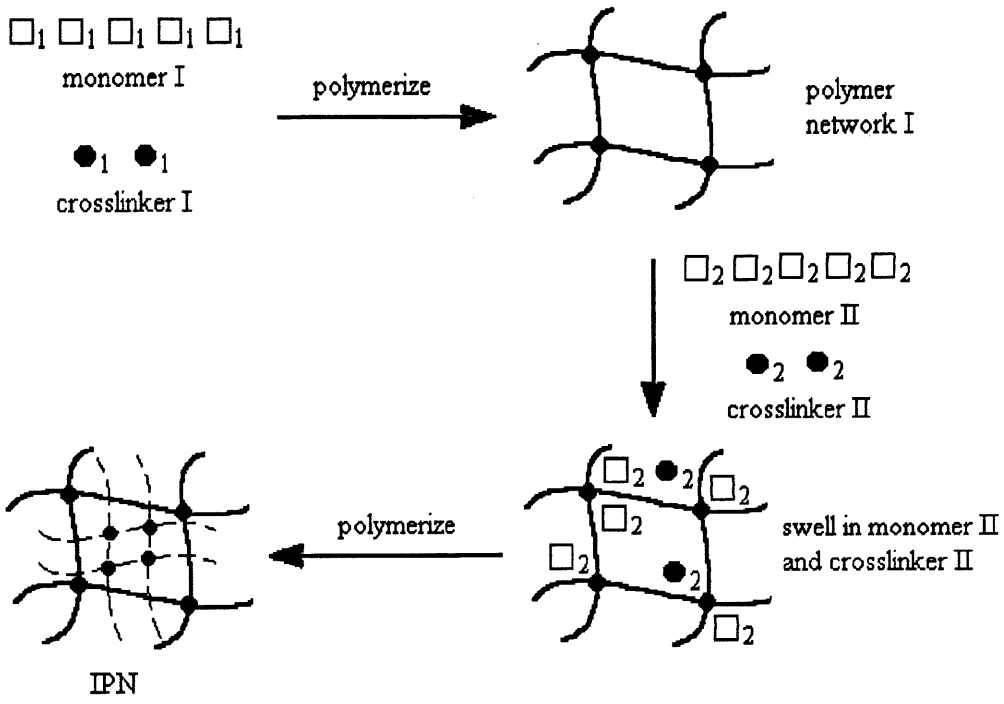

Figure 4. Basic synthesis method for sequential IPNs.

On the basis of the extensive investigations on IPNs formed from conventional non-liquid crystalline polymers, it has become clear for us to extend the concept of interpenetrating networks to SCLCPs could bring new perspectives for the development of SCLCP-based functional materials. Among the continuously increasing research activities on SCLCPs, the greatest effort is still being made for the preparation of new polymers which, hopefully, would find applications or meet the requirements for the development of specific electrooptic devices. These studies essentially involve new synthesis and characterization methods, with the synthesis methods often becoming more and more complicated. We think that it is of great interest to develop novel and efficient approaches to make new SCLCP-based materials. We believe LC-IPNs represents such an approach that needs to be explored. There is a

considerable number of studies dedicated to polymer blends. The reason is that blending two or more polymers is an important way of making new materials. Now, it is well recognized that not only miscible blends but immiscible, phase-separated blends with controlled morphology can be valuable industrial materials. In the case of SCLCPs, and for polymer liquid crystals in general, few, if any, of them are miscible. Actually, the miscibility within mesophases is still more difficult to achieve as a result of the additional long range ordering as compared to conventional polymers (16). This means that blending two SCLCPs essentially leads to no useful materials because of the severe phase separation with uncontrollable morphology. As already mentioned, interpenetrating two cross-linked conventional polymers is known as an effective way of restricting the phase separation by the cross-links, which often can result in microphases (tens of nanometers in size) like in block copolymers, or two continuous phases - a desirable morphology, or even the miscibility with one single phase for the otherwise immiscible components (17); the interest of extending the concept of interpenetrating networks to SCLCPs is obvious. Basically, an interpenetrating liquid crystalline polymer networks (ILCPNs) makes it possible to combine or to bring together intimately several SCLCPs. The potential of making new materials from ILCPNs is due to the fact that they offer a broad spectrum of structural possibilities with varying degrees of miscibility and changing interfaces. There are two basic beneficial situations that can be expected. If the miscibility is induced between two SCLCPs, changes in their mesophase behavior, such as enhanced phase stability and induction of new mesophases, could be observed. On the other hand, if no miscibility is induced but the phase-separated system has a controlled interface and morphology, the resulting stable ILCPNs as a single material could combine the features of two SCLCPs. The latter situation is as desirable as the former since it can produce designed functional materials for which the two components should not be miscible. A nice example is given by a recent study on the design of efficient photodiodes: an interpenetrating network of two phase-separated semi-conducting polymers having different electron affinities and ionization potentials was prepared to allow for efficient dissociation of the absorption-created electron-hole pairs at the spatially distributed interfaces (18). In order

to illustrate the possibilities of LC-IPNs, we mention one example of designing this sort of special material. For a film, sandwiched by two electrodes, of LC-IPNs formed from two SCLCPs with different crossover frequencies at which the sign of their dielectric anisotropy ($\Delta\varepsilon$) changes, varying the frequency of the applied electric field can have the mesogens of both SCLCPs aligned perpendicular to the film plane ($\Delta\varepsilon>0$), or have the mesogens of SCLCP-1 aligned perpendicularly while those of SCLCP-2 oriented parallel in the film plane ($\Delta\varepsilon<0$), or have the mesogens of both SCLCPs oriented parallel in the film plane.

As the first step of the strategy, developed in this laboratory, of exploring SCLCP-based ILCPNs, the purpose of the present work is to study the feasibility of making sequential ILCPNs, through the preparation of samples containing two cross-linked polyacrylate-based SCLCPs, and demonstrate the possibility of modifying the mesophase transition behavior of the polymers (13). Details on the synthesis and characterization are given below.

1.2 Synthesis of ILCPNs

A series of sequential ILCPNs based on two side-chain liquid crystalline polyacrylates were prepared through the formation of network-2 inside a pre-formed network-1. The mesogenic and diacrylate monomers used in this study have the chemical structures shown below. It can be seen that monomer I and monomer II differ in the end group of the mesogenic moiety, OCH_3 for the former and CN for the latter. Monomers I and II were synthesized according to the methods in the literature (4), while monomer III was purchased from Aldrich.

Two types of the network-1 were used to prepare ILCPNs. The first type of network-1 was prepared by co-polymerizing monomer I (or II) with the diacrylate monomer III (cross-linker). The second type of network-1 was made through polymerization of monomer II, and

I 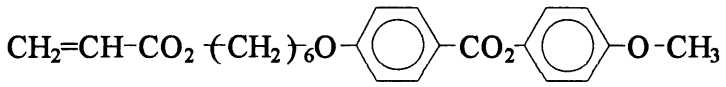

II 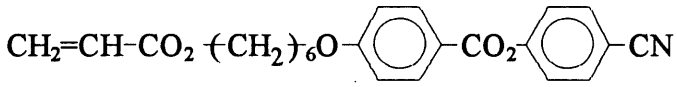

III 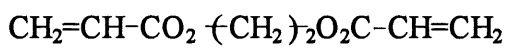

the resulting SCLCP was then partially hydrolyzed in a sodium hydroxide (NaOH) solution giving rise to ion-containing SCLCPs, called LC ionomer. The LC ionomers have a network structure because of the ionic aggregates which act as cross-links. Once the network-1 was obtained, the technique of making ILCPNs was the same, that is, after swelling monomer II (or I) and monomer III in a sample of network-1, the polymerization *in-situ* leads to network-2 interpenetrated with network-1. For the convenience of our discussion, the samples of ILCPNs prepared from the two types of network-1 will be referred to as 'ILCPNs with two covalent networks' and 'ILCPNs involving LC ionomers', respectively. Described below are the details of the preparation of ILCPNs.

1.2.1 ILCPNs with two covalent networks

The preparation was composed of two steps. First, a copolymerization of monomers I (or II) and III was performed in order to obtain the network-1. To do this, the following typical synthesis procedure was employed. A mixture of 1 g of monomer I, 0.0865 g of monomer III, which corresponds to 20 mol % of the monomers, and 1 mol % of azobisisobutyronitrile (AIBN) as the initiator was dissolved in 5 ml chlorobenzene. After a rigorous stirring and a purge with nitrogen, the solution was heated to 60 °C for 18 hours for the polymerization. After removal of the solvent, the precipitated cross-linked polymer was washed five times through swelling in tetrahydrofuran (THF) in order to extract any un-reacted monomers and un-cross-linked polymers. The collected sample was finally dried under vacuum at 60 °C for 2

days. The diacrylate monomer was freshly distilled (under a vacuum of about 0.5 mmHg at 60 °C) before the reaction. It is clear that the cross-linking level of the network is determined by the concentration of the diacrylate monomer. The network-1 sample of the above example will be denoted netOCH_3(20%). The acronym indicates that the sample is a cross-linked polymer prepared from monomer I (with the OCH_3 end unit) and the concentration of the cross-linker used is 20 mol %.

Other cross-linked networks were prepared in this study. Besides netOCH_3(20%), the samples of netOCH_3(10%) and netCN(10%) were utilized as the network-1 for the preparation of ILCPNs. To facilitate comparisons as will be discussed later, other single networks from monomer II, such as netCN(20%), as well as the un-cross-linked homopolymers from monomers I and II, denoted PolyOCH_3 and PolyCN respectively, were also prepared.

After obtaining the network-1, the ILCPNs could be prepared through the following procedure. As a typical example, one piece of the netOCH_3(20%) sample of 62 mg was immersed in 1 ml of a chlorobenzene solution containing 200 mg of monomer II mixed with 10 mol % of monomer III and 1 mol % of AIBN, and swollen in a closed system at room temperature for overnight. Then, the swollen sample was separated from the remaining solution and placed into a small bottle. After circulating the nitrogen for 10 min, the bottle was sealed and placed into a thermostat oven at 60 °C for the second polymerization *in situ* for 20 hours. After the reaction, five consecutive extractions were carried out using THF as the solvent. For every extraction the solid sample remained in the solvent for at least 4 hours. The sample was finally dried in vacuum at 80 °C for two days. The obtained ILCPN sample of the above example is denoted netOCH_3(20%)-netCN(10%), where the monomer used for the network-2 and the concentration of the diacrylate monomer are indicated.

1.2.2 ILCPNs involving LC ionomers

In this case, the ionomers prepared from PolyCN were used as the network-1. The preparation of the PolyCN-based ionomers through a partial alkaline hydrolysis was demonstrated in this laboratory (9). As a typical example, the ionomer containing 5.3 mol % of the ionic groups was prepared through the following procedure: a 5 wt % PolyCN solution was prepared using a solvent mixture of N, N-Dimethylformamide (DMF)/methanol (95/5, v/v). The solution was stirred for overnight and then purged with nitrogen for 1 h before addition of freshly prepared NaOH solution (concentration : 0.05 mol L^{-1}). After the calculated amount of NaOH was added in order to abtain an ionomer containing 5.3 mol % of the ionic groups, the reaction was performed at room temperature for 24 h, and then the mixture was precipitated into cold ether at ca. -25 °C. The solid was collected and dried. All the ionomers used in this study contain less than 10 mol % of the ionic groups. However, with the presence of the ionic aggregates, they can only be solubilized in very strong polar solvents such as dimethyl sulphoxide (DMSO), and are no longer soluble in solvents like THF and toluene. The samples used as network-1 for the preparation of ILCPNs were netCNNa(2.5%), netCNNa(5.3%) and netCNNa(7.3%). From the acronym of the network-1, the sodium cation and the mole percentage of the COO^-Na^+ units are indicated. Obviously, the cross-link level is dependent on the content of the ionic groups. The determined structure of the ionomers (9) is shown below, and the cross-linking from the ionic aggregates is schematically depicted in *Figure 5*.

The preparation procedure for the resulting ILCPNs using the above LC ionomers as the network-1 is basically the same as described above, and will not be repeated here. As monomer II was always used for network-2, the general acronym for the resulting ILCPNs is netCNNa-netCN.

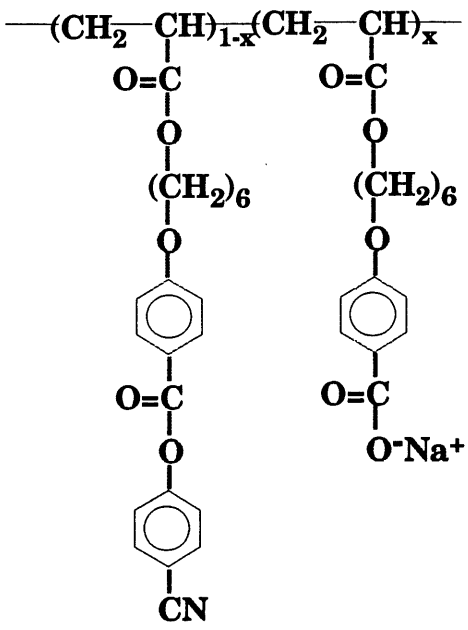

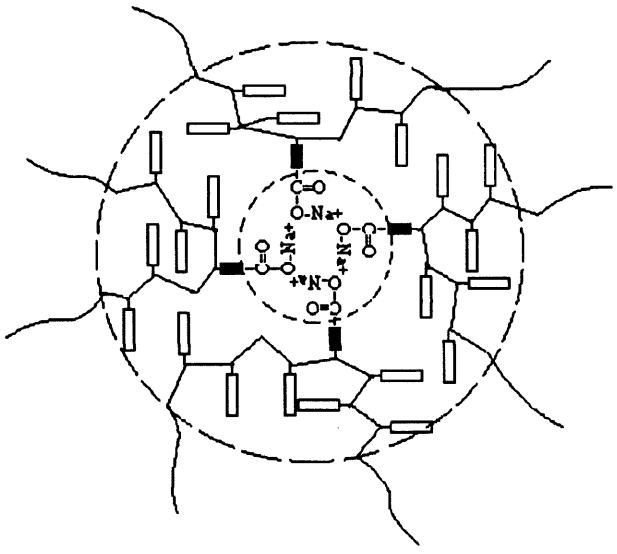

mesogenic group

side chain connected by ionic group

Figure 5. Schematic representation of the cross-linking from the ionic aggregates.

1.2.3 Factors which determine the success of the preparation of ILCPNs

Before discussing the characterization results, it should be mentioned that a number of unsuccessful attempts of preparing ILCPNs was made. From these synthesis experiences, several factors were found to be very important for obtaining ILCPNs successfully and should be considered carefully.

The first factor is the monomer concentration of the solution in which the network-1 was swollen by the mesogenic monomer with the solvent for subsequent polymerization to form the network-2 and get ILCPNs. In contrast to the preparation of a conventional sequential IPN, for which the monomer swollen into the first network for subsequent polymerization is generally a liquid, but in the present case the mesogenic monomer is a solid and must be dissolved in a solvent before being swollen into the network-I and polymerized. The monomer concentration should be high enough to expect a significant amount of the network-2 in the resulting ILCPN, but should not be too high because the monomer molecules must be kept in a mobile liquid phase during the polymerization. A number of attempts of polymerizing ILCPNs shows that the range of monomer concentration was available from 10% to 20%, but the 20% monomer concentration was found to be the most appropriate.

The second factor is the choice of the solvent for subsequent polymerization to form the network-2. Because of the solvent evaporation as the polymerization processes, the reaction temperature and the choice of the solvent affect the results. The slower the speed of the solvent evaporation, the more favored the reaction of forming network-2. For this reason, although toluene is used as a common good solvent for the synthesis of polyacrylate, chlorobenzene is a better solvent than toluene in this polymerization because of its higher boiling point (132 °C).

The third factor is the reaction temperature which determines the rate of polymerization inside the swollen samples. Although we do not know precisely how the cross-link level of network-2 changed with the advancement of the polymerization, it was likely that with a slow rate of polymerization a certain time was needed to reach an effective cross-link level that was necessary to ensure gelation or physical interlocking between the two networks. As is known for IPNs, phase separation tends to occur once the second polymer is formed. If the polymerization *in situ* is not fast enough the early-formed linear and slightly cross-linked polymer chains could be phase-separated and extracted in the purification process; and in the meantime, the swollen sample becomes drier and drier, which prevents the polymerization from occurring at later time. This seems to explain some unsuccessful experiments by swelling a network-1 sample in a 10% (or less) monomer solution and using a lower reaction temperature of 55°C. 60°C was a better reaction temperature in preparing ILCPNs.

The fourth factor is also crucial. It is the size of the network-1 sample for subsequent polymerization. Under the same conditions and with the same weight of the network-1 sample, e.g. 0.2 gram, it was necessary to have a single or a couple of big pieces which led to successful preparation of ILCPNs, while the attempts starting with fine granules (ca. <1 mm) for swelling and polymerization ended in failure, or resulted in ILCPNs containing only a very small amount of the network-2. This observation can be explained by a different evaporation rate of the solvent once the polymerization *in-situ* starts. The solvent evaporates much more rapidly with small swollen granules of the network-1 because of a much larger surface; consequently the swollen sample loses most solvent and is dried shortly after being placed in the oven, and no effective polymerization *in-situ* occurs.

Finally, the choice of the polymer as network-1 merits to be mentioned here. From a number of attempts of making ILCPN samples, it was found that the samples of netOCH_3 with different cross-linked levels were mostly suitable for the network-1 since they could absorb a larger volume of the monomer II solution than the samples of netCN which absorb the

monomer I solution, making it possible to obtain ILCPNs of netOCH$_3$–netCN containing a large amount of netCN. This result was confirmed by comparing the sample of netOCH$_3$(10%)-netCN(20%) with netCN(10%)–netOCH$_3$(20%), the former containing ca. 56 wt% netCN(20%) and the latter only having 23 wt% netOCH$_3$(20%) (see *Table 1*).

1.3 Characterization of ILCPNs

In this section, the characterization of all synthesized ILCPN samples was described. The compositions of ILCPNs were determined by using the FT-IR spectroscopy. All infrared spectra were recorded at a resolution of 4 cm^{-1} and from a total of 100 interferograms for each spectrum. The phase transition behaviors of ILCPNs were investigated by using DSC with a heating rate of 10 °C/min and a sample weight of ca. 20 mg. All presented thermograms are from the second heating scan of the respective sample.

1.3.1 Determination of the compositions of ILCPNs samples

According to the preparation method, if the second polymerization *in-situ* did not result in a cross-linked polymer, i.e., the network-2, the repeated extraction would remove the second SCLCP component. Simple calculations based on the change in the weight of the sample allowed us to estimate the composition of the resulting ILCPNs, because subtracting the initial network-1 weight from the weight of the ILCPNs yielded the weight of the network-2 present in the sample. Nevertheless, in order to confirm the results obtained from the weight of the sample, we used infrared spectroscopy to determine the compositions of all obtained ILCPNs.

For all the ILCPNs with two covalent networks, netOCH$_3$–netCN or netCN–netOCH$_3$, the presence of netCN is revealed by the characteristic –CN infrared band at 2230 cm^{-1} which is absent for netOCH$_3$, and the content of netCN can easily be calculated from the absorbance of the 2230 cm^{-1} band ($A_{.CN}$) relative to the absorbance of –C=O band at 1734 cm^{-1} ($A_{.C=O}$) which

is contributed by both components. To do that, we prepared a series of blend samples with different known compositions of two un-cross-linked polymers prepared from monomer I and monomer II, i.e., PolyOCH$_3$ and PolyCN, and measured the absorbance ratio of A_{-CN} to $A_{-C=O}$ from the infrared spectra of all the blends, which are shown in *Figure 6* for the region of 1450-2320 cm^{-1} .

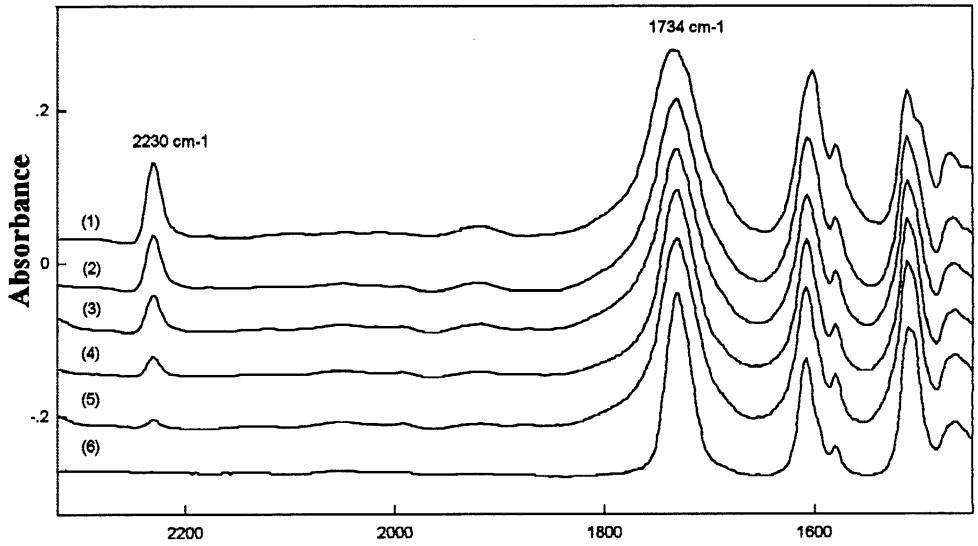

Figure 6. Infrared spectra of PolyOCH$_3$, PolyCN and their blend samples. (1) PolyCN, (2) PolyOCH$_3$/PolyCN, 30/70, (3) PolyOCH$_3$/PolyCN, 50/50, (4) PolyOCH$_3$/PolyCN, 70/30, (5) PolyOCH$_3$/PolyCN, 90/10 and (6) PolyOCH$_3$

Plotting the content of PolyCN in the blend as a function of the absorbance ratio $A_{CN}/A_{C=O}$ yielded a straight line as shown in *Figure 7*. The curve fit equation is expressed as follows:

$$(PolyCN)\% = 764.2 \times \frac{A_{-CN}}{A_{-C=O}} \qquad [1.1]$$

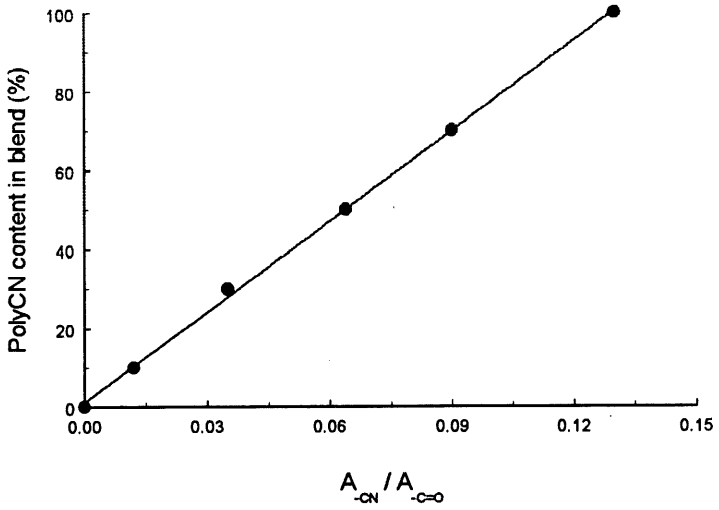

Figure 7. Content of PolyCN in the PolyCN/PolyOCH$_3$ blend vs the absorbance ratio of $A_{-CN}/A_{-C=O}$.

This equation is used to determine the content of netCN in the ILCPNs samples. The results obtained from the infrared analysis and from the weight calculation are listed in *Table 2-1*. It can be seen that both methods indicate similar compositions.

Table 1. Composition of ILCPNs with two covalent networks

Sample	The contents of the network-2 (%)	
	by I.R.	by weight
netOCH$_3$(20%)–netCN(20%)	49	50
netOCH$_3$(20%)–netCN(10%)	52	51
netOCH$_3$(10%)–netCN(20%)	56	58
netCN(10%)–netOCH$_3$(20%)	23	22

In the case of the ILCPNs involving LC ionomers, i.e., netCNNa–netCN, the infrared analysis could not be made in the same way as described above, since both network components have the CN absorption. However, it was found that a new band at 770 cm^{-1}, shifted from the 762 cm^{-1} band, was induced by the sodium salt group ($-COO^-Na^+$) in the ionomers and was sensitive to its concentration. This can easily be noticed from the infrared spectra of the ionomers used as network-1 and the non-ionic PolyCN presented in *Figure 8*.

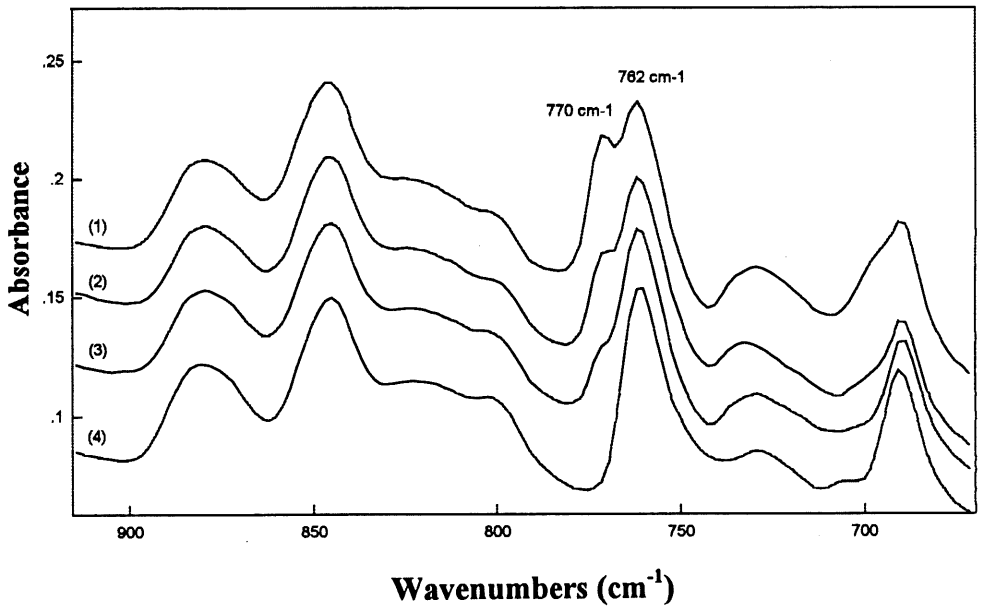

Figure 8. Infrared spectra of PolyCN and its ionomers: (1) netCNNa(7.3%), (2) netCNNa(5.3%), (3) netCNNa(2.5%) and (4) PolyCN.

Now, the presence of netCN in the ILCPNs samples of netCNNa–netCN corresponds to a dilution of the ionic groups and should be reflected by the 770 cm^{-1} band with respect to the 762 cm^{-1} band. *Figure 9* gives an example of the infrared spectra in this region for a pure ionomer, netCNNa(5.3%), the ILCPNs sample of netCNNa(5.3%)–netCN(20%) and the pure netCN(20%).

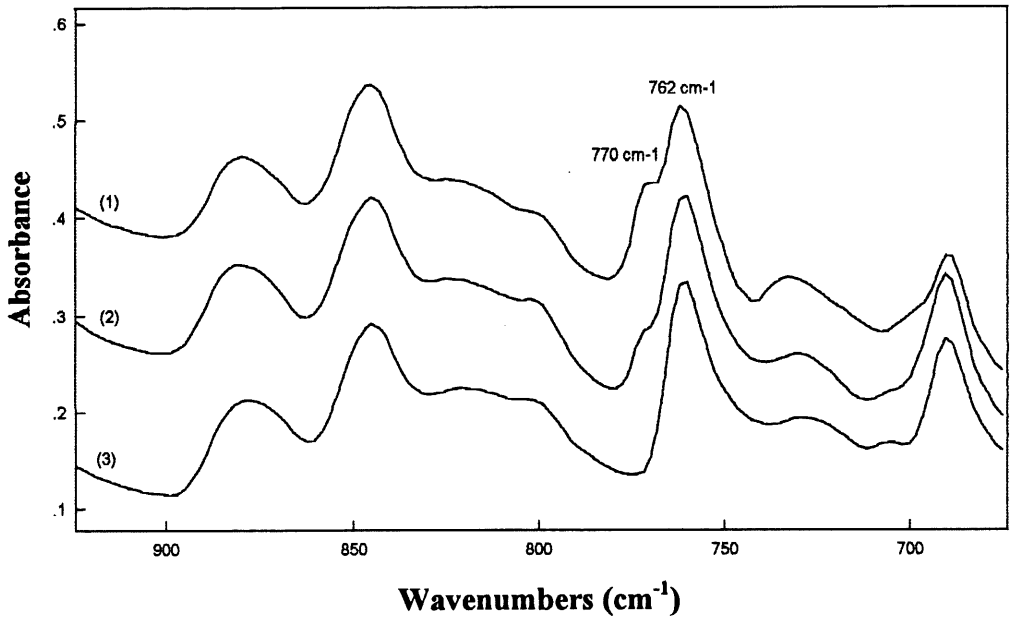

Figure 9. Infrared spectra of (1) netCNNa(5.3%), (2) netCNNa(5.3%)-netCN(20%) and (3) netCN(20%).

It is clear that the intensity of the 770 cm^{-1} band in netCNNa(5.3%)–netCN(20%) sample is decreased as compared to netCNNa(5.3%) because of the dilution by netCN(20%), while the pure netCN(20%) sample has no ionic groups and shows no band at 770 cm^{-1}. Actually, on the basis of the LC ionomers having different contents of the ionic groups, it was found that the ratio of the absorbances of the 770 cm^{-1} band (A_{770}) to the 762 cm^{-1} band (A_{762}) was linearly proportional to the concentration of the ionic groups, and this allowed the content of netCN in the ILCPNs to be estimated. The calibration line by plotting the content of sodium salt COO^-Na^+ % as a function of A_{770}/A_{762} is shown in *Figure 10*. The obtained curve fit equation is expressed as follow:

$$(-COO^-Na^+)\% = 10.8 \times \frac{A_{770}}{A_{762}} \qquad [1.2]$$

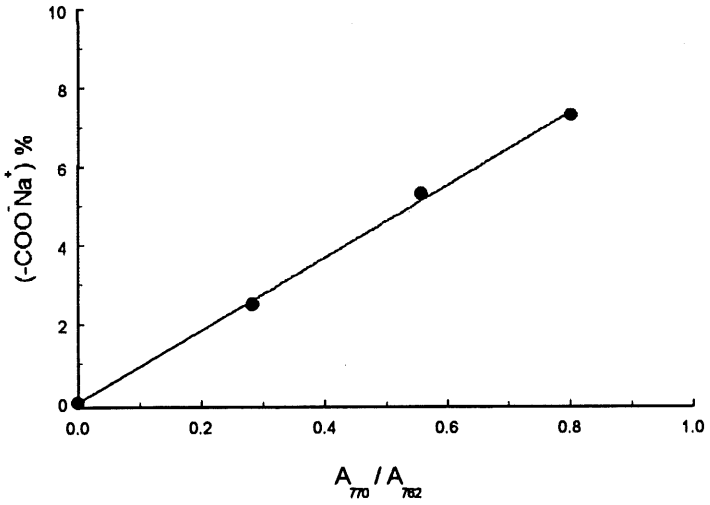

Figure 10. Linear reference curve of $-COO^-Na^+$ content as a function of A_{770}/A_{762}.

From this equation, the contents of the sodium salt for the netCNNa-netCN samples were calculated and compared with that of the pure netCNNa before the presence of the network-2. The composition of ILCPNs involving LC ionomers can thus be determined and are shown in *Table 2*, which are also confirmed by the weight calculation. For example, A_{770}/A_{762} of netCNNa(5.3%)-netCN(20%) is 0.315, and a sodium salt content of 3.4% is obtained. So the content of netCNNa is (3.4/5.3) × 100 = 64% and that of netCN thus is 36%.

Table 2. Composition of ILCPNs involving LC ionomers

Sample	The contents of the network-2 (%)	
	by I.R.	by weight
netCNNa(7.3%)–netCN(20%)	28	30
netCNNa(5.3%)–netCN(20%)	36	37
netCNNa(2.5%)–netCN(20%)	25	27

1.3.2 Phase transitions of ILCPNs

The phase transition behavior of all samples was investigated by means of DSC. Summarized in *Table 3* are the obtained data on the glass transition temperature (T_g), the smectic-nematic transition temperature (T_{sn}), its transition enthalpy (ΔH_{sn}), the nematic-isotropic transition temperature (T_{ni}) and the transition enthalpy (ΔH_{ni}).

First of all, some observations can be made on the single covalent networks as well as the ionomers based on the data in *Table 3*. Taking PolyOCH$_3$ for example. It displays a smectic and a nematic phase with a T_g at 25 °C, a T_{sn} at 94 °C, and a T_{ni} at 119 °C. Its networks, netOCH$_3$(10%) and netOCH$_3$(20%), still exhibit both liquid crystalline phases, but the transition temperatures and enthalpies are severely modified as a result of the presence of the covalent cross-links. Indeed, both T_{sn} and T_{ni} are shifted to lower temperatures, and the transition enthalpies are lowered. The effects become more important as the cross-link level increases. On the other hand, T_g of the networks increases with the cross-linking. Similar observations can be made for PolyCN and its networks, netCN(10%) and netCN(20%). In the case PolyCN-based ionomers, the increase in the content of the ionic groups, which corresponds to an increase in the number of the ionic aggregates and thus the cross-link level, also leads to a depression of the transition temperature; while T_g of the ionomers show a very slight decrease as compared to PolyCN. The disturbing effects of the cross-links leading to the decrease in the mesophase transition temperatures are well known, so is the effect of raising T_g by the covalent cross-links. The slight decrease in T_g for the ionomers can be explained in the following way. Generally, for the conventional ionomers, it is known that T_g of ionomers will rise significantly by the presence of ionic aggregates as compared to the corresponding polymer. But here the another effect due to the ionic interactions is that the partial hydrolysis reaction gives rise to a cleavage of some bulky, mesogenic groups, and the resulting smaller groups should have an effect of reducing the T_g of the polymer. Because of predomination of the latter effect the results lead to a decrease in T_g of ionomers.

Table 3. Phase transition temperatures and enthalpies of the samples.

Sample Name	T_g (°C)	T_{sn} (°C)	T_{ni} (°C)	ΔH_{sn} (J/g)	ΔH_{ni} (J/g)
PolyOCH$_3$	25	94	119	2.67	2.08
netOCH$_3$(10%)	32	80	111	2.11	1.99
netOCH$_3$(20%)	34	69	102	0.74	1.13
PolyCN	30		125		0.92
netCN(10%)	34		113		0.80
netCN(20%)	43		100		0.71
netOCH$_3$(10%)–netCN(20%)	39	79	109	0.38	1.02
netOCH$_3$(20%)–netCN(10%)	35	68	106	0.14	1.06
netOCH$_3$(20%)–netCN(20%)	37	69	104	0.26	0.48
netCN(10%)–netOCH$_3$(20%)	37	---	115	---	1.37
netCNNa(2.5%)	28		107		0.94
netCNNa(5.3%)	27		90		0.83
netCNNa(7.3%)	24		71		0.80
netCNNa(2.5%)–netCN(20%)	33		110		0.93
netCNNa(5.3%)–netCN(20%)	35		110		0.84
netCNNa(7.3%)–netCN(20%)	26		76		0.80

1.3.2.1 ILCPNs with two covalent networks

We expect to obtain ILCPNs with two interpenetrated cross-linked SCLCPs. If this is the case, small or even microphases should be induced with a large interfacial region. In other words, more mesogenic groups belonging to the two SCLCP components could be brought into an intimate contact, resulting in a certain extent of miscibility. In principle, this can be reflected in the mesophase transitions of the ILCPNs as compared to the respective single networks. In order to reveal the features of ILCPNs, we first prepared and investigated PolyOCH$_3$/PolyCN blend samples. *Figure 11* shows the DSC heating curves for PolyCN, PolyOCH$_3$ and their 50/50 blend.

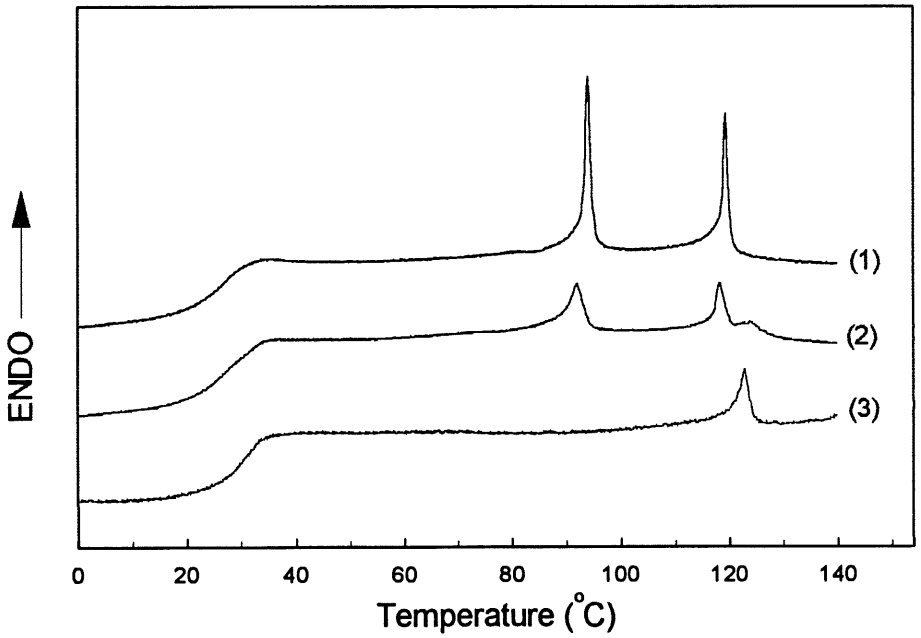

Figure 11. DSC heating curves of (1) PolyOCH$_3$, (2) PolyOCH$_3$/PolyCN 50/50 blend and (3) PolyCN.

The DSC curves of the blends are a simple addition of the curves of PolyOCH$_3$ and PolyCN. The first two peaks centered at 94 and 119 °C are due to, respectively, the smectic-nematic

and nematic-isotropic transition of PolyOCH$_3$, while the peak at 122 °C characterizes the nematic-isotropic transition of PolyCN. *Figure 12* shows a polarizing photomicrograph of 50/50 blend at 80 °C. Two distinct liquid crystalline textures are clearly seen in the phase-separated blend; the PolyCN phase exhibits a threaded nematic texture, whereas the smectic PolyOCH$_3$ displays a Schlieren texture with four brushes. The sizes of the two phases are of the order of 50 μm.

Figure 12. Polarizing optical micrograph of the 50/50 blend of PolyOCH$_3$ and PolyCN at 80 °C. Magnification: 170×.

Now, we compare the results for ILCPNs and their respective single networks. First, an interesting feature of ILCPNs can be revealed by comparing netOCH$_3$(20%)-netCN(10%) with netOCH$_3$(20%) and netCN(10%), the two corresponding to pure polymer networks. Their DSC curves are displayed in *Figure 13*. As compared with the un-cross-linked polymers, netOCH$_3$(20%) (curve 1) still exhibits both transitions, but as expected, owing to the cross-linking effects, both T_{sn} and T_{ni} are shifted to lower temperatures, with T_{sn} = 69 °C and T_{ni} = 102 °C, and the transition peaks are broadened and the transition enthalpies lowered, whereas its T_g increases to 34 °C. The same observation can be made for netCN(10%) (curve 3) which has a T_{ni} lowered to 113 °C. Now, for the ILCPN sample, netOCH$_3$(20%)-netCN(10%) containing 52 wt% of netCN(10%) (curve 2), its T_g is almost unchanged with

respect to both pure networks, but only a very weak low-temperature transition seems to persist at temperatures around 68 °C, and the drastic decrease of the transition enthalpy from 0.74 J/g for netOCH_3(20%) to the estimated 0.14 J/g for the ILCPN sample obviously cannot be accounted for only by the dilution effect arising from the presence of netCN which has no smectic phase. This result clearly indicates much interaction between the mesogenic side groups of both networks which leads to a severe perturbation effect on the smectic ordering of netOCH_3(20%). More interesting is the nematic-isotropic transition peak of the ILCPN sample which appears at 106 °C that is intermediate between T_{ni} of netOCH_3(20%) and that of netCN, i.e., 4 °C higher than the former and 7 °C lower than the latter. This change of the nematic-isotropic transition implies a single nematic phase formed by both mesogenic groups, or two nematic phases whose T_{ni}'s approach each other. In one way or another, this can only result from an intimate interlocking of both networks in the ILCPN sample.

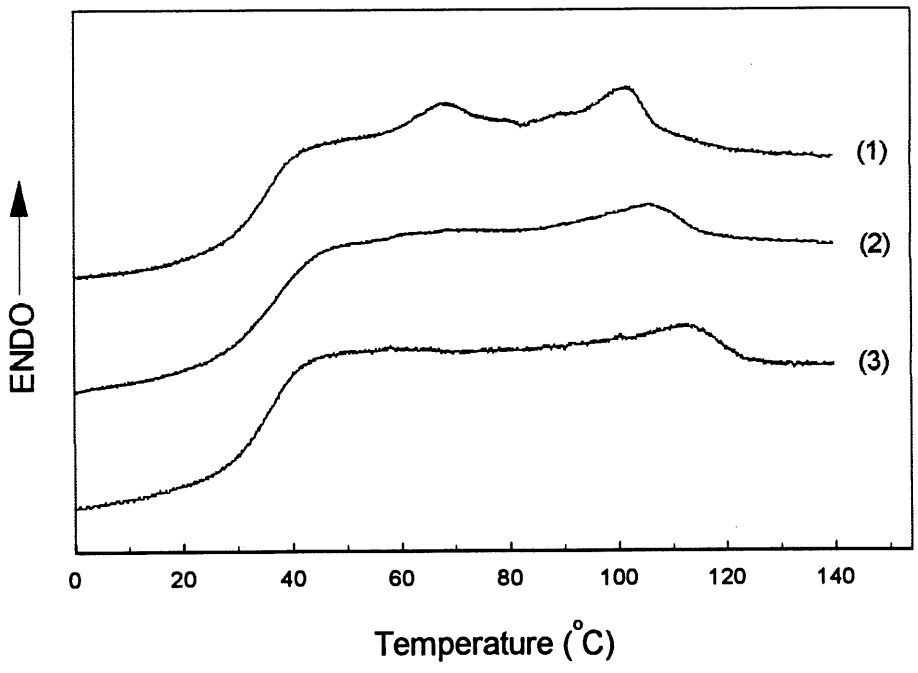

Figure 13. DSC heating curves of (1) netOCH_3(20%), (2) netOCH_3(20%)-netCN(10%) and (3) netCN(10%).

Strong effects were also observed for netOCH$_3$(20%)-netCN(20%), an ILCPN having a higher network-2 density. *Figure 14* shows the heating DSC curves of netOCH$_3$(20%)-netCN(20%) with its corresponding two pure networks, netOCH$_3$(20%) and netCN(20%). This ILCPN sample, containing 49 wt% of netCN(20%), has a T_g of 37 °C which is 3 °C higher than T_g of the netOCH$_3$(20%) and 6 °C lower than that of the netCN(20%). The smectic-nematic transition peak of netOCH$_3$ (20%) was severely weakened in the ILCPN sample. Interestingly, it is the apparently single nematic-isotropic transition peak which is higher than the transitions in both pure networks.

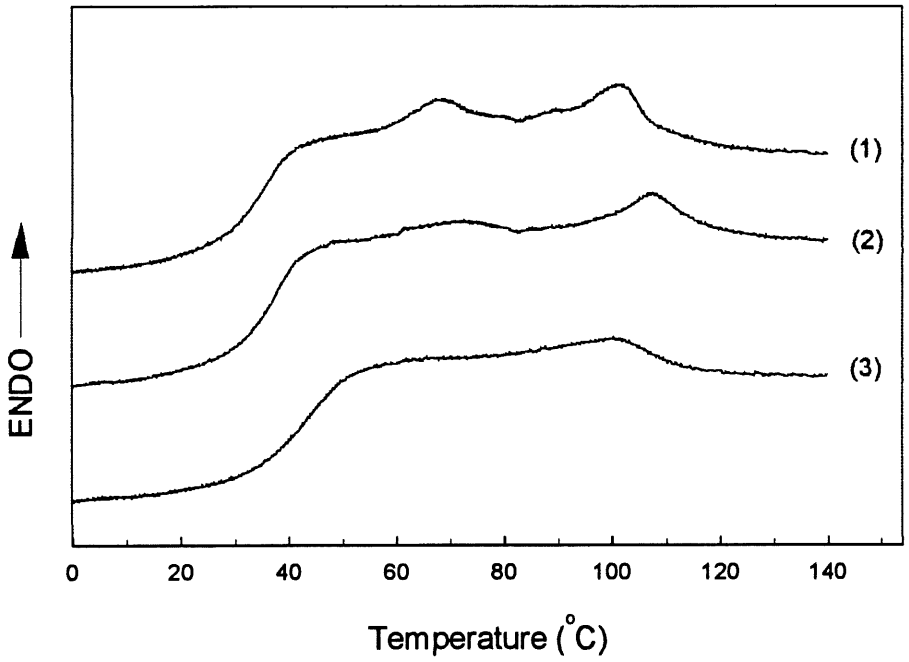

Figure 14. DSC heating curves of (1) netOCH$_3$(20%), (2) netOCH$_3$(20%)-netCN(20%) and (3) netCN(20%).

Investigations on the conventional IPNs (14) indicate that the domain sizes of IPNs are mostly determined by the cross-link levels, especially that of network-1. *Figure 15* displays the DSC curves of ILCPN, netOCH$_3$(10%)-netCN(20%) having a lower cross-link level of network-1, and its corresponding two pure networks, the netOCH$_3$(10%) and netCN(20%). Comparing

netOCH$_3$(10%)-netCN(20%) with netOCH$_3$(10%) and netCN(20%) reveals another solution. Although the apparent low-temperature transition of ILCPN, appearing at 79 °C, is also severely weakened, which indicates a strong interlocking of the two networks, some significant difference can be noted. The glass transition region is broadened, and the nematic-isotropic transition peak clearly is composed of two superimposed peaks at around 109 and 98 °C, respectively. They apparently correspond to the peaks of the two pure networks. All this indicates a lesser miscibility between the two components in this sample, which should result in larger domain sizes. This is likely to be due to the lower cross-link level of network-1 which restricts less efficiently the phase separation during the polymerization *in-situ*.

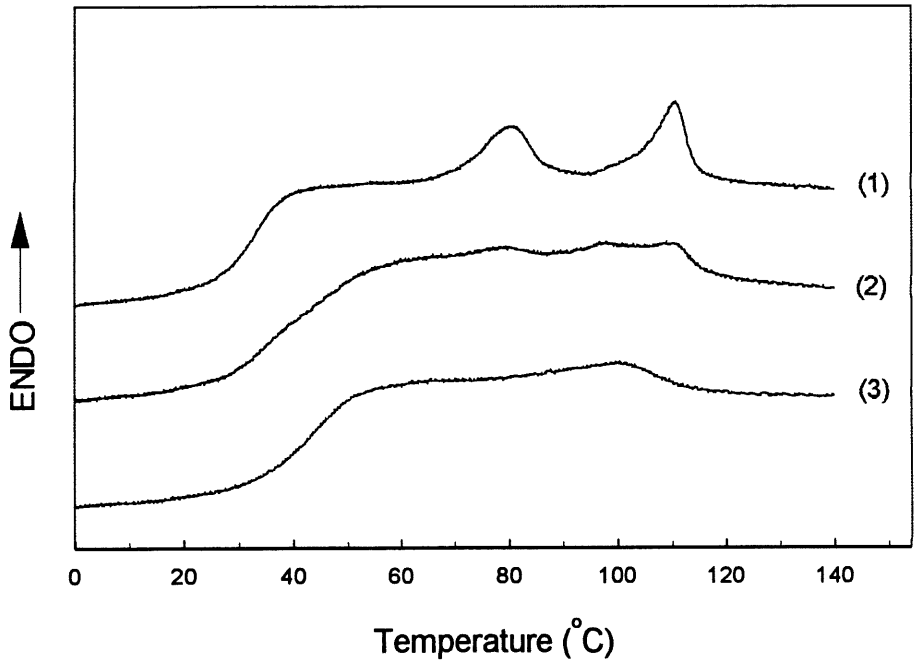

Figure 15. DSC heating curves of (1) netOCH$_3$(10%), (2) netOCH$_3$(10%)-netCN(20%) and (3) netCN(20%).

As different from the above ILCPNs which combine a netOCH$_3$ sample as network-1 and a netCN sample as network-2, the sample of netCN(10%)–netOCH$_3$(20%) is made of netCN(10%) as network-1 and netOCH$_3$(20%) as network-2. The network-2 content of this

ILCPN, i.e., 22 wt % netOCH_3(20%), is much lower than that of the above ILCPNs (ca. 50 wt %). From the DSC curves shown in *Figure 16*, it is seen that no smectic-nematic transition can be noticed for the ILCPN sample, and that the nematic-isotropic transition is a little higher that those of pure networks.

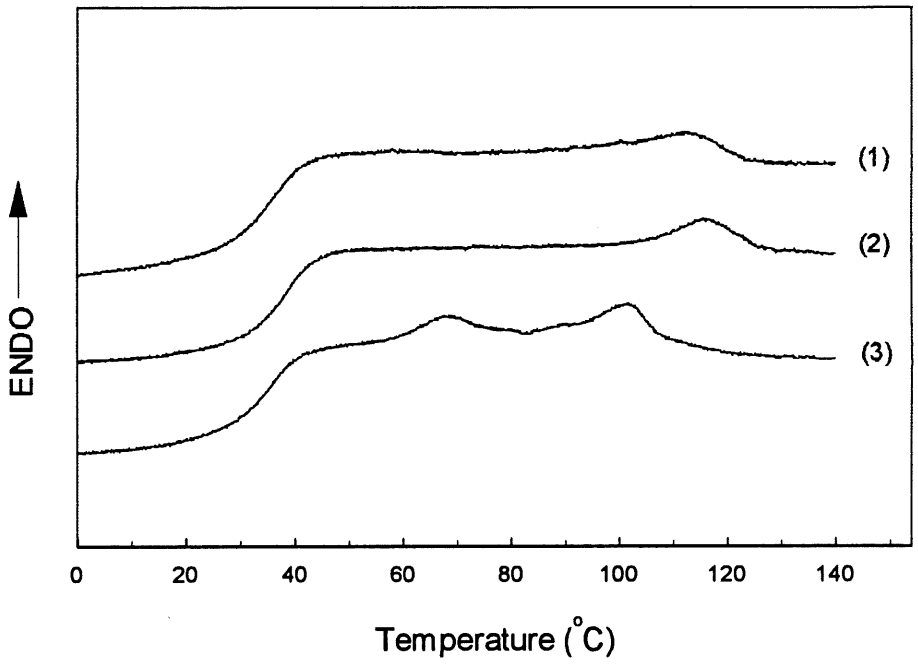

Figure 16. DSC heating curves of (1) netCN(10%), (2) netCN(10%)-netOCH_3(20%) and netOCH_3(20%).

1.3.2.2 ILCPNs involving LC ionomers

The DSC heating curves for the three LC ionomers used as network-1 and their ILCPNs with netCN(20%) and the pure netCN(20%) are displayed in *Figure 17* for comparison. In contrast with the ILCPNs of netOCH_3-netCN, the obtained content of network-2 in these ionomer-based ILCPNs is quite low (around 30 wt %). All the three ILCPNs were prepared by polymerizing *in-situ* the same monomer solution with 20 mol % of the cross-linker. Clearly, their mesophase transitions are modified as compared with the corresponding single networks.

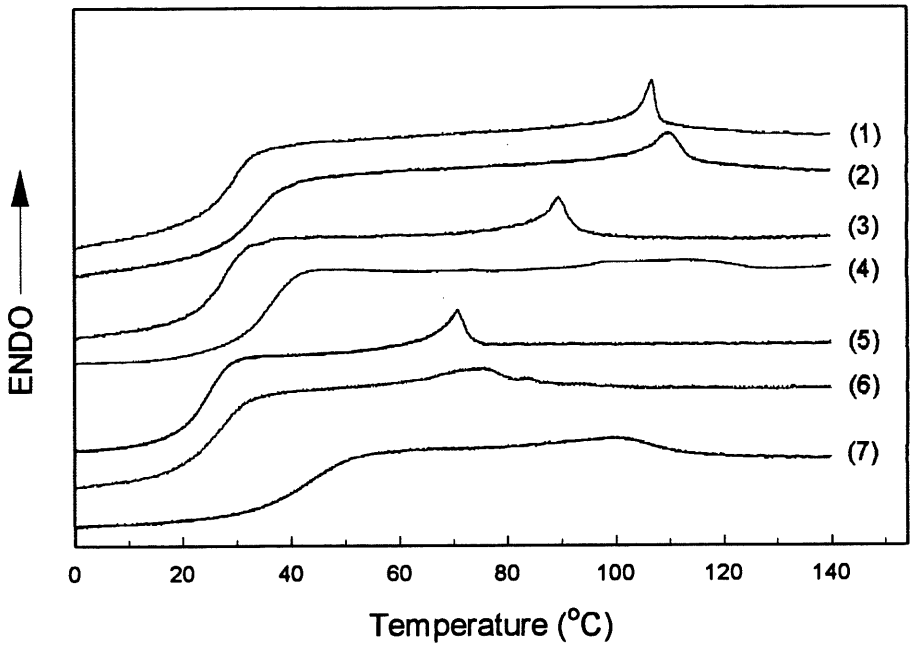

Figure 17. **DSC heating curves of (1) netCNNa(2.5%), (2) netCNNa(2.5%)–netCN(20%), (3) netCNNa(5.3%), (4) netCNNa(5.3%)–netCN(20%) (5) netCNNa(7.3%), (6) netCNNa(7.3%)–netCN(20%) and (7) netCN(20%).**

In all cases, the ILCPNs sample has a higher T_g than that of the ionomer network-1, but lower that that of netCN(20%). Interestingly, the glass transition region of each ILCPNs apparently is not broadened. This intermediate T_g with an unchanged glass transition area is indicative of a certain degree of miscibility between the two network components. As for the nematic-isotropic transition, a higher and broader peak can be noticed for all ILCPNs as compared to the respective ionomer network-1. But, unlike the samples of netOCH_3-netCN, the peak does not seem to be either intermediate between or an addition of the peaks of the two single networks. Only in the case of netCNNa(7.3%)–netCN(20%) the peak position is intermediate. These results suggest a strong interlocking between the two networks. In the case of netCNNa(2.5%)–netCN(20%) and netCNNa(5.3%)–netCN(20%), the transition temperatures

higher than those of both netCNNa and netCN(20%) could suggest that the actual cross-link level of the network-2 in the ILCPNs samples is lower than that of the pure netCN(20%). The unusual width of the transition peak, particularly for netCNNa(5.3%)–netCN(20%) should reflect a heterogeneous structure throughout the sample.

Another observation also proves an intimate interaction between the two networks in the ILCPNs samples. The ionomer network with ionic aggregates as cross-links is thermoplastic and can be dissolved in strong polar solvents like DMSO (9). Placing the ILCPN sample in DMSO, if there is no intimate interlocking between the two networks, most of the netCNNa should be expected to dissolve in the solution and be extracted. We performed the experiment with the sample of netCNNa(5.3%)-netCN(20%). In contrast to the pure ionomer sample, no visible dissolution of the ILCPNs sample could be observed. After several hours of extraction in DMSO, a small amount of netCNNa(5.3%) was extracted since the estimated content of netCNNa(5.3%) in the extracted ILCPNs sample is 44 wt% instead of 63 wt% in the un-extracted sample. This result implies a strong interlocking between the two networks which hinders the dissolution of the ionic network.

1.4 Conclusion

We have extended the concept of interpenetrating polymer networks to SCLCPs, giving rise to ILCPNs. For the first time, several polyacrylate-based sequential ILCPNs were successfully prepared through polymerization *in-situ* of a mesogenic monomer solution which is absorbed in a LC network made from another mesogenic monomer. Two types of network-1 were utilized. These are either a covalently cross-linked SCLCP or a non-covalently cross-linked SCLCP, the latter being a thermoplastic, ion-containing SCLCP with ionic aggregates acting as cross-links. We found that the success in preparing ILCPN samples was determined by a number of important factors, which includes the monomer concentration, the solvent

used for the polymerization in-situ, the reaction temperature, the size of the network-1 sample, and the choice of network-1.

As compared to single network samples, phase transitions in the obtained ILCPNs were modified to different extents depending on the achieved miscibility between the two components in the systems. We found that a first network of a greater cross-link level generally results in an ILCPN sample displaying a greater miscibility and, consequently, more profound effects on the phase transitions of the two components. This observation indicates that a greater cross-link level for the network-1 restricts more efficiently the phase separation as the second polymer is formed. Overall, the rate of gelation during the second polymerization relative to the rate of phase separation governs the extent of the phase interpenetrating.

More importantly, this study demonstrates the possibility of exploring a novel SCLCP-based system. Indeed, it is expected that ILCPNs could combine the features of two different SCLCPs into a single stable material, which opens a new route for the development of functional materials.

CHAPTER 2

GRAFTING OF LIQUID CRYSTALLINE POLYMERS ON A STYRENE-BUTADIENE-STYRENE TRIBLOCK COPOLYMER AND ORIENTATION INDUCTION

2.1 Background

There is an increasing interest in preparing block or graft copolymers containing a SCLCP. They represent one of the most exciting new materials based on SCLCPs through the combination of the self-assembled morphology in the copolymers and the anisotropic features arising from the liquid crystals. The synthesis method for the preparation of LC block or graft copolymers usually is very complex, generally involving the utilization of anionic polymerization. To date, one of the few successful systems is the styrene-SCLCP-styrene tri-block copolymer (19). The interest of the present study is twofold. Firstly, from the new-materials-making point of view, the purpose was to exploit a new and easy approach of making SCLCP-containing copolymers. It is a known industrial procedure to prepare styrene-butadiene graft copolymers by polymerizing the monomer of styrene in a solution with a dissolved polybutadiene (PB) and resulting in polystyrene (PS) grafts on PB chains (20). By employing this approach, we polymerized the monomers of SCLCPs in a solution with a dissolved SBS tri-block copolymer (15), which is commercially available. As will be shown below, the characterization results indicate the grafting of SCLCP onto the central PB block leading to graft LC copolymer system.

The other main interest of this study is related to a previous research performed in this laboratory. As part of an effort of overcoming the difficulty of casting thin SCLCPs films

which could be mechanically stretched to induce a monodomain structure, it was shown that blending a SCLCP with a conventional polymer as matrix made it possible to obtain thin blend films which could be stretched to induce effectively the monodomain structure despite the immiscibility of the blend system (21). In that study, two conventional polymers, a SBS copolymer and a poly(vinyl chloride) (PVC), were used. The choice of SBS was not arbitrary. This polymer is of particular interest because it is a thermoplastic elastomer. Although such an approach is successful in providing a new method of monodomain induction through mechanical effects, there is a main drawback for the SBS/SCLCP blends. Due to the severe immiscibility or incompatibility, the blend films prepared through solution-casting are opaque and have a very rough surface. They show a poor mechanical strength since repeated stretching rapidly leads to cracks in the films, and the films break eventually. Actually, the SCLCP's content in the blend should be limited to 30 wt% or lower. At higher concentrations the films are not elastic enough for a mechanical stretching. Clearly, by grafting the SCLCP component onto the SBS polymer, we could obtain a particular SBS/SCLCP system with an improved miscibility or compatibility between both polymers. This, consequently, should improve the mechanical strength and other properties and facilitates the induction and control of the monodomain structure.

In this chapter, we start with the details of the synthesis procedure for the preparation of the graft copolymers. Then, the characterization of the samples using several techniques is discussed, and the results are compared with those for solution-cast SBS/SCLCP blends. Finally, the orientation induction and preservation of the mesogenic side groups in the graft copolymers is described.

2.2 Preparation of Graft Copolymers

2.2.1 Synthesis procedure

In order to graft SCLCPs onto the SBS polymer, the monomer of SCLCP was radically polymerized in a solution with a dissolved SBS. The resulting samples will be referred to as SBS/SCLCP *in-situ* in order to distinguish them from the corresponding SBS/SCLCP blends cast from a solution with the same solvent. Two acrylate monomers of SCLCPs were synthesized (4, 5) and used in this study. They have the chemical structures shown below. The SBS polymer was purchased from Aldrich. It contains 30 wt% of polystyrene and has an average molecular weight of about 140,000 g/mol.

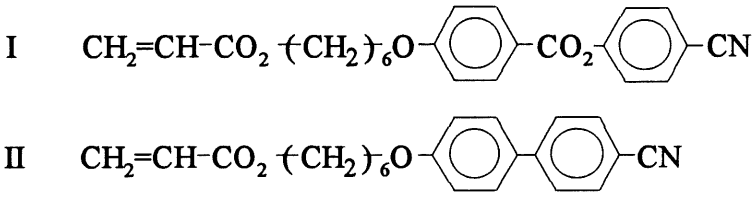

First of all, we mention that for comparison two homo-polyacrylates were prepared by polymerization of monomer-I and monomer-II, respectively, in toluene with 1 mol % AIBN with respect to monomer as the initiator at about 55 °C. More details are described in literature (4, 5). These two homopolymers are denoted as PA and BiPA, respectively.

To illustrate the typical synthesis conditions for the graft copolymers, we describe the procedure leading to a SBS/PA *in-situ* sample with 18 wt% of PA. 0.8 g of the SBS copolymer was dissolved in 16 ml of toluene and stirred overnight. During that time the solution was kept in the dark while purging with nitrogen. Then, 0.8 g of monomer-I and 4.9 mg of the initiator, benzoyl peroxide (1 mol %) (re-crystallized from chloroform by adding an equal volume of methanol before the use), were added into the SBS solution and solubilized for about 4 hours under nitrogen. The mixture solution was heated to 65 °C for the polymerization under a rigorous stirring and nitrogen atmosphere; the reaction lasted for 40 hours. After the reaction, the mixture was precipitated into cold methanol; the solid was collected and then re-dissolved in toluene for another precipitation. After several precipitation cycles in order to remove any un-reacted monomer-I and, possibly, un-grafted PA, the solid

was dried under vacuum at 50 °C for two days. The weight concentration of the monomer in the toluene solution was 5 % for all polymerizations using different weight ratio of SBS to monomer in the solution, regardless of the amount of the SBS copolymer.

The concentration of the SCLCP component in the SBS/SCLCP *in-situ* samples can be changed by changing the monomer concentration relative to the amount of SBS for the polymerization. Similarly to the method used for LC interpenetrating networks, the content of the SCLCP component in the *in-situ* samples was determined through infrared spectroscopy by using a calibration straight line obtained by plotting the concentration ratio of SCLCP to SBS in a series of the SBS/SCLCP blends of known compositions versus the ratio of the infrared absorbances at 2230 cm^{-1} (A_{PA}, –CN group in side-chain) and 967 cm^{-1} (A_{SBS}, –CH=CH– trans in PB chain) bands arisen from SCLCP and SBS, respectively. The curve is shown in *Figure 18*.

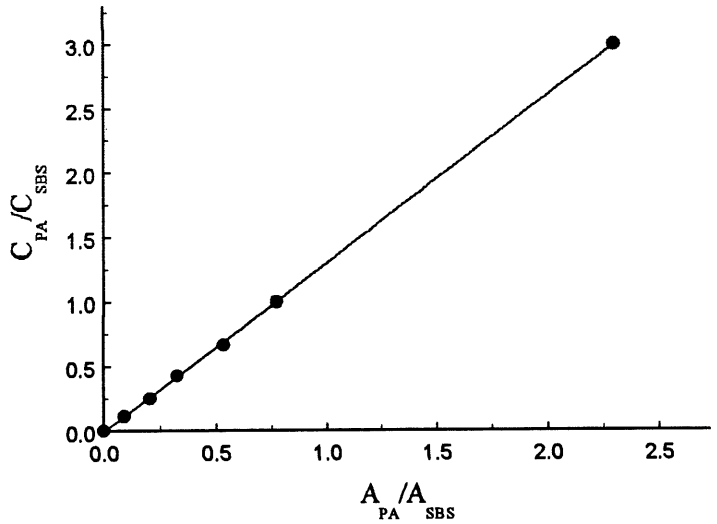

Figure 18. The concentration ratio of C_{PA}/C_{SBS} as a function of absorbance ratio of A_{PA}/A_{SBS}.

A linear curve fitting yields:

$$\frac{C_{PA}}{C_{SBS}} = 1.308\frac{A_{PA}}{A_{SBS}} \qquad [2.1]$$

The contents of the SCLCP component in the obtained SBS/SCLCP *in-situ* samples and the monomer feeding conditions are shown in *Table 4*.

Table 4. SCLCP contents in prepared *in-situ* samples.

Sample name	monomer used	weight ratio of SBS to SCLCP monomer	SCLCP content (wt %)
SBS/PA 82/18 *in-situ*	I	1:1	18
SBS/PA 70/30 *in-situ*	I	1:2	30
SBS/PA 48/52 *in-situ*	I	1:3	52
SBS/BiPA 76/24 *in-situ*	II	1:1	24

2.2.2 Characterization results

For the comparison purpose, polymer blends having the same compositions as those shown in *Table 4* for SBS/SCLCP *in-situ* samples were prepared from toluene-solution casting, and dried under the same conditions. All characterizations were performed on the *in-situ* and the respective blend samples.

2.2.2.1 Polarizing microscopy

Optical polarizing microscopy was utilized to reveal the differences between the *in-situ* and blend samples. In these measurements, the samples were first heated to 140 °C in the isotropic state for 5 min, and then cooled to a LC phase for the taking the photomicrographs of the same magnification under crossed polarizers. *Figure 19* shows the polarized photomicrographs taken at 80 °C for 1) PA, 2) SBS/PA 70/30 blend, and 3) SBS/PA 70/30 *in-situ*. Drastic differences are evident. As PA has only a nematic phase, with a nematic-isotropic transition at around 125 °C, it displays a threaded nematic texture. For the blend sample, two distinct phases are clearly seen. The SBS phase, which is amorphous, appears dark under crossed polarizers, while the birefringent regions arise from the phase of the PA component. Within the phase of the nematic polymer, the same threaded nematic textures emerge. As for the *in-situ* sample, interestingly, it displays a much more homogeneous morphology with no distinguishable phases of SBS and nematic PA like those for the blend sample. Apparently, a nematic-like, threaded texture can still be noticed, but it is more likely the result of a uniform distribution of the PA component throughout the sample.

In the case of BiPA, it has a more complex sequence of mesophases. When cooled from the isotropic state, the polymer exhibits a transition into a nematic phase at 129 °C, then a transition into a smectic-A phase at 119 °C, and finally a transition into a re-entrant nematic phase at 80 °C. *Figure 20* shows the photomicrographs, taken at 100 °C, for 1) BiPA, 2) SBS/BiPA 76/24 blend, and 3) SBS/BiPA 76/24 *in-situ*. At this temperature BiPA displays a smectic texture. For the blend sample, the result is similar to what is observed for the SBS/PA blend. There are two separated phases ; the dark areas arise from the amorphous SBS component and the birefringent regions correspond to the smectic phase of the BiPA component. Once again, by contrast, the *in-situ* sample has an almost homogeneous morphology when viewed under crossed polarizers. The smectic texture is no longer identifiable.

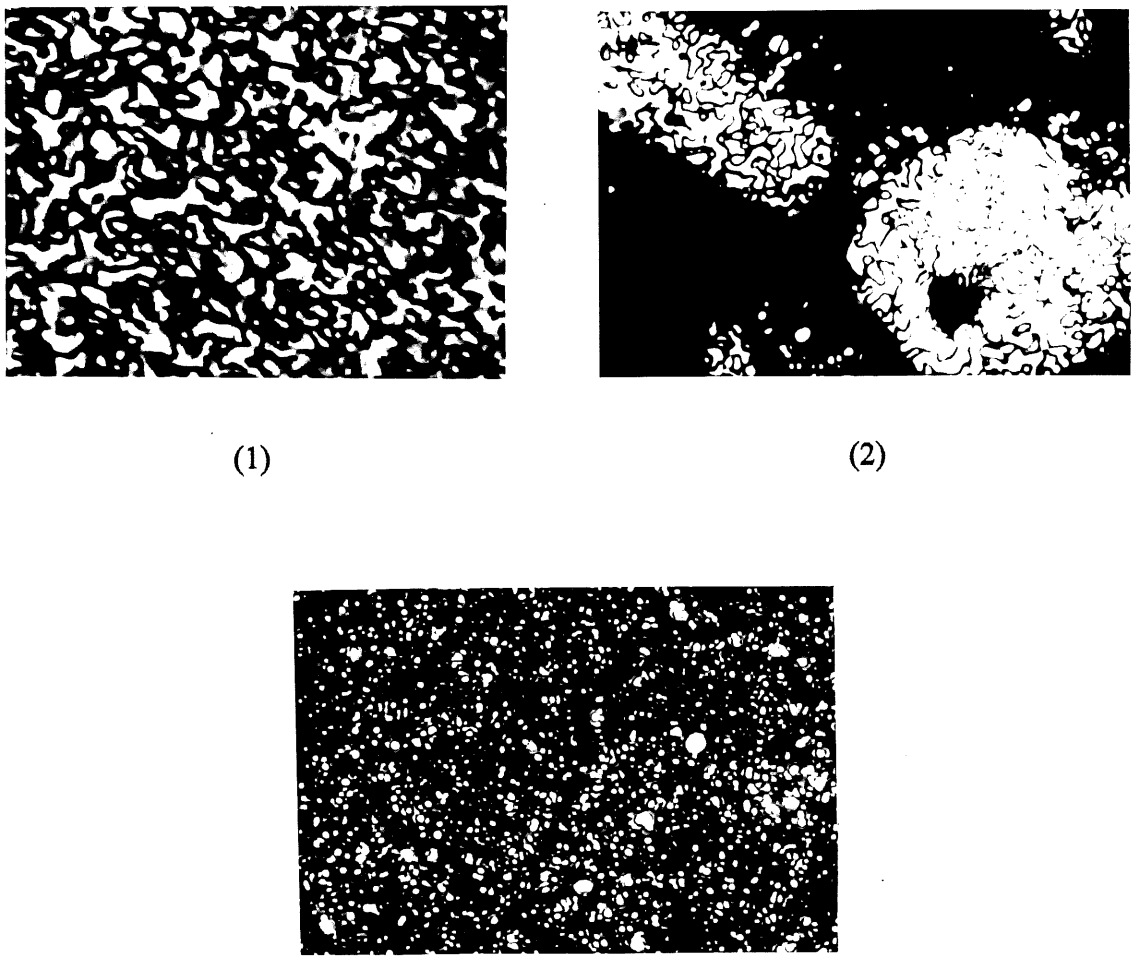

(1) (2)

(3)

Figure 19. Polarizing photomicrographs for (1) PA, (2) SBS/PA 70/30 blend, and (3) SBS/PA 70/30 *in-situ*. Magnification: 410 ×.

The above polarizing microscopic observations are very significant. The results imply that in these *in-situ* samples the SCLCP component essentially is randomly dispersed, and located in a sort of "microphase", even though we have no evidence to suggest the true, immiscibility-induced microphase conferred on block and graft copolymers.

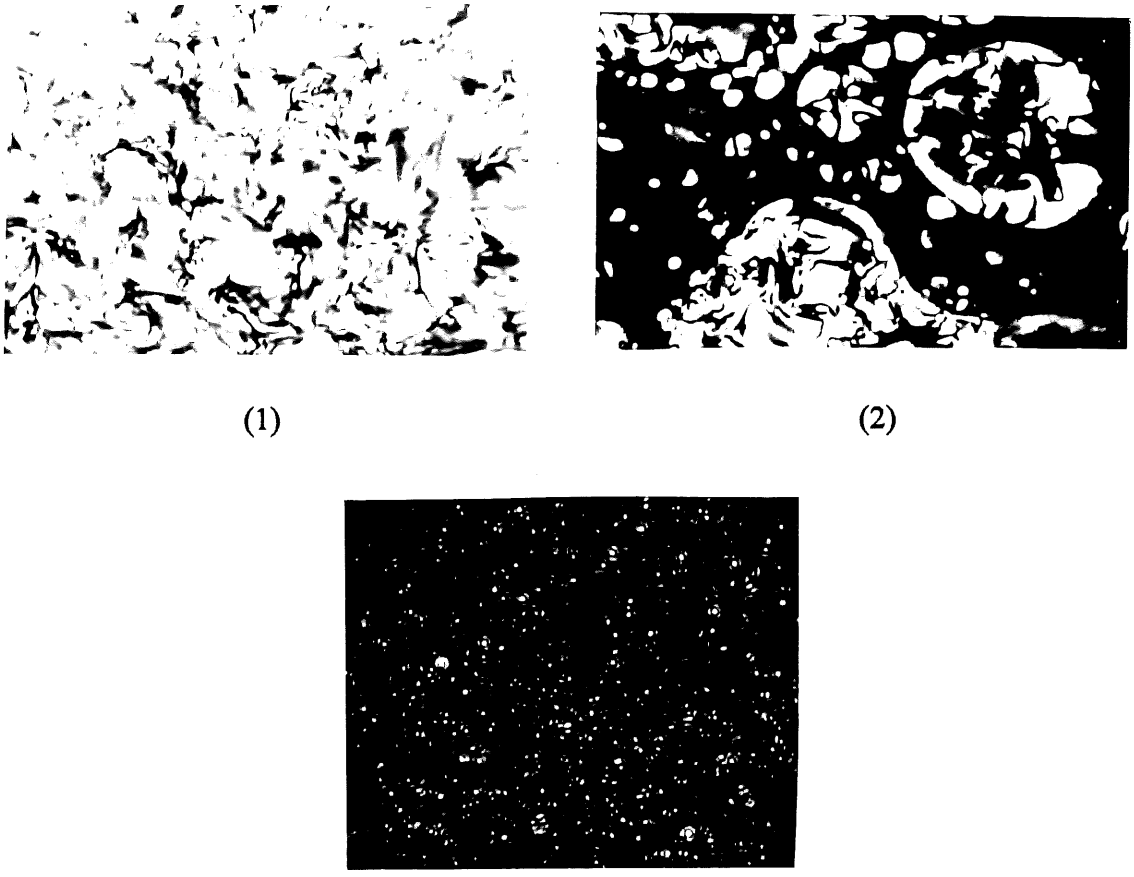

(1) (2)

(3)

Figure 20. Polarizing photomicrographs for (1) BiPA, (2) SBS/BiPA 76/24 blend, and (3) SBS/BiPA 76/24 *in-situ*. Magnification: 410 ×.

2.2.2.2 Differential scanning calorimetry

Differences in thermal transition behaviors between the *in-situ* and the blend samples were also observed. The DSC heating curves of some samples are presented in *Figure 21, 22* and *23*.

An interesting case can be found by comparing the SBS/PA 82/18 blend (curve 1 in *Figure 21*) with the *in-situ* sample (curve 2 in *Figure 21*). The 18% of PA in the blend behaves essentially like pure PA, exhibiting a T_g at about 32 °C and a nematic-isotropic transition temperature T_{ni} centered at 124 °C. While the *in-situ* sample has a T_g of PA lowered to 22 °C, and a little higher T_{ni} at 127 °C. The decrease in T_g must be induced by a plasticizing effect, suggesting that in the *in-situ* sample there is a greater interaction between the chains of PA and the PB block in the SBS copolymer which has a low T_g at about -80 °C (not shown for the sake of clarity). This should be the situation with SCLCP grafted on the PB block. Surprisingly, a plasticizing effect generally lowers both T_g and T_{ni} by a similar magnitude, here the *in-situ* sample's T_{ni} is not lowered, but instead it is higher than that of the blend.

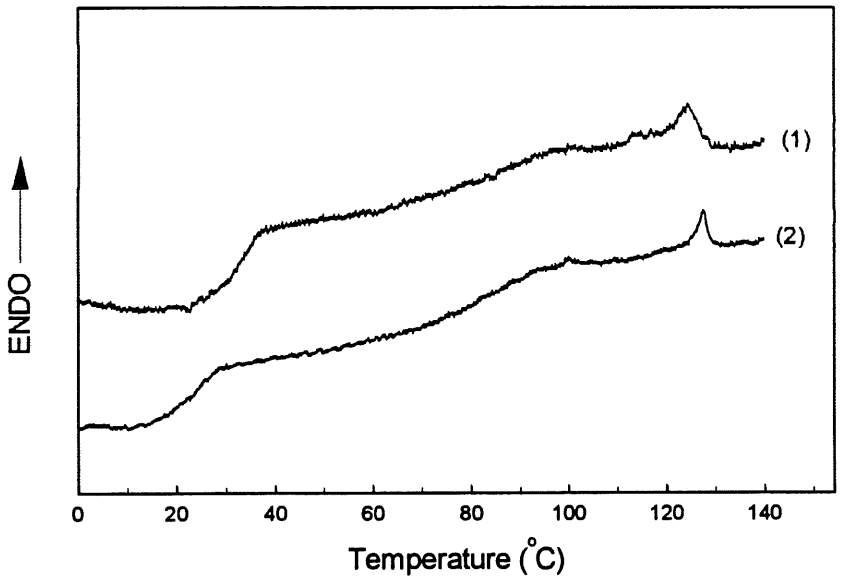

Figure 21. DSC heating curves of (1) the SBS/PA 82/18 blend sample and (2) the SBS/PA 82/18 *in-situ* sample.

Figure 22 compares SBS/PA 70/30 blend and *in-situ* samples. Similar observations can be made. Although in this case, T_g of the *in-situ* sample only lowers from 32 °C in the blend to 29 °C, the increase in its T_{ni} is greater, shifting from 124 °C in the blend to 133 °C. Also, it is interesting to notice that the nematic-isotropic transition region becomes much shaper for the *in-situ* sample. For both SBS/PA *in-situ* samples, the nematic phase between T_g and T_{ni} is significantly enlarged by about 12 °C as compared with their corresponding blends.

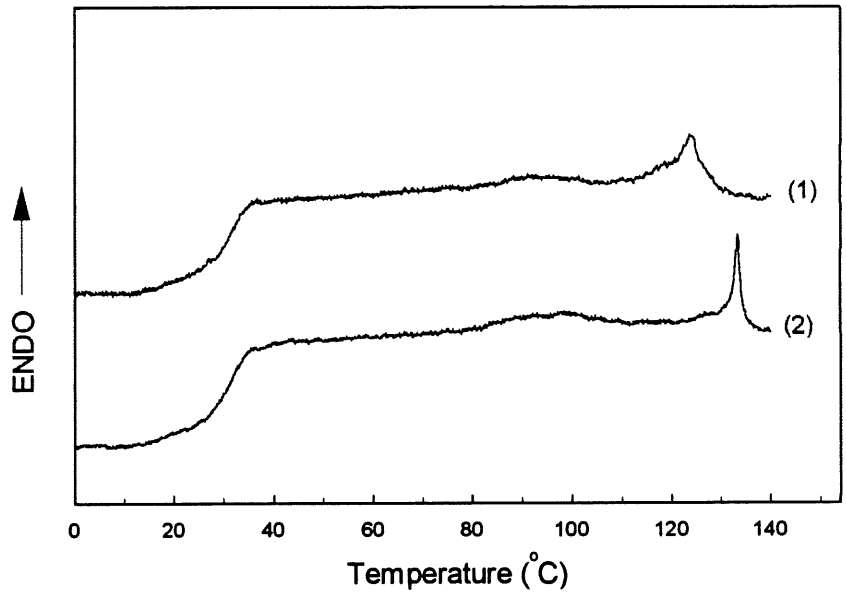

Figure 22. DSC heating curves of (1) the SBS/PA 70/30 blend sample and (2) the SBS/PA 70/30 *in-situ* sample.

In the case of SBS/BiPA 76/24, much smaller differences can be noticed between the *in-situ* and the blend samples. As revealed in *Figure 23*, the mesophase transition temperature of the SBS/BiPA 76/24 *in-situ* sample shows little change as compared with the blend sample. Nevertheless, the T_g of the *in-situ* sample is clearly below that of the blend sample. In all cases, the glass transition at about 85 °C is due to the PS microdomains in SBS.

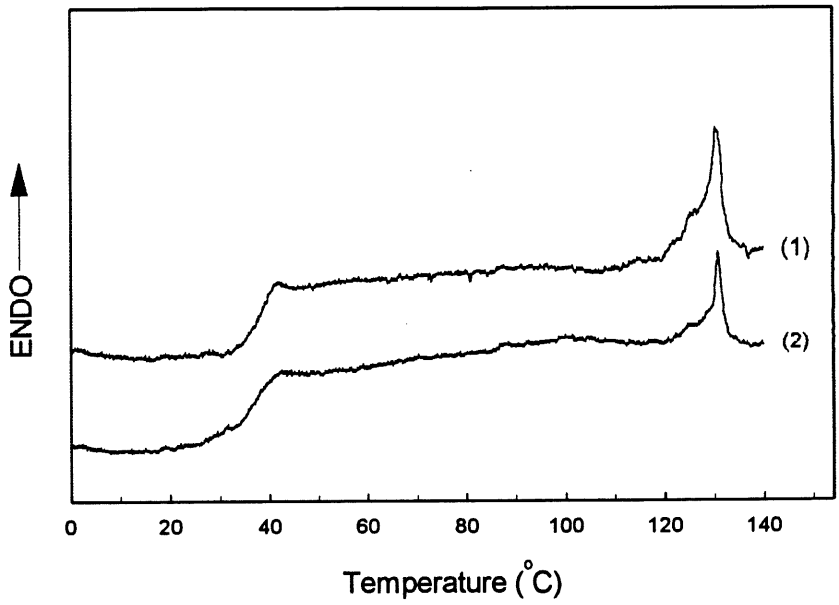

Figure 23. DSC heating curves of (1) the SBS/BiPA 76/24 blend sample and (2) the SBS/BiPA 76/24 *in-situ* sample.

2.2.3 Discussion

The possible mechanisms which lead to a grafting of the SCLCP on the SBS polymer should be similar to those for the grafting of PS on PB (20). They include 1) a radical transfer, either from a primary radical formed after the thermal decomposition of the initiator or from a propagating radical, to the methylene group of the PB block, which then initiates the polymerization of the monomer and results in SCLCP grafts on the PB block, and 2) a direct reaction between the double bonds of the PB block and the propagating radicals. The second process is known to be more important for PB containing a high vinyl groups. As the SBS sample used in this study contains more 1-4 units the radical transfer could be the main reaction for the grafting. According to the above grafting mechanisms, the *in-situ* samples could be a mixture of graft copolymer with homopolymer of SCLCP and possibly some un-grafted SBS as well. At this point we cannot say what could be the proportions of copolymer

and homopolymer, but it seems to be certain that the *in-situ* samples contain a significant amount of SBS-SCLCP graft copolymer. This copolymer in the mixture could play the role of a compatibilizing agent which tends to bring together the liquid crystalline homopolymer and the un-grafted SBS. Otherwise, such a drastic change as shown in *Figure 19* and *Figure 20* could not be possible.

The precipitation in methanol that we used for the sample purification should remove not only the un-reacted monomer but also some homopolymer of SCLCPs. This is revealed in *Figure 24* which shows the photomicrographs, which is taken at 80 °C, under cross polarizers, of the SBS/PA 48/52 *in-situ* sample before and after the first precipitation in methanol. It is seen that before the precipitation (*Figure 24* (1)) the sample contains regions displaying the typical nematic texture of the homopolymer of PA (see *Figure 19* (1)), indicating the existence of PA which is not grafted on SBS because the monomer is not liquid crystalline. The sample after the first precipitation (*Figure 24* (2)) shows no such homopolymer regions, and displays a mostly homogeneous morphology. Clearly, at least some of the homopolymer can be eliminated through this precipitation process.

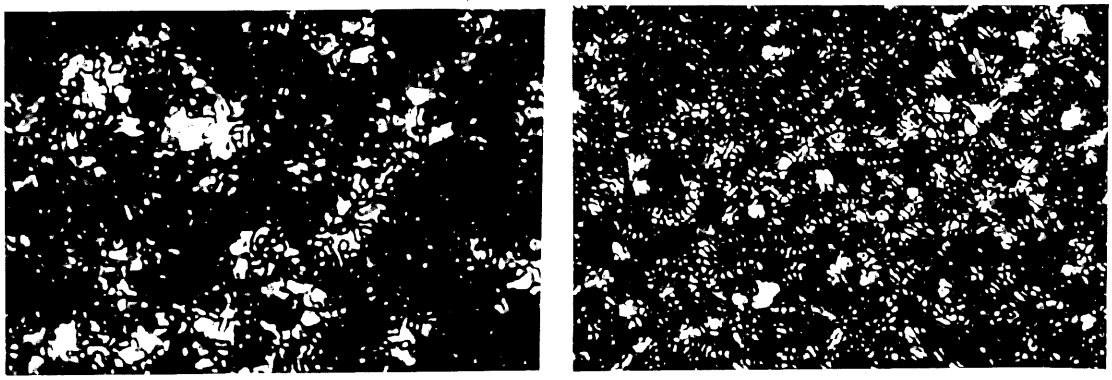

(1) (2)

Figure 24. Polarizing photomicrographs for SBS/PA 48/52 *in-situ* sample at 80 °C, (1) before, and (2) after the first precipitation in methanol, Magnification: 410 ×.

Finally, it is interesting to mention that in this study, benzoyl peroxide, instead of AIBN, was used as initiator for the radical polymerization since it is known that the peroxide favors the grafting of PS on PB (20). However, we also made some trials with AIBN as initiator, and the resulting samples look similar to those obtained with benzoyl peroxide. Even though no detailed characterizations were carried out and the results recorded, it seems that the use of AIBN leads to a grafting when polymerizing acrylate monomers in a solution with dissolved SBS.

2.3 Orientation Induction

The orientation behavior was studied by the infrared dichroism which is a particularly powerful tool for orientation characterization. We used this method to study the development of a macroscopic orientation of the mesogenic side groups in the three synthesized *in-situ* samples. The technique of the infrared dichroism will be firstly outlined. Then, the method of measurement will be described. And finally, the results of orientation induction will be presented and discussed.

2.3.1 Orientation characterization through infrared dichroism

For each vibrational mode of a molecule, there is a transition-moment vector, **M**. Because the transition-moment is a vector quantity, it has both magnitude and direction. Each of the IR vibrational modes will have a transition-moment vector at some angle to the long axis of the molecule. The intensity of the IR absorption band depends on the angle that the electric vector of the incident radiation makes with the transition moment.

The absorption of each mode of IR vibration is proportional to the square of the dot product of the electric (**E**) and transition-moment (**M**) vectors

$$I = C(\mathbf{E} \bullet \mathbf{M})^2 = (EM\cos\alpha)^2 \qquad [2.2]$$

where C is a proportionality constant and E and M are the magnitudes of the electric field of the incident beam and the transition moment, respectively. The angle, α, is the angle between the two vectors. For an oriented solid sample, in order for the light to be absorbed, a component of the oscillating electric field vector of the incident light must be oriented in a plane parallel to the electric dipole transition moment (*Figure 25*). Light polarized perpendicular to the dipole transition moment will not be absorbed.

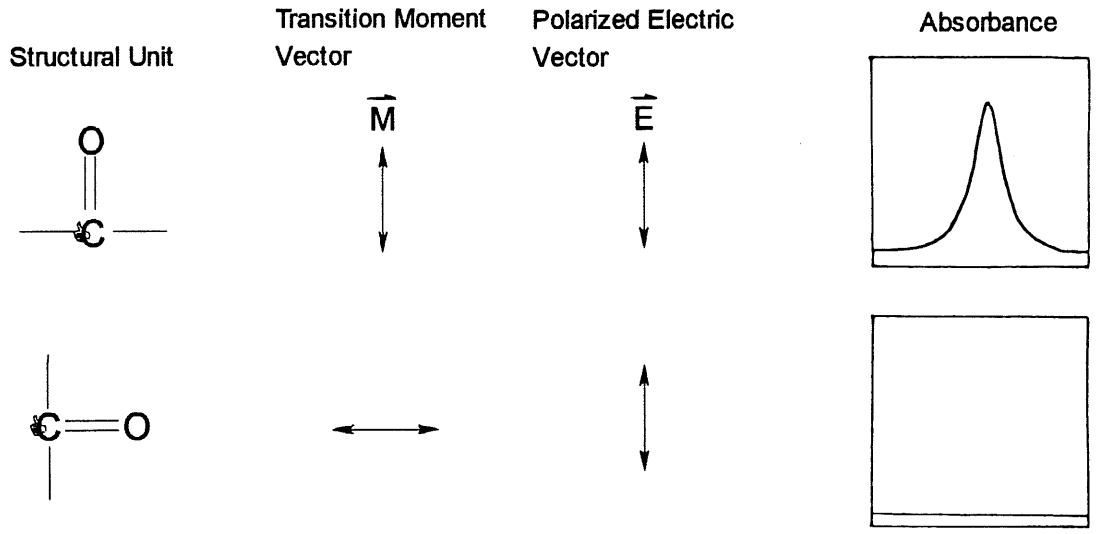

Figure 25. Linearly polarized IR absorbance of structural units

When the absorbing groups are oriented, they exhibit IR absorption that depend not only on how many groups are present in the sample but also on how the groups are oriented with respect to the beam. By using linearly polarized IR radiation, the orientation of the functional groups in a polymer system can be measured.

Measurement of IR linear dichroism requires light polarized both parallel and perpendicular to a fixed reference direction of the sample. For parallel polarized light, the absorbance is termed

$A_{\parallel}$ and the absorbance with perpendicular polarized light is termed $A_{\perp}$. The dichroic ratio, R, is defined as

$$R = (A_{\parallel}) / (A_{\perp}) \qquad [2.3]$$

For random orientation, R = 1. For unidirectional molecular orientations, such as for uniaxially drawn polymers, these dichroic parameters can be related to the orientation parameter, P_2. This quantity is equivalent to the second moment of the orientation distribution function for the molecular axis and is given by the following equation :

$$P_2 = \frac{3 < \cos^2 \theta > -1}{2} \qquad [2.4]$$

The orientation angle θ, displayed in *Figure 26*, is the angle between the draw direction and the local molecular chain axis. This orientation parameter P_2 can be calculated from measurements of the dichroic ratio by using the following equation :

$$P_2 = \frac{(R-1)(R_o+2)}{(R+2)(R_o-1)} \qquad [2.5]$$

where $R_o = 2\cot^2\alpha$.

The orientation parameter is equal to 1 (P_2 = 1) when the chain axis is parallel to the film orientation, 0 (P_2 = 0) when the system is randomly oriented (R = 1), and -1/2 (P_2 = -1/2) when the chain axis is perpendicular to the film orientation direction.

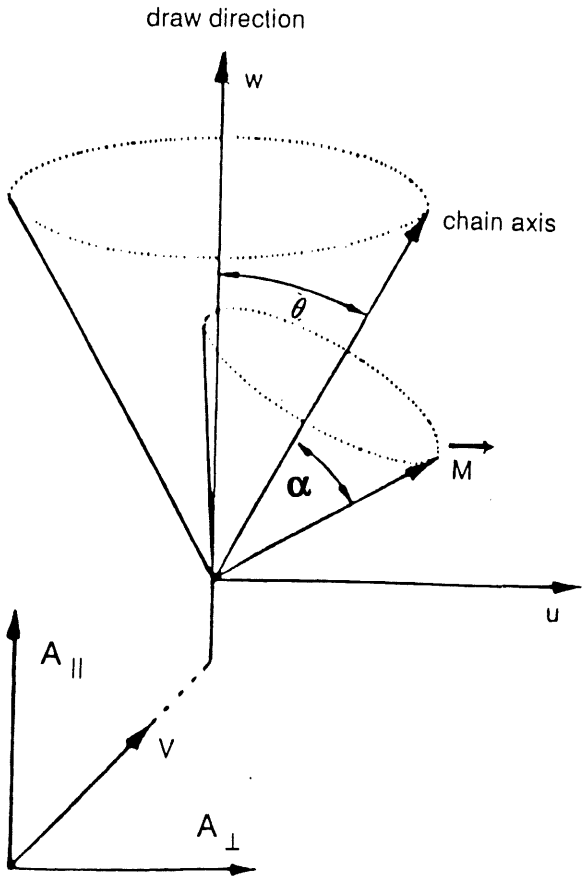

Figure 26. The orientation angle, θ, is the angle between the draw direction and the local molecular-chain axis.

2.3.2 Orientation measurements

2.3.2.1 Film Preparation

0.5 g in-situ sample was dissolved in 5 ml Toluene. The mixture was kept stirring for overnight. After complete dissolution, the solution was cast on the glass plate, and dried first in the hook for about 3 hours. When the film was formed it would be taken away from the glass plate and transformed on the Tafflon plate. The film was dried in the high vacuum oven for at least 4 hours and then at 50 °C for 2 days. This process of drying the film would

prevent the film from forming the bubbles which was formed in the film because the solvent was evaporated too fast.

2.3.2.2 Film stretching

Before stretching, all the films were annealed at 140 °C (isotropic state) for 10 min. The films were cut into a piece of 150 × 70 mm. The mechanical stretching experiments were performed on a hand-driven apparatus constructed in our laboratory. For a stretching experiment at a higher temperature than room temperature, the stretching device jawing the film was placed in an oven with a well-controlled temperature, and the film was kept at that temperature for at least 10 min before stretching, and after stretching the film was cooled at room temperature immediately. The drawing rate was about 50 mm/min. Small red ink marks were traced on the surface of the film to accurately determine the draw ratio, λ, which is defined as $\lambda = l / l_o$, l_o and l being the film length before and after the stretching, respectively.

2.3.2.3 Orientation measurements

As far as our research is concerned, we are mainly interested in investigating the orientation behavior of the mesogenic groups in SCLCPs. Therefore, we need to defined the axes of the side-chain mesogenic group and the main chain. For the case of PA as illustrated in *Figure 27*, the main chain axis is defined as the line connecting the six adjacent CH_2 units, while the mesogenic group's long axis is taken as the line connecting the centers of the two phenyl rings.

It can be seen from the infrared spectra shown in *Figure 28* that the cyano end groups (–C≡N) in a SBS/PA *in-situ* sample exhibit the characteristic stretching vibration band at 2230 cm^{-1} which is well suited to the P_2 measurement of the mesogenic groups. According to the axes

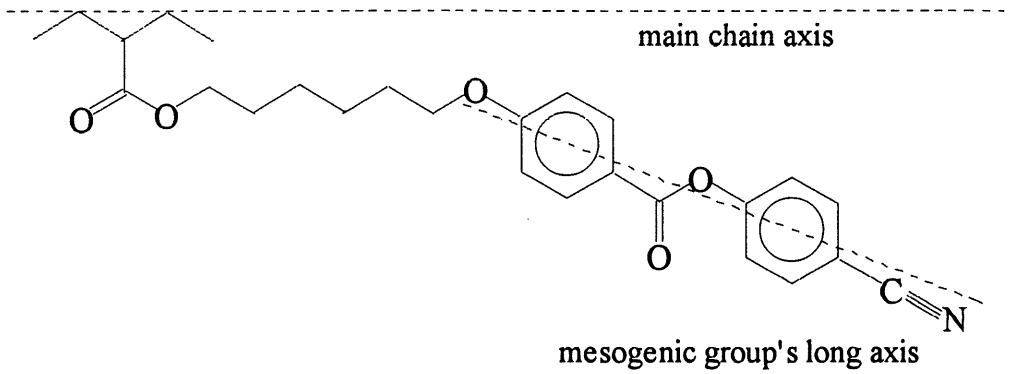

Figure 27. Definition of axes of the mesogenic group and main chain of PA

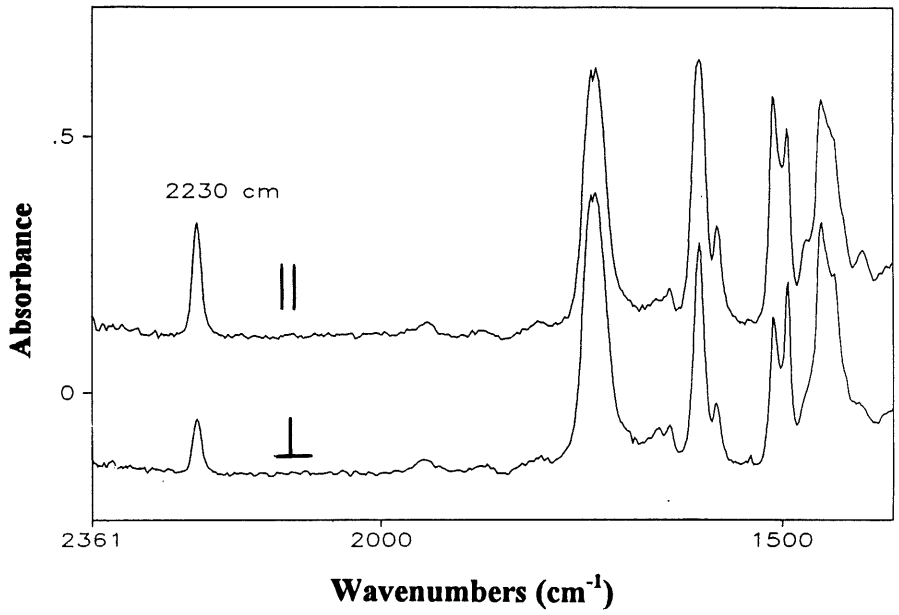

Figure 28. Infrared spectra of a SBS/PA *in-situ* sample exhibited the characteristic stretching vibration band at 2230 cm^{-1} -- the cyano end groups (–C≡N)

definition, the angle, α, between the mesogenic group and the main chain is about 11° and the P_2 of the mesogenic group for PA can be calculated from the following equation :

$$P_2 = 1.06 \times \frac{(R-1)}{(R+2)} \qquad [2.7]$$

For BiPA, the angle obviously is 0 and the P_2 can be obtained from :

$$P_2 = \frac{(R-1)}{(R+2)} \qquad [2.8]$$

where $R = A_{\parallel}/A_{\perp}$.

In contrast with the SBS/SCLCP blend films which are opaque and have rough surfaces, the films of the *in-situ* samples appear translucent, similar to a pure SBS film, and have a smooth surface. The elastic films of the *in-situ* samples are also mechanically stronger and can easily be stretched repeatedly to induce an alignment of the mesogenic groups.

2.3.3 Development of the monodomain structure

The development of a macroscopic orientation of the mesogenic side groups in SBS/PA 82/18 *in-situ* sample is illustrated in *Figure 29* by plotting the order parameter P_2 as a function of the draw ratio λ which is defined as the film length after stretching over the film length before stretching. The stretching experiments of this sample were carried out at room temperature. For this sample, a plateau P_2 value close to 0.5 is obtained after about 200% of film stretching at room temperature. This reflects the low T_g (22 °C) of this sample ; at room temperature the SCLCP component is in its nematic phase, and the stretching results in an effective alignment of the nematic domains.

In the case of SBS/PA 70/30 *in-situ* sample, the development of a macroscopic orientation of the mesogenic side groups by stretching the film at room temperature is quite different from that of the SBS/PA 82/18 *in-situ* sample. The orientation developments were displayed in *Figure 30*. This sample has a higher T_g (29 °C) which is above the room temperature, consequently, stretching at room temperature only induces a low macroscopic orientation,

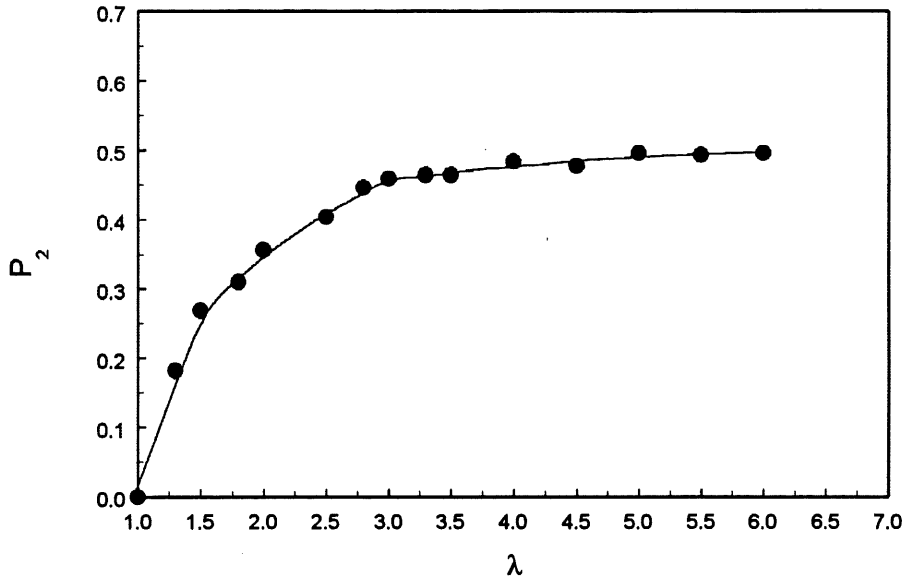

Figure 29. Order parameter P_2 vs draw ratio (λ) for SBS/PA 82/18 *in-situ* sample stretching at room temperature.

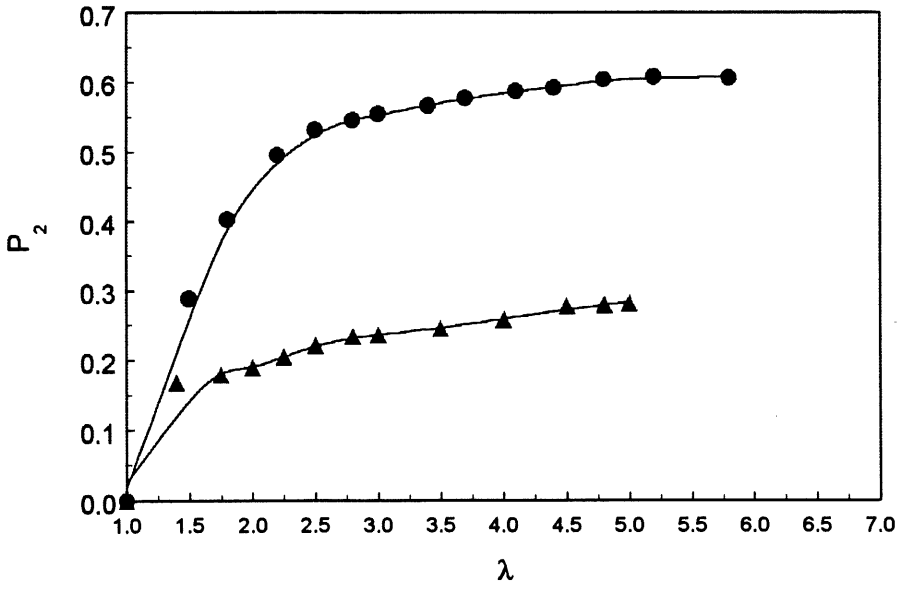

Figure 30. Order parameter P_2 vs draw ratio (λ) for SBS/PA 70/30 *in-situ* sample stretching at room temperature (▲) and at 50 °C (●), respectively.

while when stretched at 50 °C, i.e., in its liquid crystalline state, the film shows a strong macroscopic orientation as that of SBS/PA 82/18 *in-situ* sample.

The induction of a macroscopic orientation in the SBS/BiP6-CN 76/24 *in-situ* sample is also investigated, and the results are presented in *Figure 31*. It is seen that the orientation behavior is almost the same as that of SBS/PA 70/30 *in-situ* sample, because they both have a T_g which is higher than room temperature. Observed is a weak macroscopic orientation by stretching the film at room temperature and a strong macroscopic orientation by stretching the film at 50 °C .

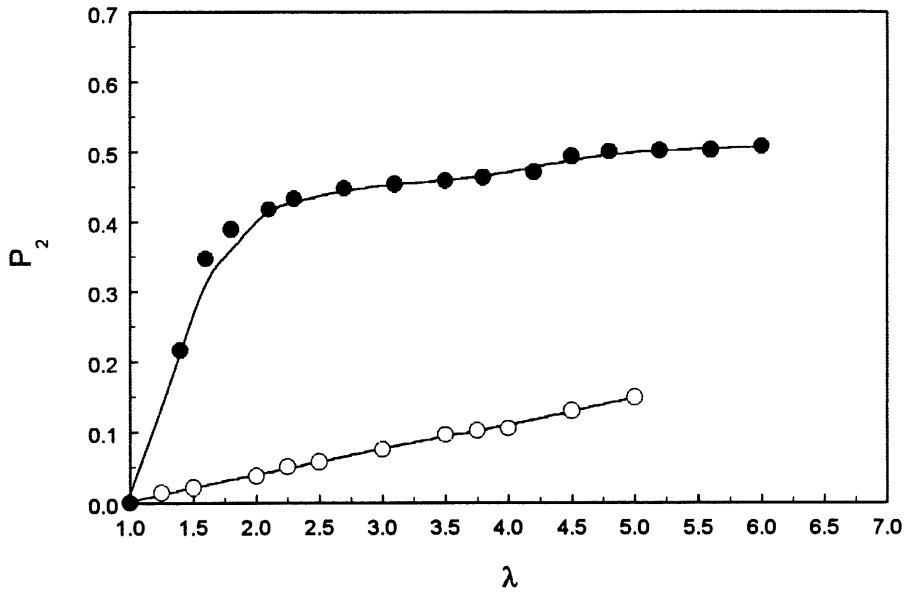

Figure 31. Order parameter P_2 vs draw ratio (λ) for SBS/BiPA 76/24 *in-situ* sample stretching at room temperature (○) and at 50 °C (●), respectively.

It should be emphasized that the almost constant P_2 value near 0.5 observed for all *in-situ* samples corresponds to a quite perfect alignment of the directors of the LC domains, since the orientation of the mesogenic groups within the LC domains along the directors (macroscopic orientation) is known to be characterized by an order parameter of this magnitude (22).

2.3.4 Orientation preservation

The orientation induction of the *in-situ* samples is similar to that observed for SCLCEs, i.e., low T_g -SCLCPs with chemical cross-links (10, 16). A known drawback for SCLCPs is that the macroscopic orientation of the mesogenic groups is lost when the film sample recovers its initial length after the removal of the mechanical force. As already mentioned, a previous work in this laboratory on SBS/SCLCP blends (21) exploited the fact that the elastic deformation of the SBS copolymer could be eliminated by thermally annealing a deformed film under strain in order to preserve the macroscopic orientation. In the present study, we further investigate the possibility of retaining the macroscopic orientation of the mesogens in the *in-situ* samples by using a special thermal annealing process which is composed of two treatments as described below.

First, a film was stretched to a deformation of 400 % at 50 °C, i.e., the initial draw ratio λ_i = 5, to reach the maximum orientation. Then the deformed film was annealed under strain at 40 °C for different times, and after each annealing time, the film was allowed to relax by removing the mechanical force. Because of the orientation relaxation of the elastic PB chains (23, 24), which occurred during each annealing under strain as a consequence of a rearrangement of the PS microdomains (cylindrical domains in SBS containing 30 wt% of PS), the relaxed film could not recover its initial length. This means that the residual draw ratio λ_r was higher than 1, and that the elastic recovery of the film, which is defined as $(\lambda_i-\lambda_r)/(\lambda_i-1)$, was less than 100%. Obviously, the elastic recovery decreases as the annealing time increases. After each annealing under strain, the residual macroscopic orientation in the relaxed film was measured.

A second treatment was subsequently conducted on a relaxed film which showed a zero elastic recovery, i.e., λ_r = 5, after having been subjected to the first thermal treatment under strain. In such a relaxed film, it is known that the arrangement of the PS microdomains is

anisotropic (23, 24); when it is heated to a temperature above the room temperature, a so-called healing effect occurs since the PS microdomains tend to recover their initial arrangement before the stretching. The film length decreases, and the apparent elastic recovery begin to increase. For the experiments, a free film with $\lambda_r = 5$ was heated to 40 °C for different times. After each time of this free film annealing treatment, the residual macroscopic orientation was also determined.

The results for SBS/PA 70/30 *in-situ* sample are shown in *Figure 32* where the residual P_2 is plotted versus the elastic recovery. It can be seen that with the first treatment of annealing under strain a macroscopic orientation of the mesogenic groups is conserved in the relaxed film. This preserved orientation increases as the elastic recovery of the film decreases. In the relaxed film exhibiting a zero elastic recovery, the same macroscopic orientation as the film

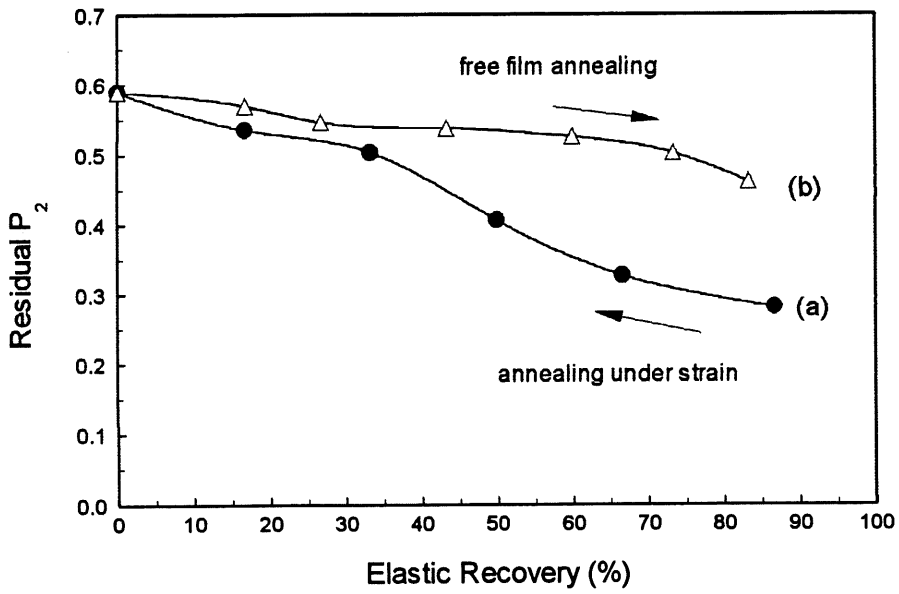

Figure 32. Residual Order parameter P_2 in relaxed film vs film elastic recovery for SBS/PA 70/30 *in-situ* after (a) thermal annealing on deformed film under strain (●), and (b) free film annealing on a relaxed film showing zero elastic recovery (Δ).

just after the 400% stretching is retained. Now, when this relaxed film is subjected to the second treatment of free film annealing at 40 °C, the film length decreases and the apparent elastic recovery is no longer zero. The elastic recovery increases with annealing time, and finally reaches 85% which corresponds to λ_r = 1.6. But, the preserved macroscopic orientation remains high, and decreases only slightly. These results indicate that with the above thermal annealing process the stretching-induced macroscopic orientation of the mesogenic groups can be preserved in a relaxed, free standing film which is thermally stable, and has a length close to the initial film length before the stretching experiment. This capacity of orientation induction and preservation is particularly interesting.

Figure 33 shows the results of residual macroscopic orientation for SBS/BiPA 76/24 *in-situ* sample annealed by the first and the second treatments, respectively. It can be known, from

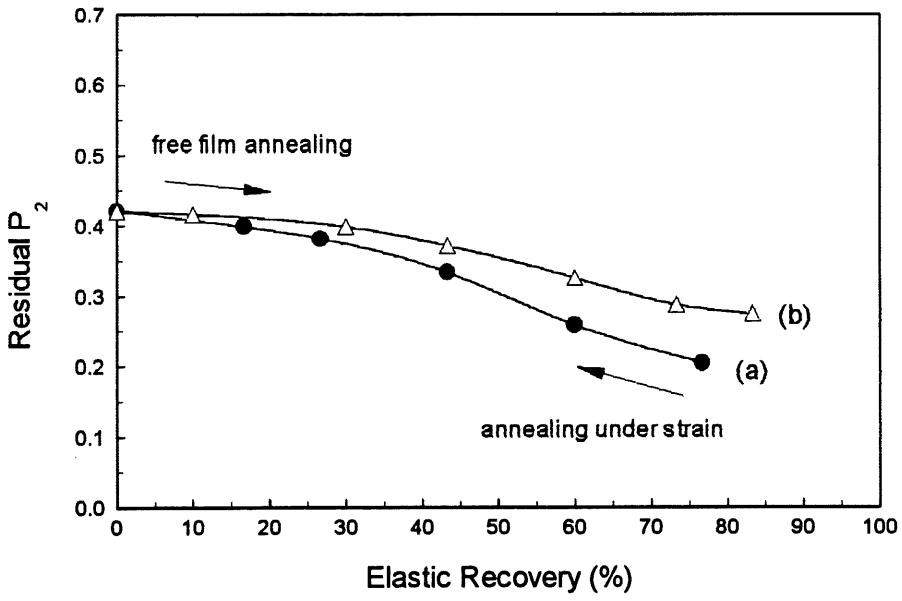

Figure 33. **Residual Order parameter P_2 in relaxed film vs film elastic recovery for SBS/BiPA 76/24 *in-situ* after (a) thermal annealing on deformed film under strain (●), and (b) free film annealing on a relaxed film showing zero elastic recovery (Δ).**

Figure 33, that the development of the residual macroscopic orientation of this sample is almost the same as that of SBS/PA 70/30 *in-situ* sample. The only one different behavior, as compared with the results of SBS/PA 70/30 *in-situ* sample, is that the preserved macroscopic orientation decreases more when the film was annealed by the second treatment.

2.3.5 Discussion

The morphology of the *in-situ* samples should be complex, which includes PS microdomains dispersed in a PB matrix and a very small size-phase, if not a microphase, of the SCLCP component. At low SCLCP content, like SBS/PA 82/18 *in-situ* sample, the SCLCP phase could also be dispersed in the PB matrix; while at high SCLCP content, like SBS/PA 48/52 *in-situ*, two continuous phases of PB and SCLCP could be present. But in any case, important interactions between the phases of PB and SCLCP must exist. Despite this complexity, the above results suggest that the orientation behaviour of the SCLCP component is mainly determined by its own response to the stretching. The macroscopic orientation of the mesogenic groups is completed at early stage of the sample's deformation, and further stretching only involves a high orientation of the rubbery PB chains and the alignment of the PS cylindrical microdomains acting as cross-links. During the annealing under strain, which induces relaxation of stretched PB chain and rearrangement of aligned PS microdomains, apparently no orientation relaxation of the mesogenic groups takes place. The treatment of free film annealing, which produces further rearrangement of the PS domains and leads to film shrinkage, has little effect on the macroscopic orientation in the SCLCP phase.

2.4 Conclusion

Polymerizing the monomers of SCLCPs in a solution which dissolved SBS can result in grafts of SCLCPs on the PB block of SBS. The resulting *in-situ* samples differ very much from the solution-casting SBS/SCLCP blend samples. In contrast with the blends, they have a much

more homogeneous morphology when viewed by microscope under crossed polarizers. Translucent films from *in-situ* samples, which are much stronger mechanically, can be obtained through solution-casting of the in-situ samples with a SCLCP content up to 52 wt %. Assuming the presence of the liquid crystalline homopolymer in the *in-situ* samples, it is, however, clear that at least a significant amount of SBS-SCLCP graft copolymer is formed during the polymerization, which accounts for drastic changes in the properties as compared with the blends.

A uniform macroscopic orientation of the mesogenic groups of the SCLCP component in the *in-situ* samples can easily be induced by mechanically stretching of the elastic films. A quite perfect orientation aligns the directors of the LC domains of all *in-situ* samples because of their almost constant orientation parameter P_2 value of near 0.5 observed. More interestingly, this macroscopic orientation can almost be totally preserved in a relaxed, free standing film after a thermal treatment process. The treatment is based on, firstly, annealing a deformed film under strain to eliminate the elastic recovery after the removal of the mechanical force and, then, annealing the relaxed film to induce film shrinkage.

CHAPTER 3

STRESS-INDUCED ORIENTATION OF SIDE-CHAIN LIQUID CRYSTALLINE IONOMERS IN BLENDS WITH POLY(VINYL CHLORIDE) AS MATRIX

3.1 Background

One important aspect of the research on SCLCPs is the control and manipulation of the macroscopic orientation of the mesogenic units under effects of the external fields such as magnetic, electric, and mechanical forces. Among the many factors which can affect the orientation process it is of interest to know the correlation between the macroscopic orientation and the intrinsically oriented microstructure which characterizes the mesophases in LCPs. To conduct this kind of investigations it is necessary to use samples with changing mesophase behaviour but keeping unchanged other parameters, such as the degree of polymerization and the length of the flexible spacer linking the mesogenic units to the chain backbone. In our laboratory, a series of liquid crystalline ionomers has been prepared through partial alkaline hydrolysis of liquid crystalline polyacrylates (9). These samples meet the requirements, since the random incorporation of a small amount, generally < 10 mol %, of ionic groups results in a perturbation of the microstructures and, consequently, a systematic depression of the nematic to isotropic transition temperature T_{ni} without, interestingly, much affecting the associated transition enthalpy and the glass transition temperature T_g. This disturbing effect is mainly due to the formation of the ionic aggregates in the ionomers (25), which reduce the polymer chain mobility and increase the internal elastic constraints for the mesogenic units.

In a previous study in our laboratory (26) the macroscopic orientation, in a strong magnetic field, of some ionomers as well as the initial polyacrylate containing no ionic groups was investigated. The ionic aggregates were found to exert strong effects on the achievable magnetic alignment. As part of the research program, this chapter reports a study focused on the macroscopic orientation of the ionomers subjected to a mechanical field, such as mechanical stretching. Studying mechanically induced orientation was usually performed on SCLCEs (27, 28) which, through formation of a network structure, possess the good deformability required for mechanical stretching. For the case of un-cross-linked LCPs, one alternative, which enables one to investigate the stress-induced orientation behavior, is to stretch a supporting medium made from a conventional polymer, i.e., a film onto whose surface a LCP film is cast or a polymer matrix in which a LCP is dispersed (21, 29). These methods allow a mechanical field to be applied on the LCP sample and are efficient enough to promote a macroscopic orientation with a level similar to that for the LC elastomers. This is why, for the present study aimed at revealing the effects of ionic aggregates on the stress-induced orientation, we have chosen the experimental approach of blending the LCP samples (10 wt %) in a PVC matrix and stretching the blend films. In this way, we have been able not only to observe the orientation behavior of the ionomers but also to reveal the underlying mechanisms involved in the orientation process under a stress.

3.2 Experimental

Two series of ionomers prepared through partial hydrolysis, using sodium hydroxide, of a polyacrylate bearing a biphenyl moiety in the side group and of a polyacrylate carrying a phenyl benzoate moiety were used. The samples are referred as to series A and series B, respectively. Their chemical structures are displayed as follows:

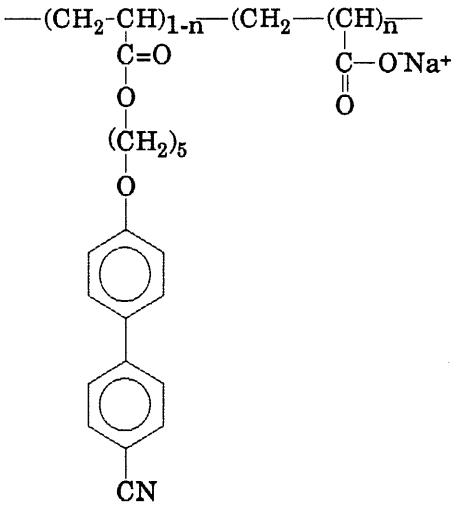

Series A

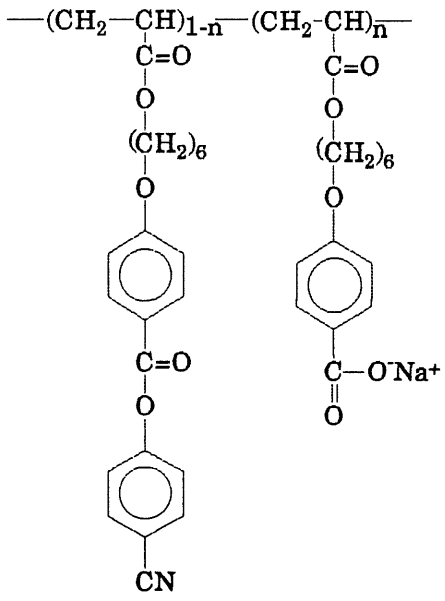

Series B

The phase transition temperatures determined by DSC (Perkin-Elmer DSC-7, 10 °C/min heating rate) are given in *Table 5*. The mole percentages of the ionic groups (COO^-Na^+) are expected values based on the amount of NaOH used in the reactions. Details about the synthesis and characterization of the ionomers are given in the literature (9). For the initial polymers containing no ionic groups, A1 has a $\overline{M}_n$ of about 79000 g/mol ($\overline{M}_w / \overline{M}_n$=1.78), and B1 47000 g/mol ($\overline{M}_w / \overline{M}_n$ =1.54), as estimated by GPC using polystyrene as standards.

All the samples were blended with PVC (Aldrich, $\overline{M}_n$ = 37500 g/mol) in a weight-based ratio of 10/90. Thin blend films of about 40 μm thick were obtained from solution-casting. For the series A-samples THF was used as the solvent while DMSO was used for the series B (the solutions were heated for dissolving both polymers and cast onto the surface of preheated glass plates). After evaporation of most solvent the films were further dried under vacuum at 60°C for several days. Prior to the mechanical stretching experiments the film samples were annealed, in vacuum, at 130°C for 10 min.

Table 5. Phase transition temperatures of the samples

Sample	*n (mol %)*	T_g (°C)	T_{ni} (°C)
A1	0	38	117
A2	7	37	107
A3	9	37	88
B1	0	30	122
B2	2.5	28	106
B3	5.3	25	90
B4	7.3	24	72

Mechanical stretching of the films (10 mm in length and 8 mm in width) was performed on a hand-driven apparatus, which was placed in a temperature-controlled oven (±1 °C). The strain rate was about 50 mm/min; and, unless otherwise stated, the films were cooled under strain at room temperature immediately following the stretching to preserve the macroscopic orientation. The extension of the films was measured by determining the draw ratio λ defined as $\lambda = l/l_o$, l_o and l being the film lengths before and after stretching, respectively.

The orientation parameter P_2 was used to characterize the macroscopic orientation and determined through the well-known infrared dichroism method (30). P_2 is a measure of the average orientation over all the molecular units considered (mesogenic groups or chain segments). Although we were mainly interested in the orientation of the mesogenic groups, for some experiments the P_2 of the matrix PVC was also measured for comparison. The details on the use of the infrared dichroism in our studies were already described in the literatures (21, 29). Here we mention that for the calculation of the P_2 of the mesogenic

groups all infrared absorbances were lower than about 0.2, ensuring the validity of Beer's law. Also, the uniaxial stretching of the samples, i.e., the fiber symmetry, has been checked by observing the absorbance which, within the error of the measurements, was proportional to $1/\lambda^{1/2}$. The polarized infrared spectra were recorded on a Bomen-MB102 FTIR spectrometer.

3.3 Results and Discussion

3.3.1 DSC measurements

As mentioned in the Introduction, in this work PVC was used essentially as a matrix for realizing the stretching experiments. The choice of PVC was based on the requirement of stretching most LCP samples in their nematic state. Although the resulting blends were expected to be phase-separated, it was interesting to characterize the blend samples, since significant interfacial interactions could exist. For these blends it is reasonable to assume that upon stretching the mechanical force mainly operates on the PVC matrix (90% in weight) and the interfacial interactions could play a role in the transfer or build up of a stress field effectively acting on the LCP samples, thereby affecting the macroscopic orientation of the mesogenic groups. DSC measurements were performed on the blend samples, confirming the phase-separated character. Two representative examples of the DSC heating curves, recorded for the blends with A2 and B2, respectively, are given in *Figure 34*. In both cases, two T_g's can clearly be seen, one arising from the LCP phase appeared around 30°C while the other one at about 70°C belonging to the PVC matrix. In the case of the blends with the series A-samples, in spite of the low LCP concentration in the blends an endothermic peak for the nematic to isotropic transition can be seen beyond the T_g region of PVC, but its position was found to shift to a lower temperature (about 5°C) as compared with the pure samples, which could be considered as an indication of the effect of the interfacial interactions between PVC and LCP. For the blends containing the samples of the series B, the transition peak cannot be found. This suggests a greater effect of the interfacial interactions in those blends.

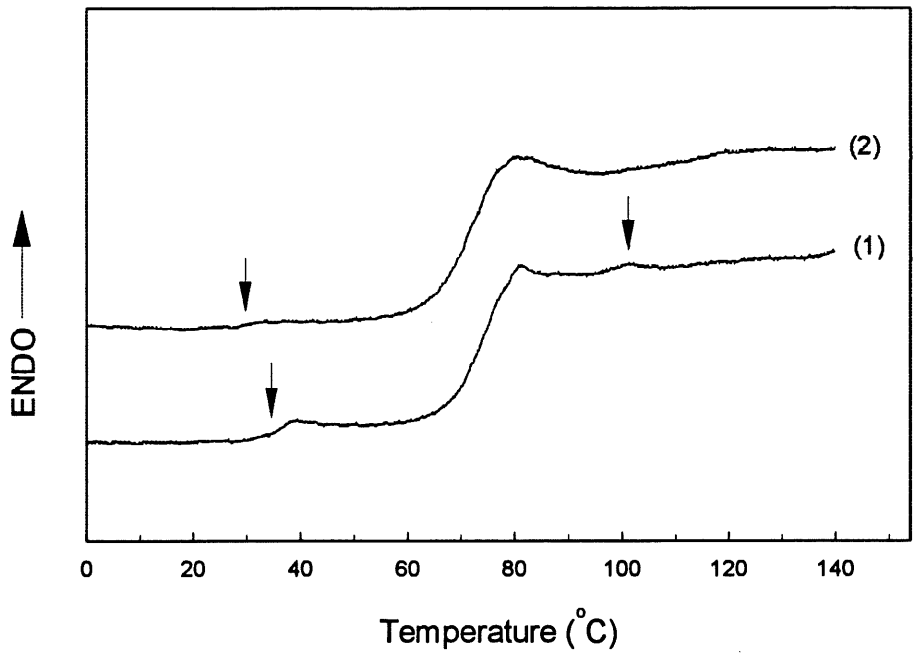

Figure 34. DSC heating curves of the blends containing 10 wt % of (1) A2, and (2) B2, showing the phase separation in the blends.

3.3.2 Orientation behaviors

Before discussing the results regarding the orientation of the mesogenic groups upon stretching, it must be emphasized that in this study the measured draw ratio was for the macroscopic deformation of the blend films and, as a first approximation, the actual draw ratio of the LCP phase in the blends was assumed to be similar. As will be shown later, as the main parameter used to characterize the orientation behavior was the maximum macroscopic orientation which was achieved at low deformations for all the samples, this assumption has no consequences on the discussion revealing the effects of the ionic aggregates.

3.3.2.1 Ionomers with biphenyl moieties

First, let us look at the stress-induced orientation behavior of the LCP samples containing a biphenyl moiety in the side group (series A). The orientation development in all blends upon stretching at 80 °C is shown in *Figure 35*, where the orientation parameter P_2 is plotted versus draw ratio. From *Figure 35a*, it is seen that the macroscopic orientation of the mesogenic groups is grown perpendicularly with respect to the stretching direction, as is revealed by the negative P_2 values. This is a phenomenon often observed for the LCPs having an odd number of CH_2 units in the flexible spacer which links the mesogenic groups to the chain backbone, and it has been attributed to a perpendicular coupling of the mesogenic groups with respect to the chain backbone, whose orientation should be parallel to the stretching direction (31). Comparing the different blend samples, it is clear that the orientation in the ionomers, regardless of the ion content, is similar to that of the polymer containing no ionic groups; the orientation in all samples seems to increase continuously with the extension, and a maximum P_2 of about -0.26 is obtained relative to -0.5 in case of a perfect perpendicular orientation of all the mesogenic groups. For comparison the orientation of the PVC matrix in the stretched samples is shown in *Figure 35b*. Based on the positive P_2 values, this orientation is along the stretching direction, and no difference is notable between the blends. A perfect orientation along the stretching direction corresponds to $P_2 = 1$.

The influence of the stretching temperature on the obtained orientation was also studied. The results for the samples stretched at different temperatures to a draw ratio of 2.5 are presented in *Figure 36*. *Figure 36a* shows the plot of P_2 of the mesogenic groups versus the stretching temperature. By inspection of the data, it is evident that when the samples are stretched at $T < T_{ni}$, i.e., in the nematic state, the orientation remains almost unchanged for all the samples while when the stretching experiments are carried out at $T > T_{ni}$ the achieved orientation drops drastically. As the samples have different T_{ni} depending on the ion content (*Table 5*), this feature is better illustrated in *Figure 36b* where P_2 is plotted versus the stretching temperature

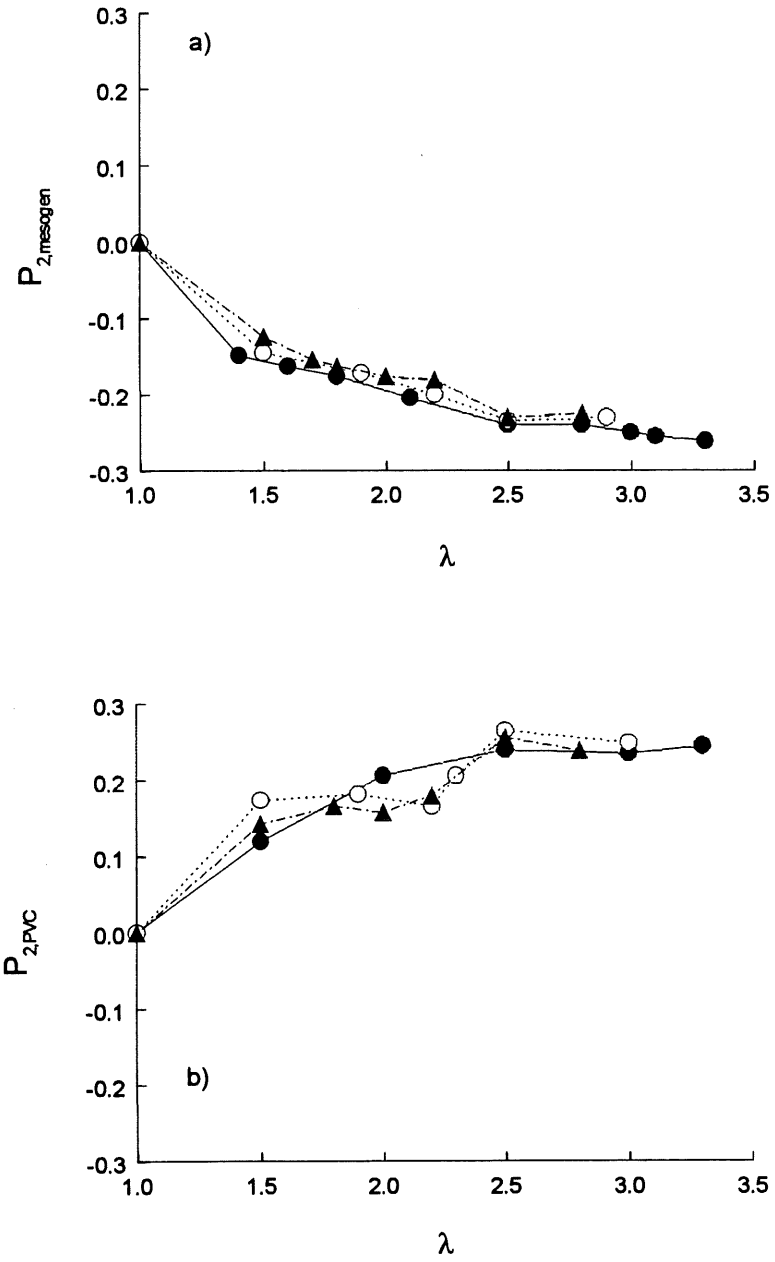

Figure 35. Orientation parameter of (a) the mesogenic groups and (b) the PVC matrix versus draw ratio for the blends containing the polymer and the ionomer samples in the series A: A1(●), A2(○) and A3(▲). The blend samples were stretched at 80°C.

normalized to T_{ni}, namely, the reduced temperature. Indeed, within the errors of the measurements, all data fall into a same curve showing the drop of P_2 at the region where T/T_{ni} = 1. Although the LCP samples were blended with PVC it was expected that their stress-induced orientation was essentially independent of the PVC matrix. This is consistent with *Figure 36c* showing P_2 of PVC at different stretching temperatures. The drop of the orientation of the mesogenic groups shows no consequence on the PVC orientation in all the blends, which is almost constant over the temperature range investigated. The results in *Figures 35* and *36* indicate that, for the series A-samples, the ionic aggregates in the ionomers have no effects on the stress-induced macroscopic orientation of the mesogenic groups, which can only be achieved by applying a mechanical stress to the samples in their nematic state.

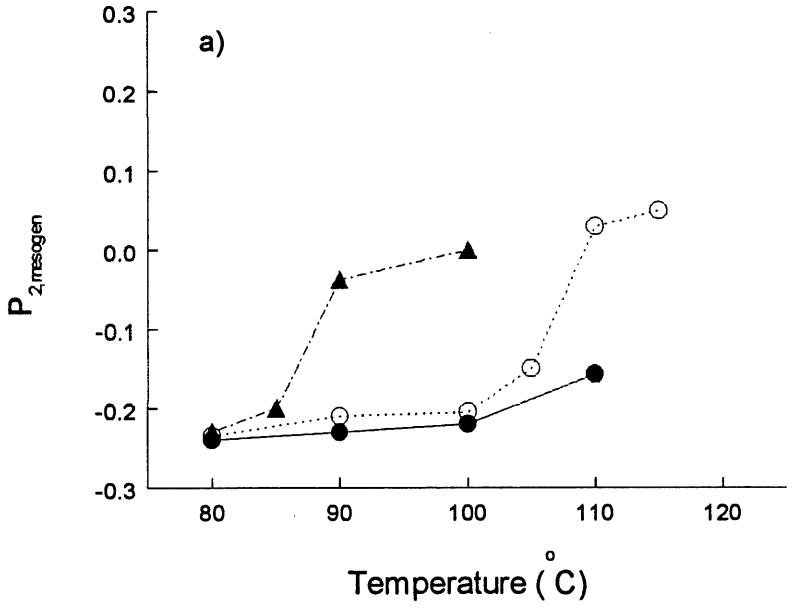

Figure 36. (a) Orientation parameter of the mesogenic groups versus stretching temperature for the blends containing the polymer and the ionomer samples in the series A: A1(●), A2(○) and A3(▲). The blend samples were stretched to λ=2.5.

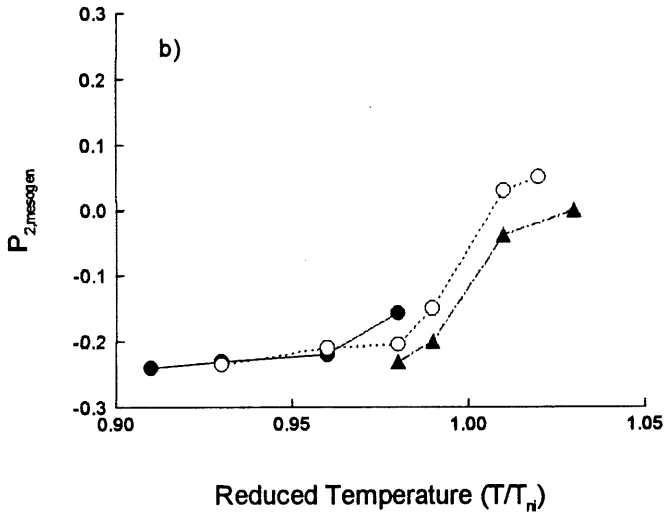

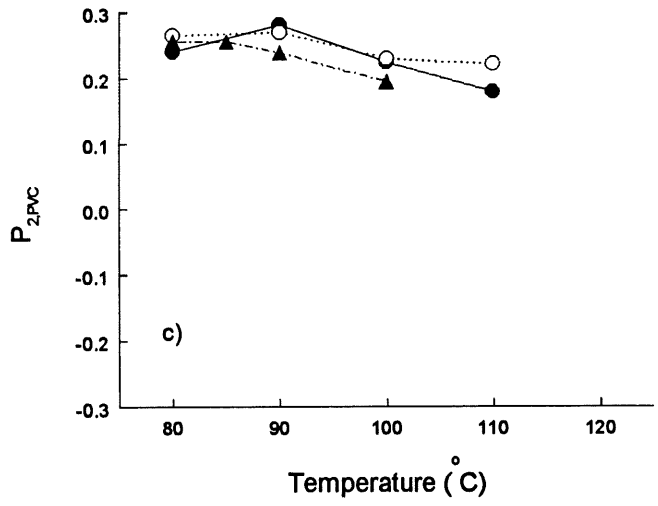

Figure 36. **(b) orientation parameter of the mesogenic groups versus reduced stretching temperature, and (c) orientation parameter of the PVC matrix versus stretching temperature for the blends containing the polymer and the ionomer samples in the series A: A1(●), A2(○) and A3(▲). The blend samples were stretched to λ=2.5.**

3.3.2.2 Ionomers with phenyl benzoate moieties

Now, for the blends with the LCP samples carrying a phenyl benzoate moiety in the side group (series B), the results on the stress-induced orientation are totally different. *Figure 37* shows the plots of P_2 versus draw ratio for the samples having different ion contents and stretched at 100°C. In contrast with the LCP samples of the series A, the macroscopic orientation of the mesogenic groups, shown in *Figure 37a*, is parallel to the stretching direction. Moreover, in all cases P_2 rapidly attains a plateau values at a draw ratio of about 1.8. This plateau value can be considered as the achievable orientation upon stretching, which corresponds to a monodomain structure with a maximum alignment of the directors of the nematic domains. Therefore, it is evident that in these systems the ionic aggregates have a strong effect on the macroscopic orientation since *Figure 37a* shows that the achievable orientation is systematically lowered as the ion content in the ionomer is higher. This result suggests that the ionic aggregates could reduce the nematic order characterizing the intrinsically oriented microstructure and, hence, lower the macroscopic orientation induced by external aligning fields. This is not unreasonable. An ionic aggregate is an association of several ion pairs, and the polymer chains which are anchored to the aggregates have a reduced number of available conformations; consequently the neighboring mesogenic side groups could suffer from this effect and distort the local nematic order. On the other hand, from *Figure 37a*, the rate of the transition from a polydomain to a monodomain structure upon extension is not affected by the ionic aggregates. Also, once again, the orientation of the PVC matrix in these blends shows no difference, as can be seen in *Figure 37b*, and it is much lower than that of the mesogenic groups.

More interestingly, the achievable orientation was determined at different stretching temperatures, and the results are given in *Figure 38*. *Figure 38a* shows that the lowering of the orientation of the mesogenic groups is observed at all the temperatures and the orientation for each sample is almost independent of the stretching temperature, and no drop of the

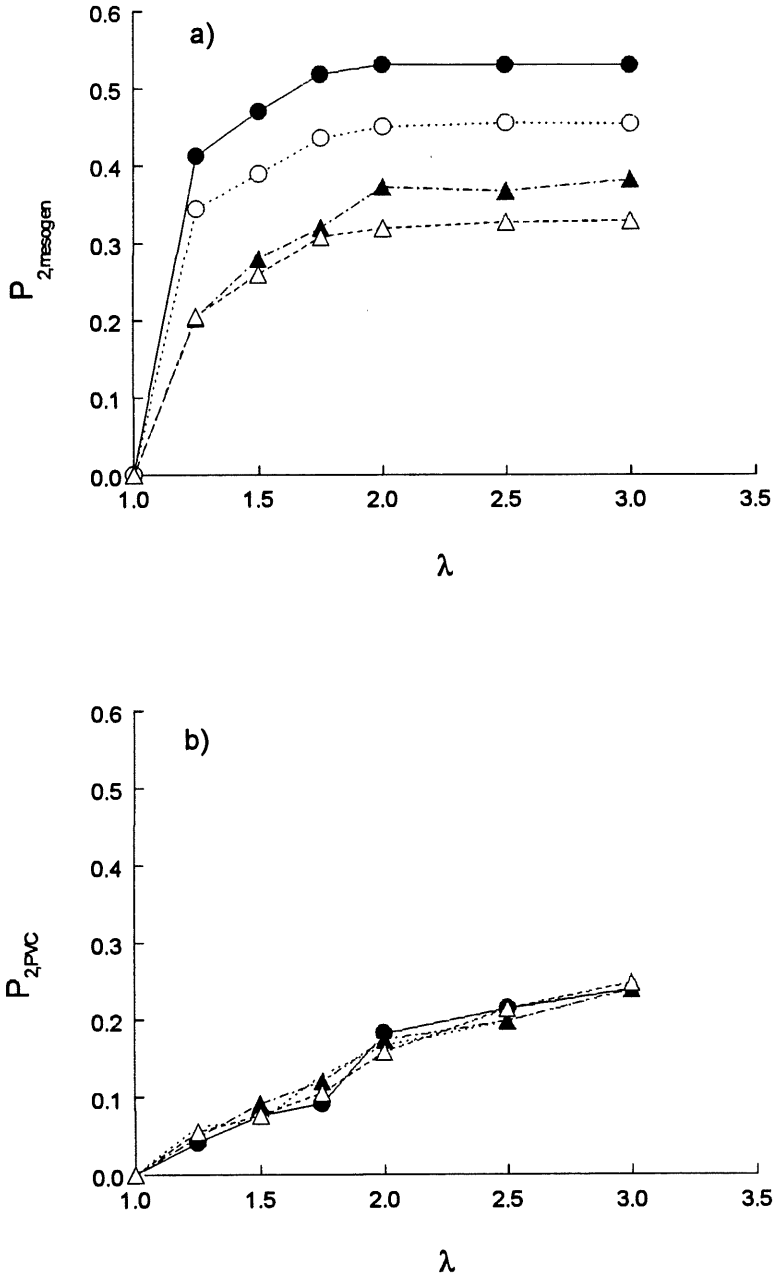

Figure 37. Orientation parameter of (a) the mesogenic groups and (b) the PVC matrix versus draw ratio for the blends containing the polymer and the ionomer samples in the series B: B1(●), B2(○), B3(▲) and B4(Δ). The blend samples were stretched at 100°C.

orientation occurs over the entire temperature range investigated. As the samples have different T_{ni} (*Table 5*), in *Figure 38b* is also shown the orientation results expressed on plotting P_2 versus T/T_{ni}. Here it should be mentioned that the range of the stretching temperatures was limited by the fact that the films broke when stretched at lower or higher temperatures. It can be seen in *Figure 38b* that for B1, the polymer containing no ionic groups, all the stretching temperatures are below its T_{ni}, i.e., $T/T_{ni} < 1$, while for two of the ionomers, B2 and B3, the temperatures cover both the nematic and the isotropic state, and for B4, which has the lowest T_{ni}, all the temperatures are above its T_{ni}. Surprisingly, even though the samples were stretched in the isotropic state almost the same achievable orientation was obtained as when they were stretched in the nematic state. This behavior is clear for B2 and B3 and, based on the whole of the results in *Figure 37* and *38*, should be expected for B1 and B4. This is an interesting and unexpected result, and contradicts the general finding revealed in *Figure 36* as well as in our previous studies (21, 29), that is, if a nematic polymer is

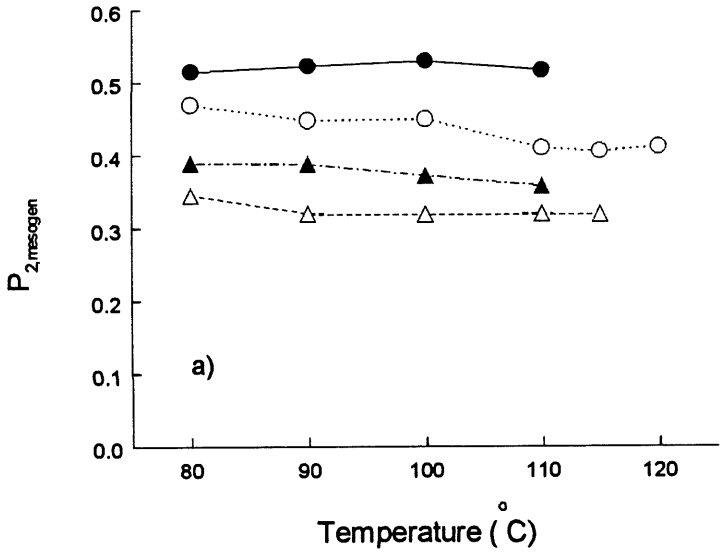

Figure 38. **(a) Orientation parameter of the mesogenic groups versus stretching temperature for the blends containing the polymer and the ionomer samples in the series B: B1(●), B2(○), B3(▲) and B4(Δ). The blend samples were stretched to $\lambda = 2$.**

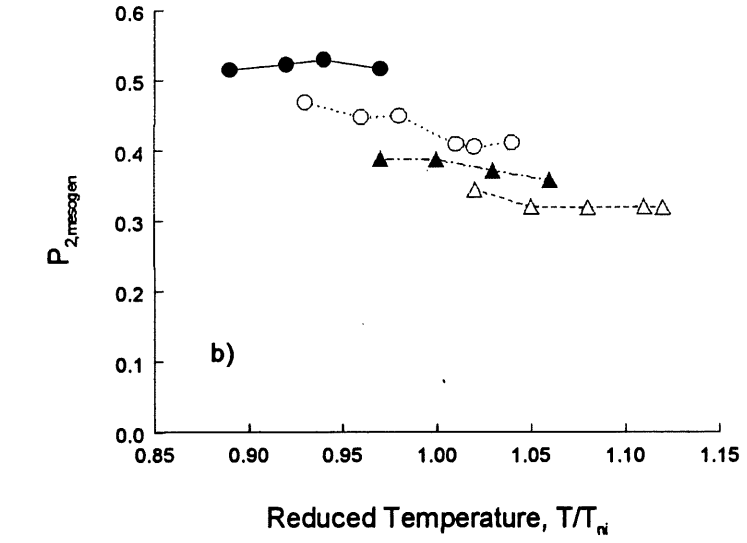

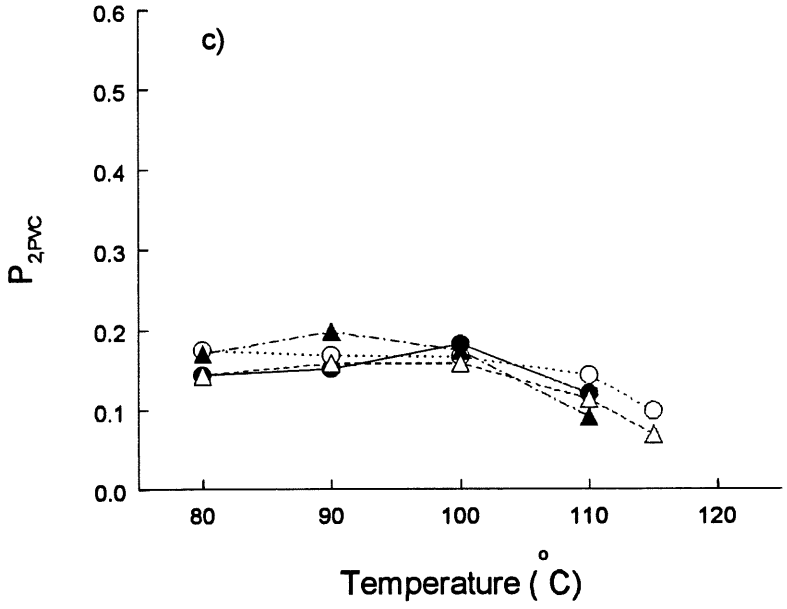

Figure 38. **(b) orientation parameter of the mesogenic groups versus reduced stretching temperature, (c) orientation parameter of the PVC matrix versus stretching temperature for the blends containing the polymer and the ionomer samples in the series B: B1(●), B2(○), B3(▲) and B4(Δ). The blend samples were stretched to $\lambda = 2$.**

stretched (or deformed) in the isotropic state the absence of the nematic domains, which means the absence of cooperative effects, there is no macroscopic orientation of the mesogenic groups. Before discussing this phenomenon it can be noted, from *Figure 38c*, that the PVC matrix in all blends shows a similar orientation. The decrease in its orientation level at the higher stretching temperatures arises from a more important chain relaxation.

The underlying orientation mechanisms which lead to this observed macroscopic orientation at stretching temperatures above T_{ni} have been investigated. *Figure 39* shows the results of a series of experiments conducted on B3, the ionomer having a T_{ni} at about 90 °C. Using a

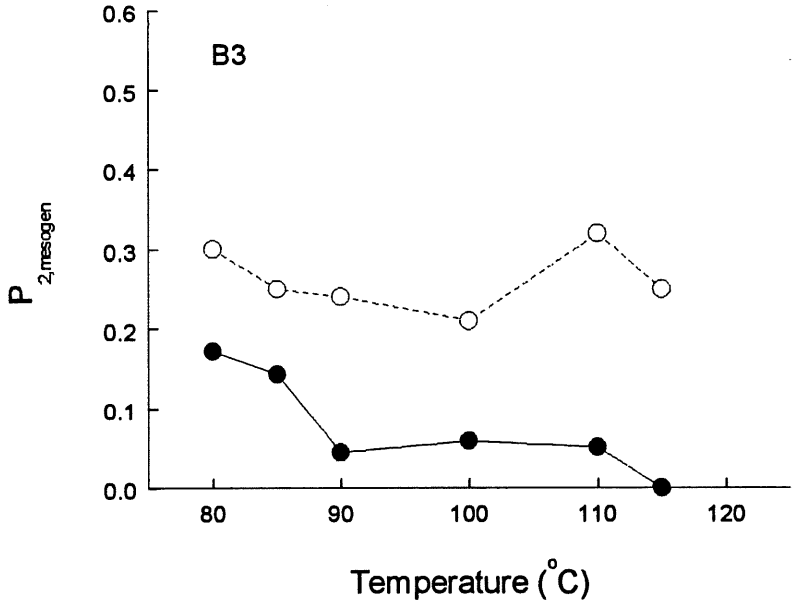

Figure 39. Orientation parameter of the mesogenic groups versus stretching temperature for the blend containing B3, stretched to $\lambda = 2$. The orientation measurements were made (1) immediately following stretching with the sample held at the stretching temperature (●), and (2) after cooling under strain of the sample to room temperature (○).

stretching apparatus placed in a temperature-controlling unit designed for making polarized infrared measurements at high temperatures, the B3 blend films were stretched to a draw ratio of 2 at different temperatures. For each film, immediately after the stretching, instead of quenching it, the orientation measurements were performed (the required time was about 8 min); then it was cooled under strain to room temperature and the orientation was determined once again. As can be seen from *Figure 39*, when the film was stretched at $T < T_{ni}$ the stretching did result in a macroscopic orientation of the mesogenic groups while at $T > T_{ni}$ there was only a slight orientation, and when the film was stretched at 115 °C there was no orientation at all. But, following the cooling under strain at room temperature a uniform macroscopic orientation was obtained for all the stretching temperatures. This result clearly indicates that, for this particular blend system, the main effect of the cooling process is not, as has been believed, to preserve the macroscopic orientation induced by the stretching, but is to induce or complete this orientation. With the stretching temperatures below T_{ni}, the orientation arising from the stretching is enhanced during the cooling while at $T > T_{ni}$ almost the whole orientation takes place during the cooling. We have further examined this phenomenon by doing other experiments. *Figure 40* shows the orientation development during the cooling process under strain. For this experiment a B3 film was stretched at 115 °C to $\lambda = 2$, and the measurements showed no orientation; then the film was allowed to cool by opening the cover of the oven, and subsequent orientation measurements were made at different temperatures. As indicated by the cooling curve of the oven, which is also given in *Figure 40*, the temperature dropped rapidly to about 82 °C after the first 3 min, and then was down at almost a constant rate (~0.6°C/min). Taking into account a probable gap of several degrees between the indicated temperature of the oven and the sample temperature, it is clear that the macroscopic orientation started to grow, apparently linearly, once the sample passed from the isotropic state into the nematic state, and it reached a plateau value at about 60 °C and remained constant at lower temperatures. Moreover, as also shown in *Figure 40*, this orientation process was totally reversible. When the film was reheated to 115 °C the

orientation was lost, and by cooling under the same conditions the same orientation growth was found.

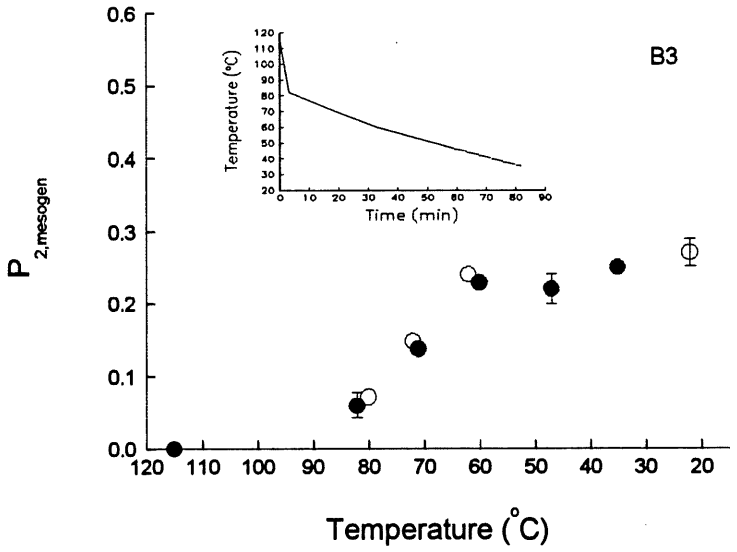

Figure 40. Orientation parameter of the mesogenic groups versus temperature for the blend containing B3, stretched to $\lambda = 2$ at 115°C and then allowed to cool under strain (●). The sample was then reheated to 115°C and re-cooled under strain (○). The cooling curve of the oven is shown, indicating a cooling rate of about 0.6°C/min.

There are two possible mechanisms responsible for the above results. A stretched film cooled under strain means that it is under the effect of a mechanical force that sustains the extension of the film. As a consequence, the nematic domains formed while the LCP sample is cooled to $T < T_{ni}$ could have a quick response to the stress field by alignment along the field direction. For the blends studied here, it is reasonable to say that most of the mechanical force is related to the extension (orientation) of the PVC matrix (90% in weight), and basically this field is effective to the stretched film until the PVC chains are completely immobilized at temperatures below its T_g. If this is the case, the interfacial interactions between the phases of both polymers could play a determining role in the transfer of the stress field to the LCP

sample, which is necessary for the alignment. We have carried out some experiments aimed at verifying this mechanism. *Figure 41* shows the results of the orientation of the B3 films quenched at room temperature after being stretched at 80 °C and 115 °C to $\lambda = 2$ and, before the quenching, held at these temperatures for different lengths of time. It was expected that the orientation relaxation of the PVC matrix could take place and, thus, reduce the mechanical force acting on the stretched film before the cooling. Although it seems that the samples immediately quenched after the stretching (with the least PVC relaxation before quenching) show the highest level of the orientation, a clear assessment about the effect of the matrix polymer's relaxation cannot be made, since the samples relaxed for different times have a similar orientation after cooling. This can be due to the fact that the orientation relaxation of the PVC at these temperatures is slow, in other words, the lowering of the stress field is not

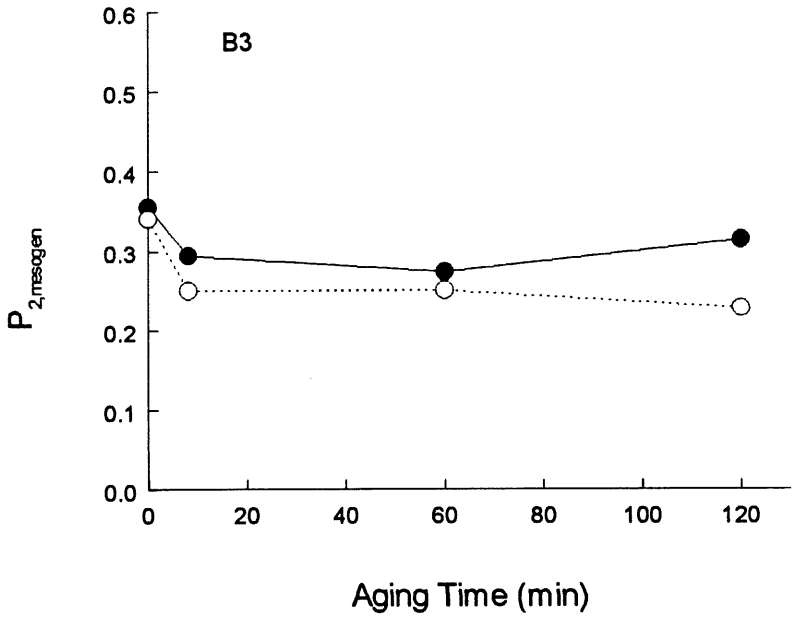

Figure 41. Orientation parameter of the mesogenic groups versus aging time for the blend containing B3, stretched to $\lambda = 2$ at 80°C (●) and 115°C (○), and held at these temperatures for different lengths of time before quenching at room temperature.

significant. Actually, even the stress field is much diminished it can still be sufficient enough to initiate the alignment of the nematic domains once the LCP samples enter into their liquid crystalline state.

The other possibility is an important role of the orientation of the LCP chain backbone in the orientation of the mesogenic groups during the cooling. The chain backbone of the LCP sample should be expected to align during the stretching along the field direction. This means an anisotropic environment for the mesogenic groups in the isotropic state, and once the nematic order is reformed among them during the cooling the nematic domain directors could tend to follow this anisotropy and to align, owing to the coupling between the mesogenic groups and the chain backbone. Unfortunately, in the present study, because of the overlapping of the infrared bands, we could not determine the orientation of the chain backbone to get a closer insight into its relation with the orientation of the mesogenic groups during the cooling. However, based on some previous investigations (21, 29, 32), the orientation of the chain backbone could be expected to be very low as compared with the orientation of the mesogenic groups.

Now, as the films of the blend containing the initial polymer B1 could not be stretched at $T > T_{ni}$, the question that can be asked is whether this orientation development during cooling under strain is a property related to the ionic aggregates in the ionomers. We conducted some experiments for answering this question. A poly(methyl methacrylate) (PMMA) sample, whose T_g, ca. 110°C, is higher than that of PVC, was utilized as the matrix, which allowed the blend samples to be stretched at higher temperatures. Two blends containing 10 wt % of the initial polymers, B1 and A1, respectively, were prepared for the experiments. The films were stretched at T_{ni} +15 °C, i.e., 137 °C for the B1 blend and 132 °C for the A1 blend, and then allowed to cool under strain, under the same conditions described for the experiment of *Figure 40*, while the orientation measurements were made at different temperatures. It can be seen in *Figure 42* that in both cases no orientation of the mesogenic groups was achieved after

stretching, and as the samples were cooled onto the liquid crystalline state a macroscopic orientation along the stretching direction was induced for B1, as occurred for its ionomers (*Figure 40*), while for A1 no macroscopic orientation perpendicular to the stretching direction was observed, as for its blend with PVC as matrix. However, it is interesting to notice that a slight parallel orientation can be seen. These results, obtained with a different polymer matrix, confirm that the orientation induction during cooling under strain is characteristic for B1, and does not result from the presence of the ionic aggregates.

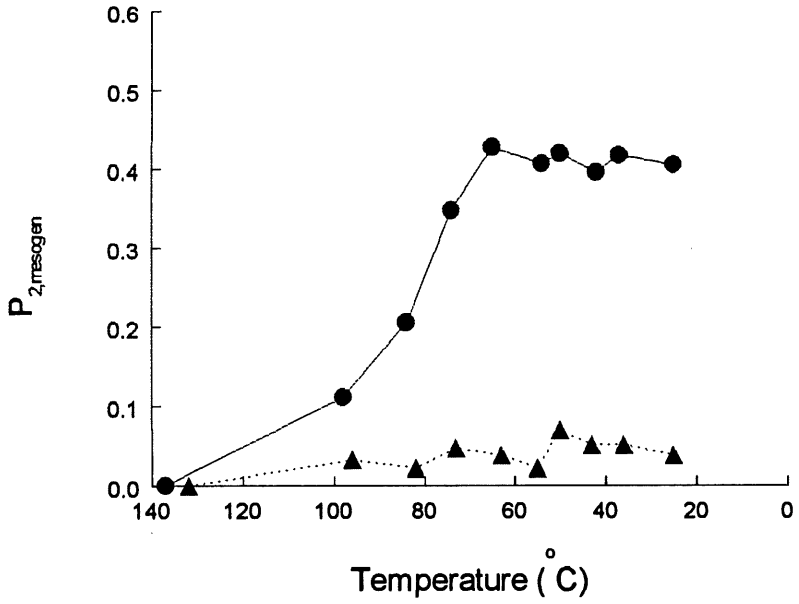

Figure 42. Orientation parameter of the mesogenic groups versus temperature for the PMMA blends containing A1 (▲) and B1 (●), stretched to $\lambda = 2$ at T_{ni} +15 °C and then allowed to cool under strain. The cooling curve is similar to that shown in *Figure 40*.

The fact that this macroscopic orientation of the mesogenic groups occurred during cooling and under strain cannot be observed for every LCP sample in the blend, like those of the series A, must be attributed to their differences in the factors discussed above. As has been mentioned, the DSC measurements seem to indicate stronger interfacial interactions in the

blends containing the samples of the series B, which is consistent with the observed orientation behavior.

3.4 Conclusion

The stress-induced macroscopic orientation of the mesogenic groups in two series of side-chain LC ionomers was studied and compared to the corresponding polymers containing no ionic groups. The investigations were made possible by blending the LCP samples with an immiscible PVC matrix and stretching the blend films. Very distinct orientation behaviors were found for the LCP samples having different mesogenic units in the side group. For the ionomers prepared from a polyacrylate bearing a biphenyl moiety in the side group (series A) their orientation behavior, regardless of the ion content, was found to be similar to that of the initial polymer: (1) the orientation develops in the same manner with extension (2) the achievable orientation is of the same magnitude and (3) the macroscopic orientation can be induced only by stretching the sample in the nematic state. In contrast, for the ionomers based on a polyacrylate carrying a phenyl benzoate moiety in the side group, the ionic aggregates display profound effects on the macroscopic orientation of the mesogenic groups; the level of the achievable orientation is systematically lowered as the ion content in the ionomer is higher. This suggests a reduced nematic order, i.e., a lesser oriented microstructure in these ionomers. More interestingly, it was found that the stress-induced orientation was almost constant when the blend films were stretched either in the nematic state or in the isotropic state. Studying the underlying orientation mechanisms, it was found that the observed macroscopic orientation was mainly achieved during the cooling of the samples under strain. Our results show that when the sample is stretched at $T < T_{ni}$, only a partial orientation of the mesogenic groups is induced, and this orientation is improved during the cooling process while when the sample is stretched at $T > T_{ni}$ only little or no orientation is induced by the stretching and the cooling under strain of the sample into the nematic state is accompanied by the appearance of the macroscopic orientation. The interfacial interactions between the phases of both

polymers, which could be important for the stress field transfer to or build up on the LCP component, as well as the orientation of the LCP backbone in the blends are suggested as being among the factors which can affect this orientation process during cooling and under strain.

CHAPTER 4

MESOPHASE TRANSITION-INDUCED REORIENTATION IN A STRETCHED SIDE-CHAIN LIQUID CRYSTALLINE POLYMER

4.1 Background

It is well known that mechanically stretching SCLCPs can lead to a monodomain structure as a result of the alignment of the liquid crystalline domains (1, 2). The monodomain structure, which is a prerequisite for the applications of SCLCPs, is characterized by a macroscopic and uniform orientation of the mesogens. It is of interest to investigate the relaxation behavior of this macroscopic orientation in stretched SCLCPs under strain. For instance, when a stretched SCLCP film is heated to the vicinity of its liquid crystalline to isotropic state transition, one would like to know whether the observed orientation relaxation is simply due to the thermally-induced disordering and isotropization eventually, or the aligned directors of the LC domains could be relaxed relative to the stretching direction before the isotropization. The infrared dichroism technique is a powerful tool for studying the molecular orientation and relaxation. But in contrast with amorphous polymers like PS or PMMA, such orientation relaxation experiments on stretched thin films of pure SCLCPs are difficult, if not impossible, to carry out because of the difficulties in preparing and stretching thin films. Nevertheless, investigations on SCLCEs have been reported (11, 12, 31). When a stretched SCLCE film is heated under strain to the isotropic state the stretching-induced macroscopic orientation is lost, but when the stretched sample is cooled again into the nematic phase the macroscopic orientation is recovered as a result of the anisotropic network conformation. For the nematic liquid single crystal elastomers (12), the network anisotropy and thus the monodomain structure can be chemically locked in by a two-step synthesis. This procedure further ensures

a permanent orientation of the mesogens at temperatures below the isotropization temperature.

In our (29) recent effort of studying the orientation in SCLCPs by means of the infrared dichroism method, two effective approaches were employed to realize a mechanical stretching of thin films of SCLCPs and to induce a macroscopic orientation. In one, the SCLCP film is cast onto the surface of a supporting poly(vinyl alcohol) (PVA) film, which is then subjected to the stretching. The other method (21) is based on making and stretching the film of an immiscible blend composed of a SCLCP and a non-liquid crystalline polymer. Though there is an obvious complication due to the interfacial or surface effects, those methods make it possible to investigate the orientation and relaxation behavior of SCLCPs through infrared dichroism. We have demonstrated that a careful analysis of the results could generate interesting and useful information (33, 34). As the orientation relaxation is concerned, we showed (35) some intriguing observations on a nematic SCLCP carrying a phenyl benzoate moiety as the mesogen and 6 methylene units in the flexible spacer, the SCLCP film being cast on the PVA film for the stretching. We showed that when the stretched film was heated under strain the stretching-induced parallel orientation of the mesogens started to disappear in the nematic to isotropic transition region, but within a narrow temperature range not far above the transition, about 4 °C, the totally relaxed macroscopic orientation could be recovered rapidly by cooling the sample into the nematic phase. The effect is similar to what is known for SCLCEs. Further, it was shown that a possible alignment effect of the supporting PVA film surface could not be the main reason for the observed orientation recovery. In order to explain this observation we have tentatively suggested a temperature regime prior to the equilibrium isotropization, over which the thermal fluctuation could make lost completely the macroscopic orientation by randomizing the mesogens, but the molecular environment (e.g. chain backbone) remained such that when the SCLCP was cooled into the nematic phase the mesogens were realigned along the oriented nematic director before the relaxation.

As a continuation of the previous study, we have investigated more SCLCPs stretched on a PVA film. In this chapter, we show the results obtained on a SCLCP displaying a broad smectic-A phase and a very narrow nematic phase below the isotropic state. A new peculiar phenomenon, namely, mesophase transition-induced reorientation, as well as a more prominent orientation recovery are observed.

4.2 Experimental

The SCLCP investigated in this work, referred to as BiPA5 hereafter, has the monomeric structure shown below, and was synthesized according to the method reported in the literature (5). The sample has a $\overline{M}_n$ of 79,000 and a $\overline{M}_w / \overline{M}_n$ of 1.8 (estimated from GPC using polystyrene standards).

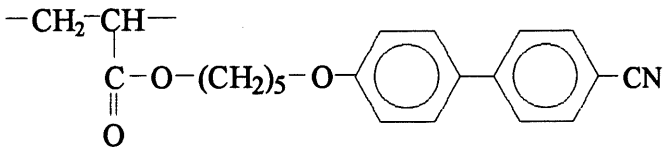

BiPA5 is known to exhibit a partially bilayered smectic-A phase over a broad temperature range and a very narrow nematic phase below the isotropic state (36, 37). The phase behavior was confirmed for our sample. *Figure 43* shows its DSC heating curve (second scan), recorded on a Perkin-Elmer DSC-7 at a heating rate of 10 °C/min. A T_g of 39 °C and two transition peaks centered at 115 °C and 118 °C can be noticed. The narrow nematic phase is located between the two transition peaks. Also in *Figure 43* are shown the polarizing optical micrographs taken respectively at 117 °C and 105 °C, using a Leitz DMR-P microscope. The Schlieren texture of the nematic phase at 117 °C changes to a focal conic texture of the smectic phase at 105 °C, and some strips associated with the nematic to smectic-A transition can also be seen. The micrographs taking at 105 °C was performed after an isothermal annealing of 20 hours. The film samples used for the mechanical stretching were prepared by

utilizing our (29) established procedure. The film of BiPA5 had a thickness of about 40 μm, and that of PVA about 100 μm. Unless otherwise stated, the films were stretched at 105 °C (in the smectic phase) to a draw ratio of 3, i.e., 200% elongation.

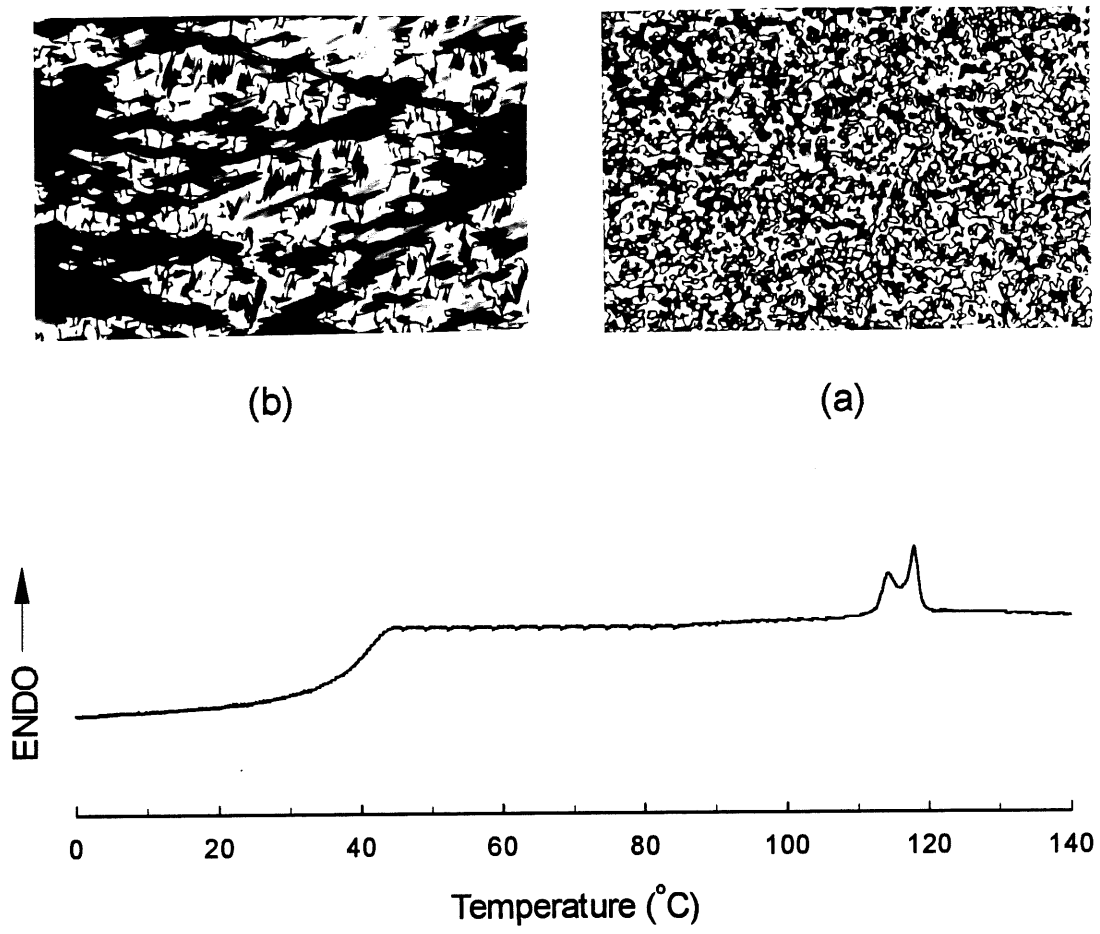

Figure 43. DSC heating curve and polarizing optical micrographs at (a) 117 °C and (b) 105 °C for BiPA5. Magnification : 280x.

The details about the experimental set-up used for monitoring the orientation relaxation through the infrared dichroism were already described in the literature (35). In essence, a temperature controlling cell, in which the stretched (oriented) film was held under constant strain, was mounted in the sample compartment of a Bomen MB-102 FTIR spectrometer, and a wire-grid polarizer was placed between the temperature controlling cell and the DTGS

detector for the taking of the polarized infrared spectra. For a given temperature the orientation parameter P_2, calculated from the infrared dichroism, could be determined as a function of the thermal annealing time. As the taking of the two infrared spectra with the polarization direction parallel and perpendicular, respectively, to the film stretching direction needed about five minutes (50 interferograms for each spectrum), each P_2 data at a given annealing time is actually the average value over a period of five minutes beginning from the indicated time. The C≡N absorption band at 2230 cm^{-1} was used for the P_2 measurement for the mesogens. The mechanical stretching direction was always taken as the reference direction for the calculations. Here, it should be recalled that for a perfect orientation of the mesogens along the reference direction P_2 equals to 1; for a perfect perpendicular orientation it is -0.5; and it is 0 for the isotropic state (or isotropic materials) and also for SCLCPs having a polydomain structure before being aligned with a mechanical field, i.e., in the absence of a macroscopic orientation of the mesogens.

4.3 Results and Discussion

Stretching BiPA5 in its smectic phase at 105 °C results in a macroscopic orientation of the mesogens perpendicular to the stretching direction, as is indicated by a negative value for the orientation parameter. This is a phenomenon usually observed for smectic SCLCPs and nematic SCLCPs having an odd number of methylene units in the spacer (32, 38). It should be mentioned that the choice of the stretching temperature in this study is quite arbitrary since, over the smectic phase, it has no effects on the induced orientation at a draw ratio of 3.

Figure 44 shows the results of the orientation relaxation with time at different annealing temperatures. After the film is stretched at 105 °C the orientation is first measured, and a P_2 of about -0.2 is obtained; then the film is heated under strain to the pre-determined annealing temperature. The data for each temperature in *Figure 44* represents a separate experiment on a new film. At temperatures below 115 °C no orientation relaxation can be noticed, and the

change in the orientation parameter begins at 115 °C. At this temperature, the orientation is relaxed slowly; P_2 is lowered with time but is stabilized at about -0.1 after 2 hours, indicating that the orientation remains perpendicular to the stretching direction. When the temperature is set to 116 °C, 1 °C higher, a dramatic change in the orientation occurs. At the beginning, the orientation relaxation appears much faster, and $|P_2|$ drops. But surprisingly, the orientation is not randomized so that P_2 is 0, instead P_2 becomes positive. This change in the sign for the orientation parameter is completed within 30 min; a P_2 of about 0.2 is achieved after 50 min, and then remains stable with time. As a positive value of P_2 indicates a macroscopic orientation parallel to the stretching direction, it is clear that at 116 °C a reorientation of the mesogens occurs, leading to a flip in their alignment direction. This reorientation can also be observed at 117 °C, but the attainable parallel orientation is lower than that at 116 °C. Now, when the film is annealed at 118 °C the orientation relaxation

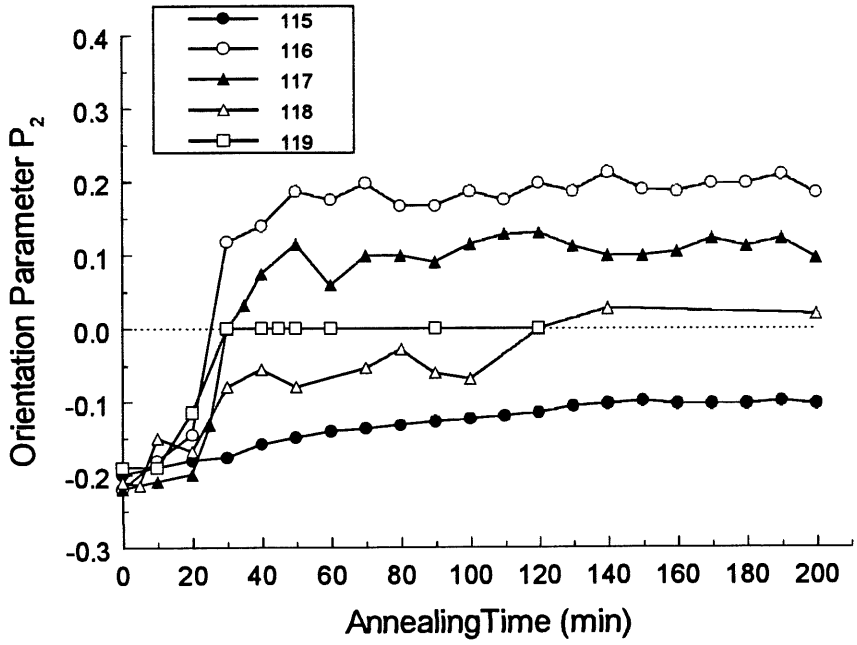

Figure 44. Orientation parameter vs annealing time for samples under strain and annealed at different temperatures as indicated in the figure.

obviously is still faster, but no rapid reorientation takes place; P_2 is lowered to a value near zero (slightly negative up to 2 hours and very slightly positive at longer times). Finally, at 119 °C it is seen that P_2 quickly falls to zero, and no macroscopic orientation is preserved in the stretched film.

Examining the phase transition behavior of BiPA5 as shown in *Figure 43*, it appears clear that the observed reorientation phenomenon would be related to the smectic-nematic transition. The narrow temperature range of 116-117 °C, over which the reorientation occurs, corresponds to the narrow nematic phase of BiPA5 beyond the smectic and below its isotropic state. In other words, this reorientation is induced by the mesophase transition. Indeed, this observation raises an interesting question as to know what will happen during a transition between different mesophases for a sample having a monodomain structure with the mesogens macroscopically oriented, and, in the present case, on the surface of a stretched PVA film. The situation is quite straightforward for un-stretched BiPA5 which has a polydomain structure having no macroscopic orientation of the mesogens. Essentially the transformation from a smectic phase to a nematic phase means that the smectic layers with randomly oriented plane normal disappear, and the nematic domains are formed with randomly oriented nematic directors. By contrast, what happens in the macroscopically oriented BiPA5 under strain remains to be understood. The reorientation revealed in *Figure 44* suggests that in the film stretched at 115 °C the aligned smectic layers have their plane normal aligned perpendicularly to the stretching direction, resulting in a negative P_2, and when the film is heated to 116 °C or 117 °C the transformation of the smectic layers to the nematic domains proceeds and is accompanied by a rotation of the mesogens, leading to nematic directors parallel to the stretching direction and a positive P_2. Now, back to the results in *Figure 44* for other annealing temperatures, it turns out that at 115 °C the sample does not reach the smectic-nematic transition temperature although the thermal fluctuations become important and lowers P_2, while at 118 °C and higher temperatures the sample enters into the isotropic phase too

quickly to stay long enough in the nematic phase, and, consequently, no reorientation can be observed.

We have performed more experiments in order to gain more information about this mesophase transition-induced reorientation of the mesogens. The results of one series of those experiments are depicted in *Figure 45*. A film, first stretched at 105 °C to reach a P_2 of -0.24, is continuously annealed under strain at different temperatures. The times at which a new temperature is set are indicated by the arrows in the figure. As has already been seen in *Figure 44*, when it is heated to 116 °C, the reorientation takes place with P_2 changing its sign rapidly and attaining a value of about 0.21. Now, after 30 min at 116 °C the stretched film is cooled back to 105 °C to make the nematic to smectic transition occur. If the reorientation process was reversible, it would be expected that P_2 change its sign again and become negative. It is seen from *Figure 45* that this is not the case. Under this nematic to smectic transition P_2 does not switch to a negative value but, contrarily, raises to about 0.34, indicating a better macroscopic orientation of the mesogens along the stretching direction in the smectic phase. The result indicates that the observed reorientation driven by the first smectic to nematic transition is not reversible during the subsequent nematic to smectic transition. The subsequent transition only results in an enhanced parallel orientation, which reflects a better ordering of the mesogens for the smectic phase as compared to the nematic phase. This is not surprising for BiPA5 considering the greater thermal fluctuations in the very narrow nematic phase close to the isotropization. The enhanced parallel orientation due to the subsequent nematic-smectic transition is, however, a reversible process since, as is seen in *Figure 45*, when the film is heated again to 116 °C P_2 is lowered to 0.21; and when it is cooled again to 105 °C P_2 recovers to 0.34. Now, when the stretched film is heated to 118 °C, closer to temperature of the isotropic state, P_2 drops to near zero ($\approx$ 0.07), and becomes 0.34 again upon cooling to 105 °C. This temperature changing cycle is repeated twice, as can be noted in *Figure 45*. Finally, heating the film to 121 °C gives rise to the isotropization, and P_2 falls to zero quickly. However, the parallel macroscopic orientation is totally recovered by

switching the temperature to 105 °C. The isotropization-orientation recovery cycle is observed for higher isotropization temperatures up to 140 °C (data till 130 °C are shown in *figure 45*). This orientation recovery behavior is similar to what is observed in our previous study for a nematic polymer (35), but it is much more prominent and is observed for a much wider range of the isotropization temperatures.

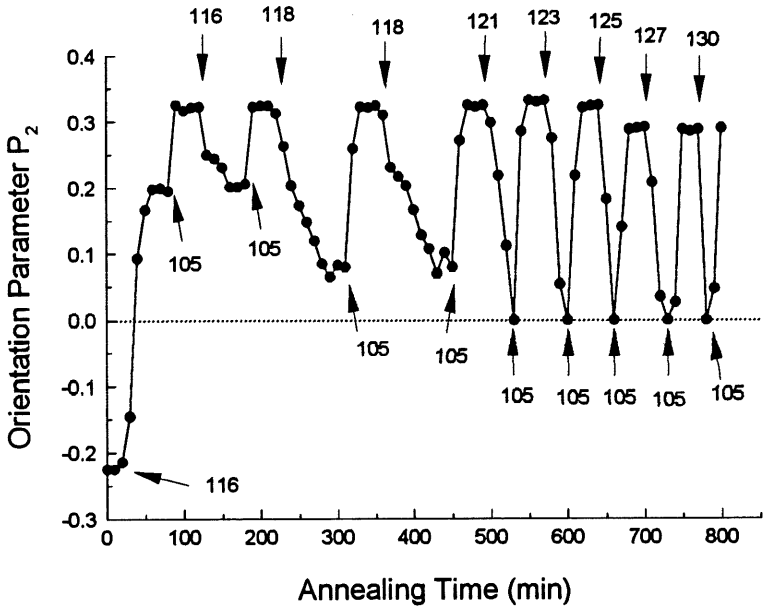

Figure 45. Orientation parameter vs annealing time for a sample under strain and annealed continuously at different temperatures indicated in the figure. The times at which the temperature changes are made are indicated by the arrows.

The essential of the above observations can be summarized by the schematic representation given in *Figure 46*. At this point the mechanism for the reorientation through rotation of the mesogens, i.e., from (a) to (b), is not clear yet and we will discuss this later. But the irreversibility of this phenomenon seems to be understandable. Energetically, a change from (b) to (c) should be easier than a change from (b) to (a), since the former necessitates only the displacement of the mesogens and their layering, while the latter needs a rotation as well as the displacement of the mesogens to form the smectic layers. It is interesting to mention that

when the stretched film in the situation (c) is subjected to a second stretching a perpendicular orientation is obtained again, confirming the formation of the smectic layers in the situation (c).

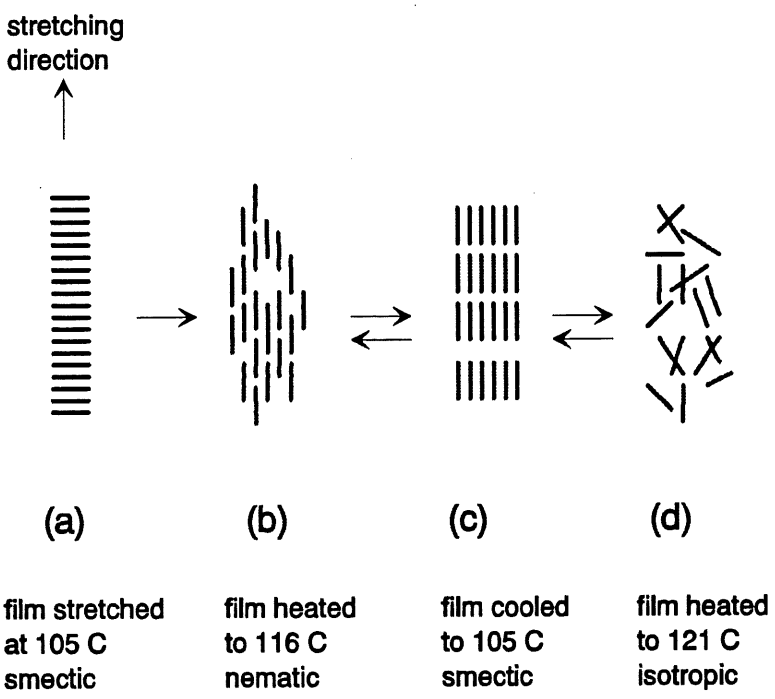

Figure 46. Schematic representation of the irreversible, mesophase transition-induced reorientation process (a-c) and the reversible orientation recovery (c-d).

The results of another experiment are also worth being presented. The reorientation during the first smectic-nematic transition is shown to be irreversible. In other words, once P_2 switches from a negative value to a positive value, the subsequent temperature change (and phase transitions) can no longer bring P_2 back to a negative value. The question we ask then is if the reorientation is interrupted somewhere in the course of the process by cooling the film back to the smectic phase, can P_2 return to the initial negative value. *Figure 47* shows the results for a stretched film heated to 115 °C, 1 °C below the smectic-nematic transition, to make sure that P_2 can not change its sign. It is clear that when the perpendicular orientation is

relaxed to $P_2 \approx$ -0.1, cooling the film to 105 °C can bring P_2 back to almost the initial value, -0.21. *Figure 48* shows the results for a stretched film heated to 116 °C. At this temperature the negative P_2 falls rapidly, but we manage to be able to change the temperature to 105 °C at the time where P_2 is about to cross the zero line and to change its sign (as can be seen in *Figure 48*, the temperature change is made at $P_2 \approx$ -0.02,). Interestingly, the reorientation is effectively stopped, but P_2 can no longer recover its initial value at 105 °C (P_2 = -0.22). Instead, a zero P_2 is found at this temperature, and it is stable over a period of time of 70 min. Afterwards, when the film is re-heated to 116 °C, the reorientation process just continues from the zero-P_2 state, and is completed quickly to attain a positive P_2 of about 0.2. Now, when the film is cooled back to 105 °C or a still lower temperature in the smectic phase, as discussed above from *Figure 45*, only an enhanced parallel orientation can be induced.

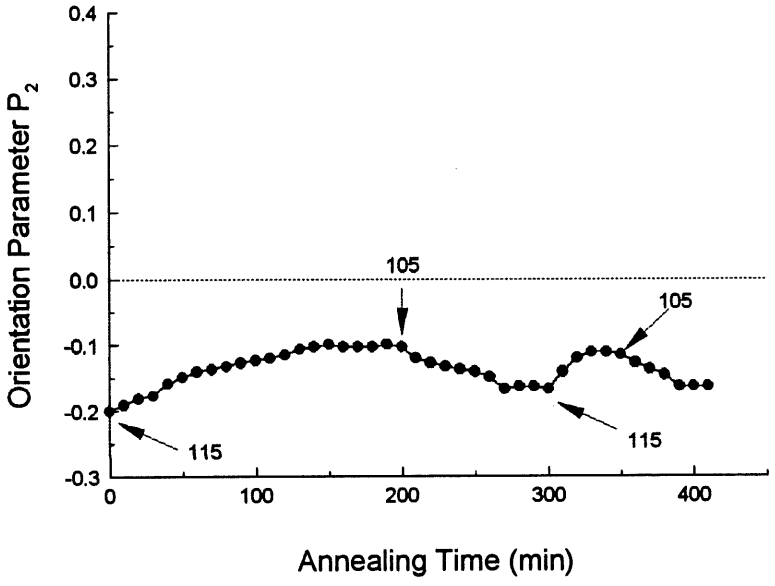

Figure 47. Orientation parameter vs annealing time for a sample under strain and annealed alternatively at 115 and 105 °C. The times at which the temperature changes are made are indicated by the arrows.

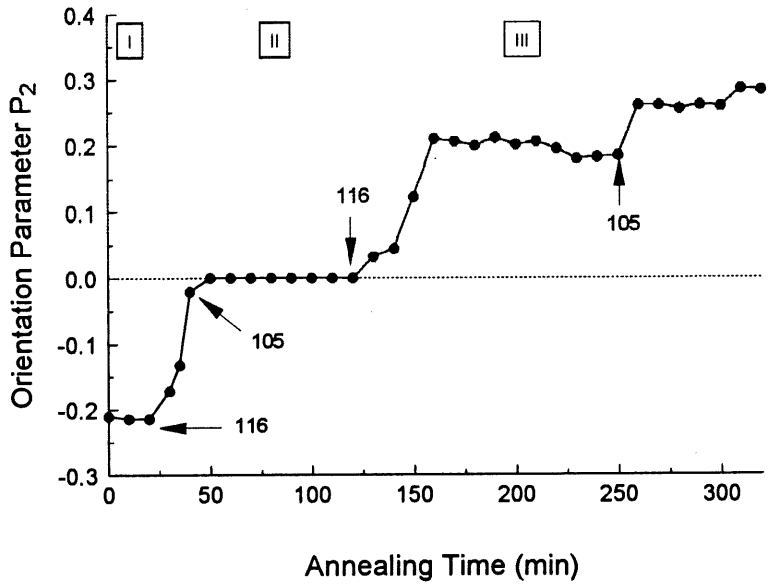

Figure 48. Orientation parameter vs annealing time for a sample under strain and annealed alternatively at 116 and 105 °C. The times at which the temperature changes are made are indicated by the arrows.

The results in *Figure 48* are interesting because they allow us to see more features of the reorientation process. Basically, the results indicate that the reorientation, once started, can be stopped before the mesogens change the orientation direction, and then can re-start under appropriate conditions. For the convenience of our discussion, three regions are assigned in *Figure 48*. On the basis of the observed orientation of the mesogens, the state of alignment of the LC domains in the three regions can be schematically represented in *Figure 49*. The question is about the mechanism via which the reorientation from region I to region III takes place during the smectic to nematic transition. One thing is certain: the transition involves a melting of the smectic layers and the formation of the nematic domains. Obviously, if no rotation of the mesogens occurred during the transition, the nematic domains formed would have the nematic directors aligned perpendicularly to the stretching direction, hence preserving the perpendicular orientation. Therefore, there must be a rotation of the mesogens

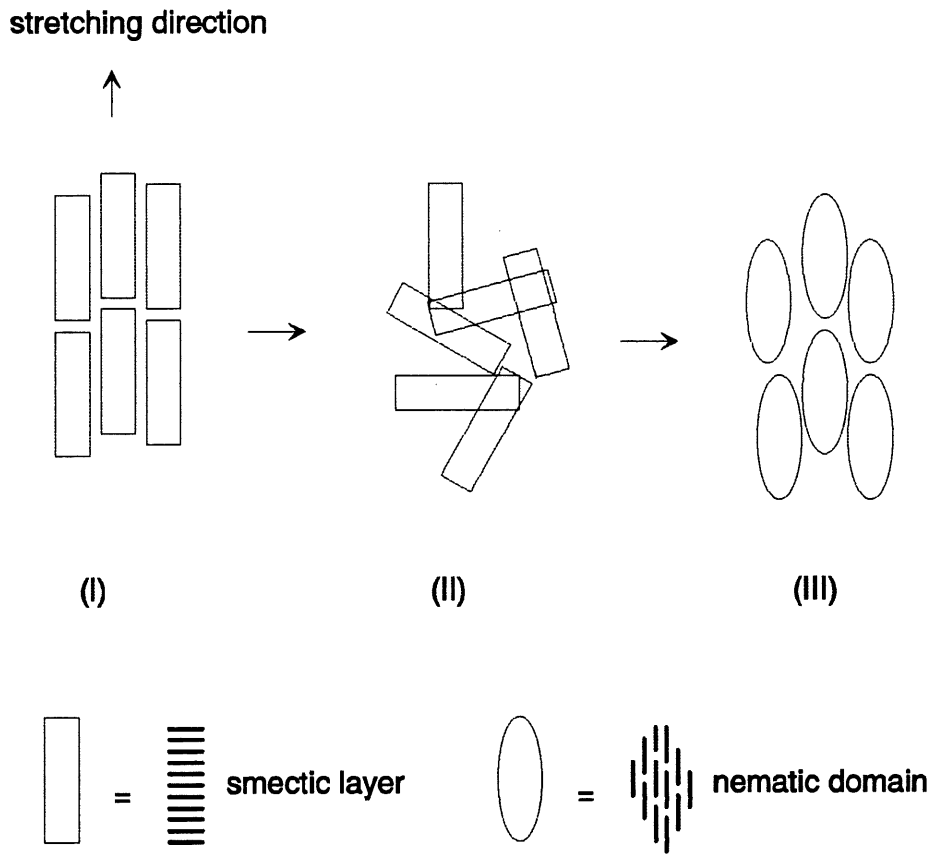

Figure 49. Schematic representation of the state of alignment of the liquid crystalline domains in the three regions indicated in *Figure 48*.

which accompanies the smectic to nematic transition. Essentially, we can envisage two possible mechanisms for explaining the reorientation process started at 116 °C. The first consists of the following steps: 1) melting of the aligned smectic layers, 2) formation of aligned nematic domains without rotation of the mesogens (i.e., there is still a monodomain structure with nematic director perpendicular to the stretching direction), and 3) alignment of the nematic director along the stretching direction, which implies rotation of the nematic domains. The second mechanism is characterized by 1) melting of the aligned smectic layers, 2) formation of randomly aligned nematic domains with rotation of the mesogens (i.e., the sample has now a polydomain structure), and 3) alignment of the nematic directors along the

stretching direction, leading to a new monodomain structure. As is depicted in *Figure 49*, the stable zero macroscopic orientation in region II corresponds to randomly aligned smectic layers (at 105 °C). This observation favors the second mechanism, since it is clear that if the film is cooled back to 105 °C after the first two steps, i.e., before the alignment of the nematic directors, randomly aligned smectic layers should be formed. The first mechanism seems to be unlikely, because if the reorientation process is stopped somewhere while cooling the sample back to the smectic phase, randomly aligned smectic layers would not be expected. On the other hand, with the first mechanism when the film in region II is heated again to 116 °C, as is shown in *Figure 48*, the reorientation process should just continue and complete, leading to region III.

However, we still can not answer the fundamental question as what is the driving force for the realignment of the nematic director accompanying the mesophase transition. Is this a sort of general behavior during the smectic-nematic transition in a monodomain structure induced by a mechanical elongation? Or is it specific to the present experimental conditions and, particularly, related to the surface of the stretched supporting PVA film? We have performed experiments in order to get some answers to these questions. Here we make a brief discussion of the experimental observations.

First, the stretched PVA film seems to play an important role for this reorientation phenomenon. We observed that when BiPA5 was directly stretched in its nematic phase, at 117 °C for example, the induced macroscopic orientation was also perpendicular to the stretching direction (negative P_2). This seems to rule out the possibility that the reorientation of the mesogens is due to an alignment of the nematic domains, formed after the smectic-nematic transition, as response to a remaining mechanical field on the film under strain, as is the case in other circumstances (34). In other words, the switching from perpendicular to parallel orientation is not the consequence of a mechanical effect on the nematic domains. A different experiment is also indicative. BiPA5 was stretched in the isotropic state at 120 °C ,

and no macroscopic orientation was induced ($P_2 = 0$). When the stretched film was cooled to 117 °C under strain, a small but non-negligible positive P_2 was observed after 30 min ($P_2 \approx 0.05$). In this case, after being cooled to 117 °C, randomly aligned nematic domains should be formed. The observed slight parallel orientation is likely to be induced by the surface effect of the elongated PVA film (the domains in the interfacial region would be more aligned than those distant from the interface, and the small P_2 is due to the fact that this parameter measures the average orientation over all domains). We could thus suspect that for the film under strain and undergoing the smectic to nematic transition, this nematic domain-aligning capability of the PVA film, although very little apparently, could start the reorientation process.

On the other hand, it also seems clear that this reorientation process is related to the nature of the mesophase transition and the formation of the LC domains. For comparison, we have investigated a different SCLCP, whose structure is shown below

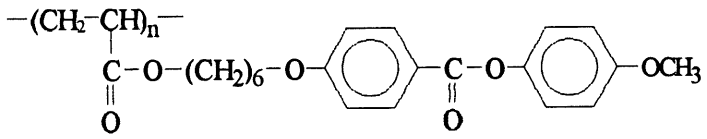

This polymer displays both a smectic-A and a nematic phase, like BiPA5, but differs from the latter in that it has a much wider nematic phase below the isotropization. It shows a smectic-nematic transition at 94 °C and the nematic-isotropic transition at 119 °C. When it is cast onto the surface of a PVA film and stretched in the smectic phase a perpendicular orientation is induced (33). But under the same experimental conditions, when it is heated through the smectic-nematic transition, the orientation remains perpendicular and no reorientation can be observed. If a possible effect of the PVA film surface is the only reason for the reorientation process to take place, we would expect the same result for this polymer as for BiPA5. As a matter of fact, it is known that the smectic-A-nematic transition depends on the width of the nematic phase (39). This transition would be second order if the temperature range of the

nematic phase is large, but become first order with a narrow nematic phase. Therefore, it seems that the very narrow nematic phase of BiPA5 before the isotropic state could be one of the factors responsible for the observed reorientation phenomenon. One thing at least is clear: BiPA5 must have a much lower viscosity while entering into the nematic phase as compared to this wide nematic phase-SCLCP.

4.4 Conclusion

Stretching BiPA5 in its smectic phase results in a perpendicular macroscopic orientation of the mesogens with respect to the stretching direction. When the stretched film is heated under strain into the smectic-nematic transition a reorientation of the mesogens occurs, leading to a parallel macroscopic orientation. The reorientation process is not reversible when the stretched film is cooled back to the smectic phase, the orientation remaining parallel. The interesting questions raised by the observations of this study are as follows. How do the mesophase transitions, such as the smectic-A-nematic transition in the present case, proceed in SCLCP samples under strain with macroscopically oriented mesogens? And how different are they as compared to un-oriented SCLCPs with a polydomain structure, i.e., with randomly aligned oriented microstructures. In the case of BiPA5, our investigations suggest that in the course of the smectic-nematic transition, the melting of the macroscopically aligned smectic layers in the monodomain structure would lead to the formation of randomly aligned nematic domains before their alignment which gives rise to a parallel orientation of the mesogens. This point of view is particularly supported by the observation that the reorientation process, once started, can be stopped before the change of the orientation direction by cooling the polymer back to its smectic phase, and that this can result in randomly aligned smectic layers indicated by a stable zero macroscopic orientation in the stretched film. The surface of the stretched supporting PVA film used for the mechanical stretching is believed to play a role in starting the reorientation process, but it cannot be the only reason. The observed reorientation is not a common feature for all SCLCPs undergoing a smectic-nematic transition

under those conditions. The width of the temperature range for the nematic phase appears to be a factor which makes this mesophase transition-induced reorientation to take place.

CONCLUSION

This thesis describes several research works on SCLCPs and related systems. The apparently separate projects are centered on two main aspects : 1) development of new SCLCP-based materials, and 2) physical studies of monodomain induction, relaxation and reorientation. The obtained results are significant and of interest. Regarding the first research objective, we have succeeded in preparing two novel SCLCP-based systems. These are ILCPNs and elastomeric graft copolymers containing a SCLCP component. As for the second research front, we have investigated the induction of the monodomain structure in the new graft copolymers, in a series of ion-containing SCLCPs whose ionic aggregates perturb the molecular order within nematic domains. We have also studied the relaxation behavior of the monodomain structure in the vicinity of mesophase transitions in stretched SCLCP films under strain.

Despite the preliminary nature of the results presented in Chapter 1, the work represents the first demonstration of a novel SCLCP-based system that could incite interest. Indeed, we have proposed to extend the concept of interpenetrating networks to SCLCPs and shown the feasibility of preparing such materials (13). Several polyacrylate-based ILCPNs were obtained by using a sequential synthesis method that consists in swelling a network sample in a mesogenic monomer solution and polymerizing the monomer afterwards. Our characterization results show that the phase transition behaviors of the SCLCP components could be modified to different extents depending on the miscibility reached in the ILCPNs. The partial miscibility is due to the restriction of phase separation by the cross-links, and a higher cross-link level of the first network hinders more efficiently the phase separation. On the other hand, we have also made attempts to prepare ILCPNs containing non-covalent networks through the use of LC ionomers. On the basis of this study, more research on ILCPNs would be expected. One can use not only the sequential method but also the

simultaneous technique - making two networks in the same time via two non-interfering routes - to prepare ILCPNs having controlled microphases. One can also develop ILCPNs which is a combination of two non-covalent LC networks. Such a system could be thermoplastic and facilitates the processing. In essence, this study could be the beginning of research effort that eventually opens a new route for the search of functional polymer materials.

The work described in Chapter 2 is also original (15). A radical polymerization of mesogenic monomers in a solution containing a dissolved SBS tri-block copolymer results in a grafting of the SCLCP component on the polybutadiene block of SBS. The resulting materials are thermoplastic elastomers, like pure SBS. They differ from the corresponding blends prepared from solution-mixing and casting of SCLCPs and SBS by showing a number of improved properties. They have much smaller phases, probably microphases, which give rise to a homogeneous texture when viewed through an optical microscope under crossed polarizers. They are mechanically much stronger, and can be stretched repeatedly to induce very easily a monodomain structure for the SCLCP component. We show that, using a two-step thermal treatment which involves a rearrangement of polystyrene microdomains and the relaxation of polybutadiene chains, the mechanically-induced orientation of the mesogens can be preserved in relaxed and free standing films. This provides an effective way of controlling the monodomain structure in SCLCPs. Applications requiring liquid crystalline monodomain in elastomeric materials could be possible. The interest of this study is also due to the fact that this special technique is, in principle, applicable to grafting any SCLCPs, as long as they are made through radical polymerization like acrylate and methacrylate-based polymers, onto a number of polymers containing double bonds in their backbone. For instance, in addition to SBS, SCLCPs should be able to be grafted to other commercially very important polymers, such as styrene-isoprene-styrene tri-block copolymer, styrene-butadiene and styrene-isoprene two-block copolymers, their random copolymers of varying compositions, and polybutadiene

or polyisoprene homopolymer as well. A large variety of materials containing a SCLCP component can thus be prepared.

The main purpose of the study discussed in Chapter 3 was to investigate a possible correlation between the mechanically-induced macroscopic orientation of the mesogens (34), which is the average orientation over all mesogens throughout the film sample, and the intrinsically oriented microstructure in SCLCPs, i.e., the molecular order inside each nematic domain. The orientation parameter determined from infrared dichroism, denoted S_{macro} (or P_2), is given by $S_{macro} = S_{director} \cdot S_{micro}$, where $S_{director}$ measures the alignment of nematic directors along the stretching direction and S_{micro} characterizes the orientation of the mesogens inside each nematic domain along the nematic director. In the case of polyacrylate-based SCLCPs, S_{micro} is generally near to 0.5. Before the mechanical stretching, the sample has a polydomain structure, that is $S_{director} = 0$; no macroscopic orientation is observable. The mechanical stretching leads to the alignment of nematic domains, and a monodomain structure is reached when $S_{director} = 1$. At this point the sample has a uniform orientation of the mesogens, and the measured S_{macro} is determined by S_{micro}. In our study, as model polymers we have used a series of LC ionomers carrying less than 10 mol % of COO^-Na^+ units, and presumed that S_{micro} in the ionomers be affected by the presence of ionic aggregates. It turned out that for two different groups of ionomers the orientation behaviors are completely different. In the case of the ionomers containing mesogenic biphenyl moieties, the orientation increases with stretching in a same way as for all samples, regardless of the ionic content. Whereas for the ionomers with phenyl benzoate moieties, the achievable macroscopic orientation is lowered with increasing the ionic concentration. Furthermore, a plateau value of S_{macro} is rapidly reached for all samples upon stretching, which is indicative of a uniform macroscopic orientation with $S_{director} = 1$. Therefore, at least for this group of ionomers, it is clearly revealed that the ionic aggregates perturb the molecular order inside the nematic domains, i.e., lowering S_{micro}. This is reflected by a less ordered monodomain structure induced by mechanical stretching. Another notable finding in this study is that when a SCLCP is stretched in the isotropic state,

no macroscopic orientation of the mesogens is induced because of the absence of a liquid crystalline phase, but when the stretched film is cooled under strain from the isotropic state, a macroscopic orientation could occur during the course of cooling. This surprising effect is attributed to a rapid response of the nematic domains, formed once the temperature is lowered through the isotropic-nematic transition, to the residual mechanical field acting on the film under strain. This result explains some literature data concerning orientation in fibers drawn from the isotropic state.

Generally, when a transition from polydomain to monodomain is induced by a mechanical stretching, the molecular order of the mesogens remains nematic or smectic depending on the mesophase from which the sample is stretched. In other words, in a stretched film of SCLCP having a monodomain structure, a nematic or smectic order extends over a macroscopic scale. The interesting question one can raise is what could happen when such a stretched film is heated, under strain, to the vicinity of mesophase transitions. Would the phase transitions of a monodomain proceed just like for a polydomain structure, or would it be done differently ? The work (40) presented in Chapter 4 is a first attempt to observe the possible phenomena associated with the phase transitions in a stretched film of SCLCP, and to answer those questions. We have used a SCLCP having a smectic phase and a very narrow nematic phase before the isotropic state. When this polymer is stretched in its smectic phase, a macroscopic orientation of the mesogens develops in the direction perpendicular to the stretching direction as a result of smectic layers' alignment. When the stretched film is heated under strain to the smectic-nematic transition, an interesting mesophase-transition-induced reorientation process occurs. The aligned mesogens flip 90°, and the macroscopic orientation becomes parallel to the stretching direction. This reorientation was found to be irreversible, and to take place only for transition from smectic to a narrow-temperature-range nematic phase. Also, when the stretched film is heated into the isotropic state, the macroscopic orientation no longer exists. However, cooling the SCLCP back to its liquid crystalline phases allows for the stretching-induced orientation to be recovered. We have tried to get some insight into the

mechanisms leading to this reorientation and other related phenomena, but it is clear that a full understanding of those observations need much more investigation.

BIBLIOGRAGHY

1. C. B. McArdle, *"Side-chain Liquid Crystal Polymers"*, Blackie, Glasgow, 1989
2. A. M. Donald and A. H. Windle, *"Liquid Crystalline Polymers"*, Cambridge University Press, 1992
3. L. Noirez, P. Keller and J. P. Cotton, *Liquid Crystals*, **18,** 129 (1995)
4. M. Portugall, H. Ringsdorf and R. Zentel, *Makromol. Chem.*, **183,** 2311 (1982)
5. V. P. Shibaev, S. G. Kostromin and N. A. Plate, *Eur. Polym. J.*, **18,** 651 (1982)
6. G. Galli, E. Chiellini, Y. Yagci and E. I. Serhatli, *Makromol. Chem., Rapid Commun.*, **14,** 185 (1993)
7. M. Blankenhagel and J. Springer, *Makromol. Chem.*, **193,** 3031 (1992)
8. A. Gottschalk and H.-W. Schmidt, *polym. Prepr. (Am. Chem. Soc., Div. Polym. Chem.)* **34(1),** 188 (1993)
9. Y. Zhao and H. Lei, *Macromolecules,* **27,** 4525 (1994)
10. J. Schatzle, W. Kaufhold and H. Finkelmann, *Makromol. Chem.*, **190,** 3269 (1989)
11. M. Brehmer and R. Zentel, *Makromol. Chem. Phys.*, **195,** 1891 (1994)
12. J. Kupfer and H. Finkelmann, *Makromol. Chem. Phys.*, **195,** 1353 (1994)
13. Y. Zhao and G. Yuan, *Macromolecules,* **29,** 1067 (1996)
14. D. Klempner, L. H. Sperling and L. A. Utracki, *"Interpenetrating Polymer Networks"*; Advances in Chemistry Series 239; American Chemical Society, Washington, DC, 1994.
15. G. Yuan and Y. Zhao, *Polymer*, **38,** 119 (1997)
16. F. Barnes, F. J. Davis and G. R. Mitchell, *Mol. Cryst. Liq. Cryst.*, **163,** 13 (1989)
17. H. L. Frisch and P. Zhou, In ref 13.
18. J. J. M. Halls, C. A. Walsh, N. C. Greenham, E. A. Marseglia, R. H. Friend, S. C. Moratti & A. B. Holmes, *Nature*, **376,** 498 (1995)

19. J. Adams and W. Gronski, *Macromol. Chem., Rapid Commun.*, **10,** 553 (1989)
20. G. Odian, *"Principles of Polymerization"*, 3rd Edn, John Wiley & Sons, New York, 1991 and references therein
21. H. Lei and Y. Zhao, *Polymer*, **35,** 104 (1994)
22. H. Finkelmann and G. Rehage, *Adv. Polym. Sci.*, **60/61,** 99 (1984)
23. T. Pakula, K. Saijo, H. Kawai and T. Hashimoto, *Macromolecules,* **18,** 2037 (1985)
24. Y. Zhao, *Macromolecules,* **25,** 4705 (1992)
25. A. Eisenberg, B. Hird and R.B. Moore, *Macromolecules* **23**, 4098 (1990)
26. P. Roche and Y. Zhao, *Macromolecules,* **28,** 2819 (1995)
27. I. J. Davis and G. R. Mitchell, *Polym. Commun.* **28**, 8 (1987)
28. J. Schätzlz, W. Kaufhold and H. Finkelmann, *Makromol. Chem.* **190**, 3269 (1989)
29. Y. Zhao and H. Lei, *Polymer*, **35,** 1419 (1994)
30. J. L. Koenig, *"Spectroscopy of Polymers"*, American Chemical Society, Washington, DC, 1992
31. W. Guo, F. J. Davis and G. R. Mitchell, *Polymer*, **35**, 2952 (1994)
32. G. R. Mitchell, M. Coulter, F. J. Davis and W. Guo, *J. Phys. II France*, **2**, 1121 (1992)
33. Y. Zhao, P. Roche and G. Yuan, *Macromolecules,* **29,** 4619 (1996)
34. G. Yuan and Y. Zhao, *Polymer*, **36,** 2725 (1995)
35. G. Yuan and Y. Zhao, *Macromol. Chem. Phys.*, **195,** 3281 (1994)
36. J.-C. Dubois, G. Decobert, P. Le Barny, S. Esselin, C. Friedrich and C. Noël, *Mol.Cryst Liq. Cryst.*, **137,** 349 (1986)
37. C. Noël, personal communication.
38. Y. Zhao, *Polymer*, **36,** 2717 (1995)
39. W. L. McMillan, *Phys. Rev. A*, **4,** 1238 (1971)
40. Y. Zhao and G. Yuan, *J. Polym. Sci., Polym. Phys. Ed.*, in press